

Modeling and Control of the Unified Power Flow Controller (UPFC)

Azra Hasanovic

**Thesis submitted to
The College of Engineering and Mineral Resources
at West Virginia University
in partial fulfillment of the requirements
for the degree of**

**Master of Science
in
Electrical Engineering**

**Ali Feliachi, Ph.D., Chair
Asad Davari, Ph.D.
Powsiri Klinkhachorn, Ph.D.**

Department of Computer Science and Electrical Engineering

**Morgantown, West Virginia
2000**

**Keywords: UPFC, load flow, dynamic model,
transient stability, fuzzy control, PST**

ABSTRACT

Modeling and Control of the Unified Power Flow Controller (UPFC)

Azra Hasanovic

The focus of this thesis is a FACTS device known as the Unified Power Flow Controller (UPFC). With its unique capability to control simultaneously real and reactive power flows on a transmission line as well as to regulate voltage at the bus where it is connected, this device creates a tremendous quality impact on power system stability. These features become even more significant knowing that the UPFC can allow loading of the transmission lines close to their thermal limits, forcing the power to flow through the desired paths. This will give the power system operators much needed flexibility in order to satisfy the demands that the deregulated power system will impose.

The most cost-effective way to estimate the effect the UPFC has on a specific power system operation is to simulate that system together with the UPFC by using one of the existing simulations packages. Specifically, the objective of this thesis is to (1) develop a UPFC model that can be incorporated into existing MATLAB based Power System Toolbox (PST), (2) design basic UPFC controllers, and (3) design on supplementary damping control scheme based on fuzzy logic to enhance power system stability. The proposed tools will be tested on the two-area-four-generator system to prove their effectiveness.

ACKNOWLEDGMENTS

First I want to thank my family for always being there for me. Their love, constant support and encouragement to pursue my goals made this thesis possible.

I would like to acknowledge Professor Feliachi, an excellent teacher and advisor, for his guidance throughout this work. His readiness to help and valuable suggestions were highly appreciated.

I would also like to thank Professors Davari and Klinkhachorn for serving on my examining committee, Professor Choudhry, my TA supervisor, for helping me in the lab, and Professor Cooley, ECE Graduate Coordinator, for helping me come to the States to continue my education.

Special thanks to my colleague and dear friend Karl Schoder for useful advice, help and support.

TABLE OF CONTENTS

TITLE PAGE	i
ABSTRACT	ii
ACKNOWLEDGMENTS.....	iii
TABLE OF CONTENTS	iv
LIST OF FIGURES	vi
LIST OF TABLES	viii
Chapter 1 INTRODUCTION	1
Chapter 2 LITERATURE SURVEY	3
Chapter 3 UPFC BASIC OPERATION AND CHARACTERISTICS	7
3.1 Basics of Voltage Source Converters and Pulse Width Modulation	7
Technique	
3.2 UPFC Description and Operation	9
3.3 Power Flow on the Transmission Line	11
3.4 Series Converter: Four Modes of Operation.....	15
3.5 Automatic Power Control Mode	16
3.6 Comparison of the UPFC to Series Compensators and Phase Angle	18
Regulators	
Chapter 4 UPFC MODELING AND INTERFACING	23
4.1 UPFC Load Flow (LF) Model	23
4.2 UPFC Dynamic Model	25
4.3 Interfacing the UPFC with the Power Network.....	26
4.4 Linearized Model	29
4.4.1 Basic Terms and Definitions	30
4.4.2 Linearized Model Derivation	31
4.5 Linearization of a Power System with the PST and Modal Analysis	34
4.5.1 Description	34
4.5.2 Method	34
4.5.3 States, Input and Output Signals	36

4.5.4	Minimum realization	37
Chapter 5	CONTROLLER DESIGN	38
5.1	Basic Control	38
5.1.1	Series control scheme	38
5.1.2	Shunt control scheme	40
5.2	Damping Controller Design	41
5.2.1	Introduction	41
5.2.2	Structure of a Fuzzy Controller	42
5.2.3	Fuzzy Logic UPFC Damping Controller	45
Chapter 6	CASE STUDY	47
6.1	Test System	47
6.2	Load Flow	48
6.3	Linearized Model	48
6.4	Nonlinear Simulations and Modal Anaysis	50
6.4.1	Tracking Active and Reactive Powers Reference Values	50
6.4.2	Operation Under the Fault Condition	51
Chapter 7	CONCLUSION	59
	REFERENCES	61
	APPENDIX A	64
	Test System and UPFC Data	64
	APPENDIX B	69
	Load Flow Solution	69
	APPENDIX C	71
	Two Machine/UPFC Power System: Linearized Model	71

LIST OF FIGURES

Fig. 3.1	Three-phase voltage sourced-converter	7
Fig. 3.2	PWM converter (a) A phase-leg (b) PWM waveforms	9
Fig. 3.3	Fundamental frequency model of UPFC	10
Fig. 3.4	Transmission line	12
Fig. 3.5	P-Q locus of the uncompensated system	14
Fig. 3.6	Phasor diagrams	15
Fig. 3.7	Transmission line with UPFC	16
Fig. 3.8	P-Q relationship for simple two-bus system with a UPFC at $\delta=0^0, 30^0, 60^0$ and 90^0	18
Fig. 3.9	Transmission line with controlled series capacitive compensation	19
Fig. 3.10	Transmission line controlled with a Phase Angle Regulator	20
Fig. 3.11	P-Q relationship attainable with transmission line controlled with series compensators and a UPFC at (a) $\delta=0^0$, (b) 30^0 , (c) 60^0 and (d) 90^0	21
Fig. 3.12	P-Q relationship attainable with transmission line controlled with a PAR and a UPFC at (a) $\delta=0^0$, (b) 30^0 , (c) 60^0 and (d) 90^0	22
Fig. 4.1	Power network with a UPFC included (a) schematic (b) Load Flow Model	24
Fig. 4.2	Load flow algorithm	24
Fig. 4.3	Interface of the UPFC with power network	26
Fig. 4.4	Algorithm for interfacing the UPFC with the power network	27
Fig. 5.1	Phasor diagram	39
Fig. 5.2	Series control scheme-automatic power flow mode	40
Fig. 5.3	Shunt control scheme	40
Fig. 5.4	Lead –lag controller structure	41
Fig. 5.5	Fuzzy controller structure	42
Fig. 5.6	Mamdani Max-Product Inference	43
Fig. 5.7	Mamdani (Max-Min) Inference	44
Fig. 5.8	Centroid method	44
Fig. 5.9	Obtaining the input signals for fuzzy controller	45

Fig. 5.10	Fuzzy logic controller input and output variables	45
Fig. 6.1	Two-area-four-generator test system	47
Fig. 6.2	Two-machine/UPFC system	48
Fig. 6.3	Changing real power reference value	51
Fig. 6.4	Changing reactive power reference value	52
Fig. 6.5	Test system with PSS: Nonlinear simulation	53
Fig. 6.6	Nonlinear simulation results: dashed lines-system with PSS; solid lines-system with PSS/UPFC	55
Fig. 6.7	Case 3 b: Nonlinear simulation results	56
Fig. 6.8	Case 3 c: Nonlinear simulation results	56
Fig. 6.9	Relative machine angle δ_{13} in degrees for operating conditions (a)-(d): 1 without damping controller; 2 lead-lag damping controller; 3 fuzzy damping controller	58

LIST OF TABLES

Table 4.1	Stability criteria for linear system	31
Table 5.1	Fuzzy rules	46
Table 6.1	System state matrices and eigenvalues using the derived equations	49
	and the PST	
Table 6.2	Input matrices of the power system using the derived equations	49
	and the PST	
Table 6.3	Eigenvalues for two-machine/UPFC system	49
Table 6.4	States and input signals of the linearized power system	50
Table 6.5	Dominant eigenvalues for the test system with exciters and governors	53
	as only controls	
Table 6.6	Dominant eigenvalues for the test system with the PSS	53
Table 6.7	Dominant eigenvalues for the test system with the PSS and the UPFC	54
	operated in the automatic power control mode	
Table 6.8	Operating conditions (values are in MW)	57
Table 6.9	Dominant eigenvalues for the test system with the PSS and the UPFC	57
	operated in the power oscillation damping control mode	
Table B.1	Load flow solution	69
Table B.2	UPFC steady-state quantities	70

Chapter 1

INTRODUCTION

The power system is an interconnection of generating units to load centers through high voltage electric transmission lines and in general is mechanically controlled. It can be divided into three subsystems: generation, transmission and distribution subsystems. Until recently all three subsystems were under supervision of one body within a certain geographical area providing power at regulated rates. In order to provide cheaper electricity the deregulation of power system, which will produce separate generation, transmission and distribution companies, is already being performed. At the same time electric power demand continues to grow and also building of the new generating units and transmission circuits is becoming more difficult because of economic and environmental reasons. Therefore, power utilities are forced to rely on utilization of existing generating units and to load existing transmission lines close to their thermal limits. However, stability has to be maintained at all times. Hence, in order to operate power system effectively, without reduction in the system security and quality of supply, even in the case of contingency conditions such as loss of transmission lines and/or generating units, which occur frequently, and will most probably occur at a higher frequency under deregulation, a new control strategies need to be implemented.

In the late 1980s the Electric Power Research Institute (EPRI) has introduced a new technology program known as Flexible AC Transmission System (FACTS) [4]. The main idea behind this program is to increase controllability and optimize the utilization of the existing power system capacities by replacing mechanical controllers by reliable and high-speed power electronic devices.

The latest generation of FACTS controllers is based on the concept of the solid state synchronous voltage sources (SSTATCOMs) introduced by L. Gyugyi in the late 1980s [5]. The SSTATCOM behaves as an ideal synchronous machine, i.e. generates fundamental frequency three-phase balanced sinusoidal voltages of controllable amplitude and phase angle. It can internally

generate both inductive and capacitive reactive power. If coupled with an appropriate energy storage device, i.e. dc storage capacitor, battery, etc, SVS is able to exchange real power with the ac system. The SVS can be implemented by the use of the voltage sourced-converters (VSC). Basics of the VSCs will be given in the third chapter.

The SVS can be used as shunt or series compensator. If operated as a reactive shunt compensator it is called static condenser (STATCON), operated as a reactive series compensator it is called static synchronous series compensator (SSSC). A special arrangement of two SVSs, one connected in series with the ac system and the other one connected in shunt, with common dc terminals is called Unified Power Flow Controller (UPFC). It represents series - shunt type of controller. The Interline Power Flow Controller (IPFC) is recently introduced series-series type of controller. It consists of two or more SSSCs coupled through a common DC link. IPFC provides independently controllable reactive series compensation of each selected line as well as transfer of real power between the compensated lines.

The advantages of SVS based compensators over mechanical and conventional thyristor compensators are

- improved operating and performance characteristics
- uniform use of same power electronic device in different compensation and control applications
- reduced equipment size and installation labor.

The FACTS device this thesis will focus on is the UPFC. The thesis will be organized as follows. A literature survey will be given in Chapter 2. UPFC basic operation and characteristics will be described in Chapter 3. Chapter 4 will discuss UPFC modeling and interfacing. UPFC "basic" and damping controller design will be presented in Chapter 5. The effect of the UPFC on the power system operation will be illustrated using a two-area power system in Chapter 6. Concluding remarks will be given in the last Chapter.

Chapter 2

LITERATURE SURVEY

In this chapter a literature survey of topics related to UPFC operation, modeling and control will be given.

The UPFC, which was proposed by L. Gyugyi in 1991 [3], [6], [7], is one of the most complex FACTS devices in a power system today. It is primarily used for independent control of real and reactive power in transmission lines for a flexible, reliable and economic operation and loading of power system. Until recently all four parameters that affect real and reactive power flow on the line, i.e. the line impedance, voltage magnitudes at the terminals of the line or power angle, were controlled separately using either mechanical or other FACTS devices such as a Static Var Compensator (SVC), a Thyristor Controlled Series Capacitor (TCSC), a phase shifter, etc. However, the UPFC allows simultaneous or independent control of these parameters with transfer from one control scheme to another in real time. Also, the UPFC can be used for voltage support, transient stability improvement and damping of low frequency power system oscillations. Because of its attractive features, modeling and controlling an UPFC have come into intensive investigation in the recent years.

Several references in technical literature can be found on development of UPFC steady state, dynamic and linearized models. Steady state model referred as an injection model is described in [9]. UPFC is modeled as a series reactance together with the dependent loads injected at each end of the series reactance. The model is simple and helpful in understanding the UPFC impact on the power system. However, the amplitude modulation and phase angle control signals of the series voltage source converter have to be adjusted manually in order to find the desired load flow solution.

If a UPFC is operated in the automatic control mode (i.e. to maintain a pre-specified power flow between two power system buses, the sending and the receiving buses, and to regulate the sending end voltage at the specific value) the UPFC sending end is transformed

into a PV bus while the receiving end is transformed into a PQ bus, and conventional load-flow (LF) program can be performed [10]. This method is simple and easy to implement but it will only work if real and reactive power flows and the sending bus voltage magnitude are controlled simultaneously. It should be also mentioned that there is no need for an iterative procedure used in [10] to compute UPFC control parameters. They can be computed directly after the conventional LF solution is found. Due to the advantages that the automatic power flow control mode offers, this mode will be used as the basic operation mode for the most of the practical applications. Therefore, this model will be discussed in the fourth chapter of this thesis. Series and shunt transformer losses are taken into account.

A Newton-Rhapson based algorithm for large power systems with embedded FACTS devices is derived in [12]. In [13] this algorithm was extended to include UPFC application. It allows simultaneous or independent control of real and reactive powers and voltage magnitude. The algorithm itself is very complicated and hard to implement. It considerably increases the order of the Jacobian matrix in the iterative procedure and is quite sensitive to initial condition settings. Improper selection of initial condition can cause the solution to oscillate or diverge.

UPFC dynamic model known as a fundamental frequency model can be found in [10], [16], [20] and [22]. This model consists of two voltage sources one connected in series and the other one in shunt with the power network to represent the series and the shunt voltage source inverters. Both voltage sources are modeled to inject voltages of fundamental power system frequency only. Model in [16] neglects the DC link capacitor dynamics which might make results obtained using this model inaccurate, models in [10], [20] and [22] include DC link capacitor dynamics and can be used for study of UPFC effect on the real power system behavior.

The linearized model of the power network including UPFC is useful for small signal analysis and damping controller design. The UPFC linearized model can be found in [16] and [19]. While deriving these models some simplification have been made, i.e. the model described in [16] does not include DC link dynamics, the model derived in [19] assumes that the UPFC sending and receiving buses are also generator terminal buses. However, UPFC can be connected between any two buses in the network. Therefore, these models do not

represent the general form of the linearized network. General form of the linearized model of the network with UPFC included will be derived in the fourth chapter of this thesis.

UPFC basic control design involves control of real and reactive power flow, sending bus voltage magnitude and DC voltage magnitude. The most frequently used control scheme is based on the vector-control approach proposed by Schauder and Metha in 1991 [14]. This scheme allows decoupled control of the real and reactive powers which makes it suitable for UPFC application. This can be accomplished by transforming the three-phase balanced system into a synchronously rotating orthogonal system. A new coordinate system is chosen in such way that its d component coincides with the instantaneous voltage vector and q component is orthogonal to it. In this coordinate system the d-axis current component contributes to the instantaneous real power and q-axis current accounts for the reactive power. This control scheme can be applied both for series and shunt converter control [3], [15]-[17], [20]. Another approach for automatic power flow control for the series converter is to decompose the voltage drop between the sending and the receiving buses into two components: one in phase with the sending bus and the other one orthogonal to it. The component in phase with the sending bus has strong influence on the reactive power flow and the component orthogonal to it mainly influences the real power flow [22]. The shunt converter can be controlled using two PI controllers to control the sending bus voltage magnitude and the dc link voltage [21]-[22]. This control scheme is simple and easy to implement and it will be used in this thesis.

UPFC damping controller design can be found in [17]-[19], [21] and [22]. The supplementary control can be applied to the shunt inverter through the modulation of voltage magnitude reference signal or to the series inverter through modulation of power reference signal. In [17] and [21] the slip of the desired machine $\Delta\omega$ is used as the input signal to the damping controller. In general it is difficult to obtain this signal. Therefore, this kind of control is not feasible, and controllers depending on local measurements such as the tie-line power flow or the UPFC terminal voltage phase angle difference are more appropriate [19], [22]. All controllers in references above are of lead-lag type. They are designed for a specific operating condition using linearized model. However, changes in operating conditions might have negative effect on the controller performance. More advanced control schemes such as self-tuning control, sliding mode control, and fuzzy logic control offer

better dynamic performance than conventional controllers. Power system stabilizers and SVC damping controllers have been designed using some of these techniques [24]-[30]. A fuzzy logic UPFC damping controller is proposed in this thesis. Fuzzy control design is attractive because it does not require mathematical model of the system under study, it can cover wider range of operating conditions and is simple to implement.

The objective of this thesis is to develop a UPFC model, design its controls, incorporate the model and its controls in the MATLAB based commercial power system simulation software Power System Toolbox (PST) [23], and use the UPFC to enhance operation and control of electric power systems. To achieve the stated objective, the following research tasks are performed:

- Development of a UPFC load flow or steady-state model, which is needed to initialize the simulation
- Development of a UPFC dynamic model with its controllers that can be used for transient stability studies
- Interfacing the model with PST
- Derivation of a linearized model of the entire system, which can be used for analysis and control of power system low frequency oscillations.

To demonstrate the performance of the controller under dynamic conditions, a power system, extensively used in the literature, consisting of two-areas, each with two generating plants, is used. When a large disturbance is applied, simulation results show that the UPFC can significantly enhance power system operation and performance.

Chapter 3

UPFC BASIC OPERATION AND CHARACTERISTICS

This chapter will explain basic operation and characteristics of the UPFC. Since UPFC consists of two voltage-sourced converters (VSCs), basics of VSCs will be briefly discussed at the beginning of the chapter.

3.1 Basics of Voltage Source Converters and Pulse Width Modulation Technique

Typical three-phase VSC is shown in Fig. 3.1 [3].

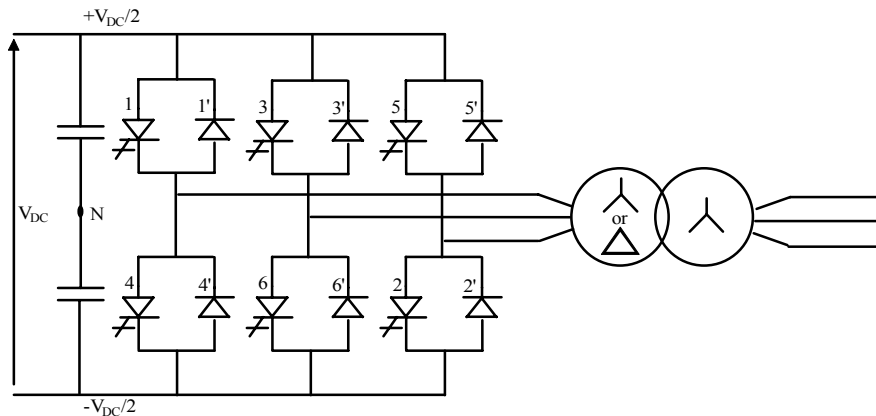


Fig. 3.1 Three-phase voltage sourced-converter

It is made of six valves each consisting of a gate turn off device (GTO) paralleled with a reverse diode, and a DC capacitor. An AC voltage is generated from a DC voltage through sequential switching of the GTOs. The DC voltage is unipolar and the DC current can flow in either direction.

Controlling the angle of the converter output voltage with respect to the AC system voltage controls the real power exchange between the converter and the AC system. The real power flows from the DC side to AC side (inverter operation) if the converter output voltage is controlled to lead the AC system voltage. If the converter output voltage is made to lag the AC system voltage the real power will flow from the AC side to DC side (rectifier

operation). Inverter action is carried out by the GTOs while the rectifier action is carried out by the diodes. Two switches on the same leg cannot be on at the same time.

Controlling the magnitude of the converter output voltage controls the reactive power exchange between the converter and the AC system. The converter generates reactive power for the AC system if the magnitude of the converter output voltage is greater than the magnitude of the AC system voltage. If the magnitude of the converter output voltage is less than that of the AC system the converter will absorb reactive power.

The converter output voltage can be controlled using various control techniques. Pulse Width Modulation (PWM) techniques can be designed for the lowest harmonic content. It should be mentioned that these techniques require large number of switching per cycle leading to higher converter losses. Therefore, PWM techniques are currently considered unpractical for high voltage applications. However, it is expected that recent developments on power electronic switches will allow practical use of PWM controls on such applications in the near future. Due to their simplicity many authors, i.e. [10], [19], [20], [22], have used PWM control techniques in their UPFC studies. Hence, the same approach will be used in this thesis.

When sinusoidal PWM technique is applied turn on and turn off signals for GTOs are generated comparing a sinusoidal reference signal v_r of amplitude A_r with a sawtooth carrier waveform v_c of amplitude A_c as shown in Fig. 3.2 (b) [33]. The frequency of the sawtooth waveform establishes the frequency at which GTOs are switched.

Consider a phase-leg as shown in Fig. 3.2 (a).

In this case

$v_r > v_c$ results in a turn on signal for the device one and gate turn off signal for the device four

and

$v_r < v_c$ results in a turn off signal for the device one and gate turn on signal for the device four.

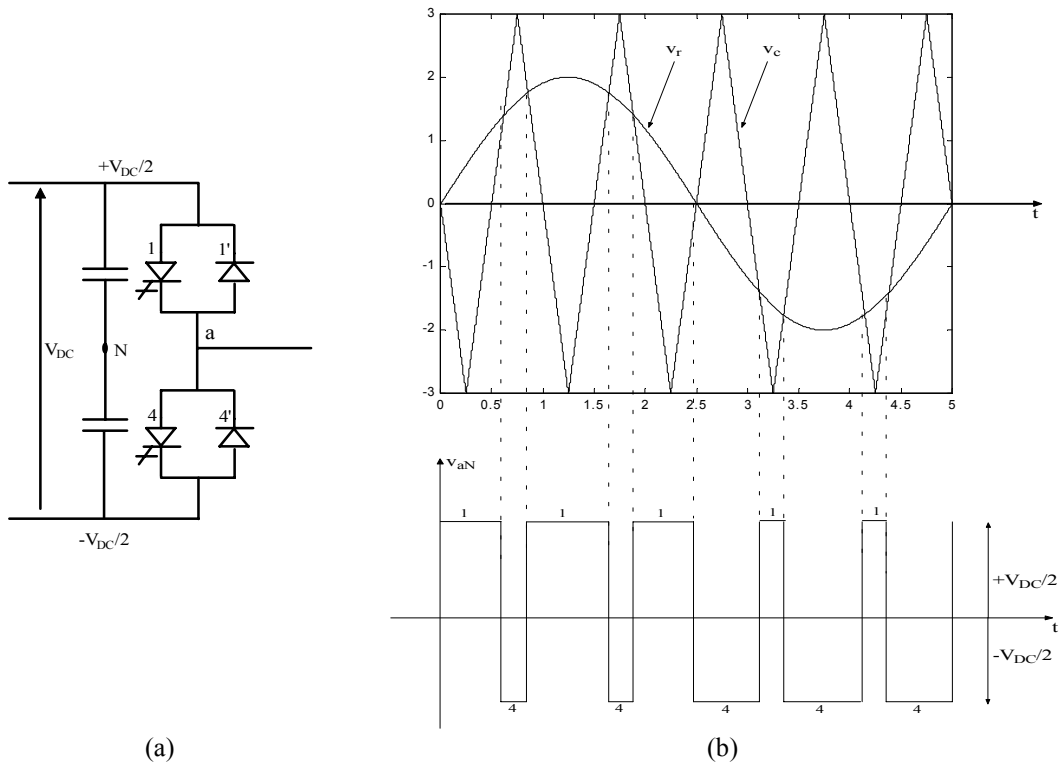


Fig. 3.2 PWM converter (a) A phase-leg (b) PWM waveforms

The fundamental frequency of the converter output voltage is determined by the frequency of the reference signal. Controlling the amplitude of the reference signal controls the width of the pulses. The amplitude modulation index is defined as ratio of A_r to A_c

$$m = \frac{A_r}{A_c} \quad (3.1)$$

For $m \leq 1$ the peak magnitude of the fundamental frequency component of the converter output voltage can be expressed as

$$V = m \frac{V_{DC}}{2} \quad (3.2)$$

3.2 UPFC Description and Operation

The UPFC is a device placed between two busses referred to as the UPFC sending bus and the UPFC receiving bus. It consists of two Voltage-Sourced Converters (VSCs) with a common DC link. For the fundamental frequency model, the VSCs are replaced by two controlled voltage sources as shown in Fig. 3.3 [22]. The voltage source at the sending bus is connected in shunt and will therefore be called the shunt voltage source. The second source,

the series voltage source, is placed between the sending and the receiving busses. The UPFC is placed on high-voltage transmission lines. This arrangement requires step-down transformers in order to allow the use of power electronics devices for the UPFC.

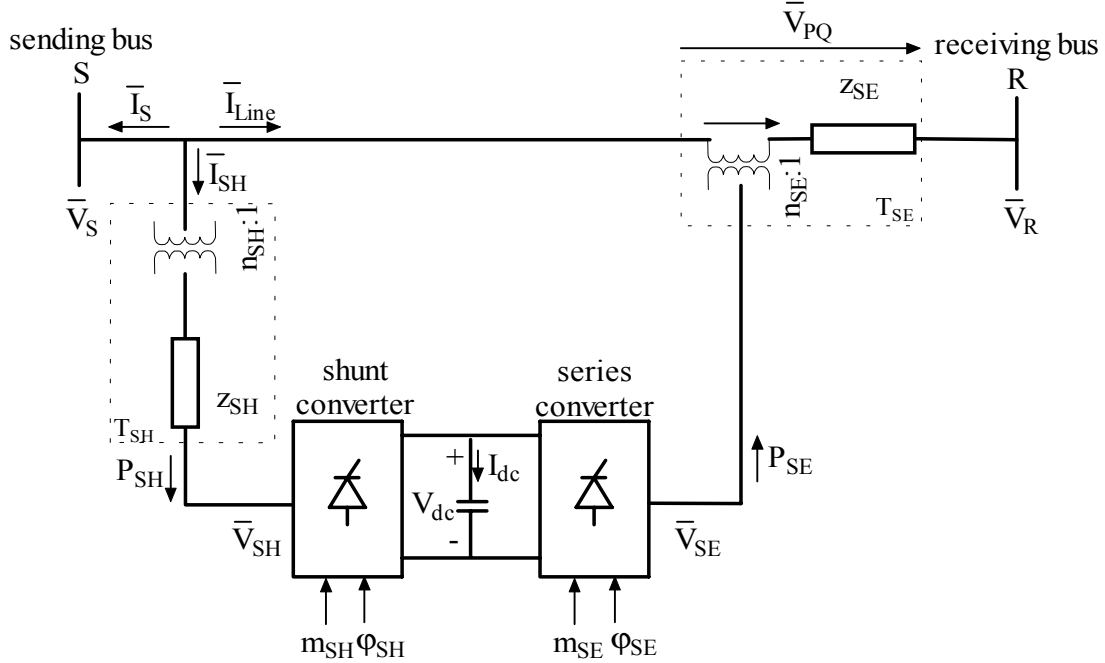


Fig. 3.3 Fundamental frequency model of UPFC

Applying the Pulse Width Modulation (PWM) technique to the two VSCs the following equations for magnitudes of shunt and series injected voltages are obtained

$$\begin{aligned} V_{SH} &= m_{SH} \frac{V_{DC}}{2\sqrt{2}n_{SH} V_B} \\ V_{SE} &= m_{SE} \frac{V_{DC}}{2\sqrt{2}n_{SE} V_B} \end{aligned} \quad (3.3)$$

where:

- m_{SH} – amplitude modulation index of the shunt VSC control signal
- m_{SE} – amplitude modulation index of the series VSC control signal
- n_{SH} – shunt transformer turn ratio
- n_{SE} – series transformer turn ratio
- V_B – the system side base voltage in kV
- V_{DC} – DC link voltage in kV

The phase angles of \bar{V}_{SH} and \bar{V}_{SE} are

$$\begin{aligned}\delta_{SH} &= \angle(\delta_s - \varphi_{SH}) \\ \delta_{SE} &= \angle(\delta_s - \varphi_{SE})\end{aligned}\quad (3.4)$$

where:

- φ_{SH} – firing angle of the shunt VSC with respect to the phase angle of the sending bus voltage
- φ_{SE} – firing angle of the series VSC with respect to the phase angle of the sending bus voltage

The series converter injects an AC voltage $\bar{V}_{SE} = V_{SE} \angle(\delta_s - \varphi_{SE})$ in series with the transmission line. Series voltage magnitude V_{SE} and its phase angle φ_{SE} with respect to the sending bus are controllable in the range of $0 \leq V_{SE} \leq V_{SEmax}$ and $0 \leq \varphi_{SE} \leq 360^\circ$. The shunt converter injects controllable shunt voltage such that the real component of the current in the shunt branch balance the real power demanded by the series converter. The real power can flow freely in either direction between the AC terminals. On the other hand the reactive power cannot flow through the DC link. It is absorbed or generated locally by each converter. The shunt converter operated to exchange the reactive power with the AC system provides the possibility of independent shunt compensation for the line. If the shunt injected voltage is regulated to produce a shunt reactive current component that will keep the sending bus voltage at its pre-specified value, then the shunt converter is operated in *the Automatic Voltage Control Mode*. Shunt converter can also be operated in *the Var Control Mode*. In this case shunt reactive current is produced to meet the desired inductive or capacitive Var request.

3.3 Power Flow on a Transmission Line

In this section a power flow on a transmission line between two buses S and R (line sending and receiving buses), Fig. 3.4, will be briefly reviewed. For the system shown in Fig. 3.4 the RMS phasor voltages of the sending and receiving buses are $\bar{V}_s = V_s \angle \delta_s$ and $\bar{V}_r = V_r \angle \delta_r$, \bar{I}_{Line} is phasor current on the line, R and X are resistance and reactance of the line respectively.

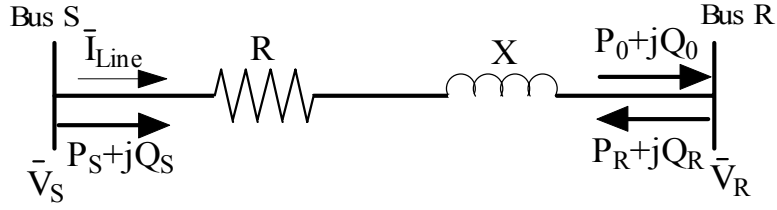


Fig. 3.4 Transmission line

The complex power injected into the sending bus is given by

$$S_S = P_S + jQ_S = \bar{V}_S \bar{I}_{Line}^* \quad (3.5)$$

where P_S and Q_S are the real and reactive powers injected into the sending bus, * denotes conjugate complex value.

Using Ohm's law line current can be written as

$$\bar{I}_{Line} = \frac{\bar{V}_S - \bar{V}_R}{R + jX} = (\bar{V}_S - \bar{V}_R)(G + jB) \quad (3.6)$$

where $G = \frac{R}{R^2 + X^2}$ is line conductance and $B = -\frac{X}{R^2 + X^2}$ is line susceptance.

Taking the complex conjugate of (3.5) and using (3.6) the following expression can be obtained

$$S_S^* = P_S - jQ_S = (V_S^2 - \bar{V}_S^* \bar{V}_R)(G + jB) \quad (3.7)$$

Using Euler's identity, which states that $V \angle -\delta = V(\cos \delta - j \sin \delta)$, to write

$$\bar{V}_S^* \bar{V}_R = V_S \angle -\delta_S V_R \angle \delta_R = V_S V_R \angle (-\delta_S - \delta_R) = V_S V_R (\cos(\delta_S - \delta_R) - j \sin(\delta_S - \delta_R)) \quad (3.8)$$

and separating real and imaginary parts of (3.7) the following expressions for the real and reactive powers injected into the sending bus are obtained

$$\begin{aligned} P_S &= V_S^2 G - V_S V_R G \cos(\delta_S - \delta_R) - V_S V_R B \sin(\delta_S - \delta_R) \\ Q_S &= -V_S^2 B - V_S V_R G \sin(\delta_S - \delta_R) + V_S V_R B \cos(\delta_S - \delta_R) \end{aligned} \quad (3.9)$$

Similarly, the real and reactive powers received at the receiving bus are

$$\begin{aligned} P_0 &= -P_R = -V_R^2 G + V_S V_R G \cos(\delta_S - \delta_R) - V_S V_R B \sin(\delta_S - \delta_R) \\ Q_0 &= -Q_R = V_R^2 B - V_S V_R G \sin(\delta_S - \delta_R) - V_S V_R B \cos(\delta_S - \delta_R) \end{aligned} \quad (3.10)$$

In the above equations P_R and Q_R represent the real and reactive powers injected into the receiving bus.

The power losses on the line are given by

$$\begin{aligned} P_L &= P_S - (-P_R) = (V_S^2 + V_R^2)G - 2V_S V_R G \cos(\delta_S - \delta_R) \\ Q_L &= Q_S - (-Q_R) = -(V_S^2 + V_R^2)B + 2V_S V_R B \cos(\delta_S - \delta_R) \end{aligned} \quad (3.11)$$

For typical transmission line $X \gg R$. Therefore, the conductance G is usually neglected and susceptance B is replaced by $B = -\frac{1}{X}$. Using these approximations, the expression for

real power transmitted over the line from the sending to the receiving bus becomes

$$P_S = -P_R = -V_S V_R B \sin(\delta_S - \delta_R) = \frac{V_S V_R}{X} B \sin(\delta_S - \delta_R) = \frac{V_S V_R}{X} B \sin \delta = P_0(\delta) \quad (3.12)$$

The angle $\delta = \delta_S - \delta_R$ is called the power angle.

The reactive power sent to the line from the sending bus and received from the line at the receiving bus are

$$\begin{aligned} Q_S &= -V_S^2 B + V_S V_R B \cos(\delta_S - \delta_R) = \frac{V_S^2 - V_S V_R \cos(\delta_S - \delta_R)}{X} \\ -Q_R &= V_R^2 B - V_S V_R B \cos(\delta_S - \delta_R) = \frac{-V_R^2 + V_S V_R \cos(\delta_S - \delta_R)}{X} = Q_0(\delta) \end{aligned} \quad (3.13)$$

It can be seen from equation (3.12) that the amount of the real power transmitted over the line can be increased by

- increasing the magnitude of the voltages at either end, i.e. voltage support
- reducing the line reactance, i.e. line compensation
- increasing the power angle, i.e. phase shift.

Power flow can be reversed by changing the sign of the power angle, i.e. a positive power angle corresponds to a power flow from the sending to the receiving bus, while a negative power angle corresponds to a power flow from the receiving to the sending bus.

Hence, the four parameters that affect real and reactive power flow are V_S , V_R , X and δ . To further understand this relationship, equations (3.12) and (3.13) can be combined as

$$(P_0(\delta))^2 + (Q_0(\delta) + \frac{V_R^2}{X})^2 = (\frac{V_S V_R}{X})^2 \quad (3.14)$$

This equation represents a circle centered at $(0, -\frac{V_R^2}{X})$, and with a radius of $\frac{V_S V_R}{X}$. It relates the real and reactive power received at the receiving bus to the four parameters V_S , V_R , δ , and X . To see for example how the power angle δ affects P_0 and Q_0 , assume that

$V_S = V_R = V$ and $\frac{V^2}{X} = 1$. The P-Q locus for this case is shown in Fig. 3.5 [3]. For a specific power angle δ , values of P_0 and Q_0 can be found, i.e. if $\delta = \frac{\pi}{4}$ (point A on the circle) then $P_{0A} = 0.707$ and $Q_{0A} = -0.293$. Note that the power angle δ might be constrained by stability limits.

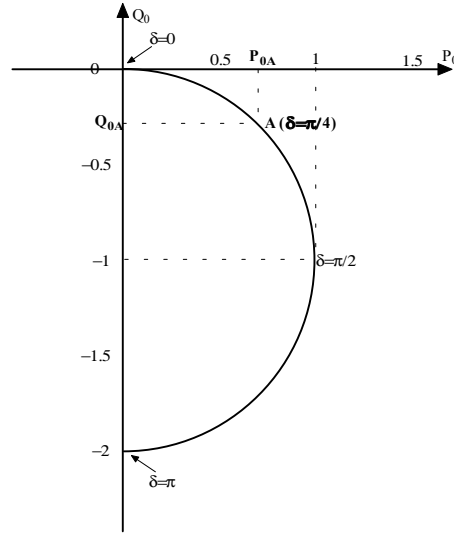


Fig. 3.5 P-Q locus of the uncompensated system

Similarly, the relationship between the real and reactive powers sent to the line from the sending bus can be expressed as

$$(P_S(\delta))^2 + (Q_S(\delta) - \frac{V_S^2}{X})^2 = (\frac{V_S V_R}{X})^2 \quad (3.15)$$

The average reactive power flow is defined as

$$Q_{SR} = \frac{Q_S - Q_R}{2} = -\frac{V_S^2 - V_R^2}{2} B = \frac{V_S^2 - V_R^2}{2X} \quad (3.16)$$

It can be seen from (3.16) that both voltage magnitudes and line reactance will affect the reactive power flow. If both voltage magnitudes are the same, i.e. flat voltage profile, each bus will send half of the reactive power absorbed by the line. The power flow is from the sending to the receiving bus if $V_S > V_R$.

3.4 Series Converter: Four Modes of Operation

As mentioned before the UPFC can control, independently or simultaneously, all parameters that affect power flow on the transmission line. This is illustrated in the phasor diagrams shown in Fig. 3.6 [3].

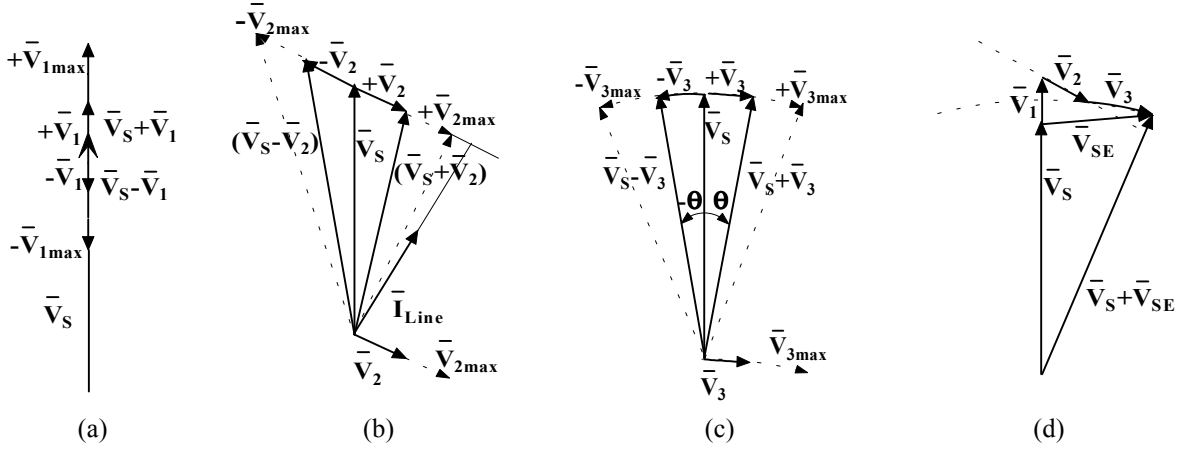


Fig. 3.6 Phasor diagrams

Voltage regulation is shown in Fig. 3.6(a). The magnitude of the sending bus voltage \bar{V}_s is increased (or decreased) by injecting a voltage \bar{V}_1 , of maximum magnitude V_{1max} , in phase (or out of phase) with \bar{V}_s . Similar regulation can be accomplished with a transformer tap changer.

Series reactive compensation is shown in Fig. 3.6(b). It is obtained by injecting a voltage \bar{V}_2 , of maximum magnitude V_{2max} , orthogonal to the line current \bar{I}_{Line} . The effective voltage drop across the line impedance X is decreased (or increased) if the voltage \bar{V}_2 lags the current \bar{I}_{Line} by 90° (or \bar{V}_2 leads current \bar{I}_{Line} by 90°).

A desired phase shift is achieved by injecting a voltage that shifts the phase angle of \bar{V}_3 , of maximum magnitude V_{3max} , that shifts \bar{V}_s by $\pm\theta$ while keeping its magnitude constant as shown in Fig. 3.6(c).

Simultaneous control of terminal voltage, line impedance and phase angle allows the UPFC to perform multifunctional power flow control. The magnitude and the phase angle of the series injected voltage $\bar{V}_{SE} = \bar{V}_1 + \bar{V}_2 + \bar{V}_3$, shown in Fig. 3.6(d), are selected in such a

way as to produce a line current that will result in the desired real and reactive power flow on the transmission line.

Therefore, the UPFC series converter can be operated in four modes:

- direct voltage injection mode
- line impedance compensation mode
- phase angle regulation mode
- automatic power flow control mode.

3.5 Automatic Power Control Mode

The automatic power control mode cannot be achieved with conventional compensators. In order to show how line power flow can be affected by the UPFC operated in the automatic power flow mode UPFC is placed at the beginning of the transmission line connecting buses S and R as shown in Fig. 3.7 [3]. Line conductance was neglected. UPFC is represented by two ideal voltage sources of controllable magnitude and phase angle. Bus S and fictitious bus S₁ shown in Fig. 3.7 represent UPFC sending and receiving buses respectively.

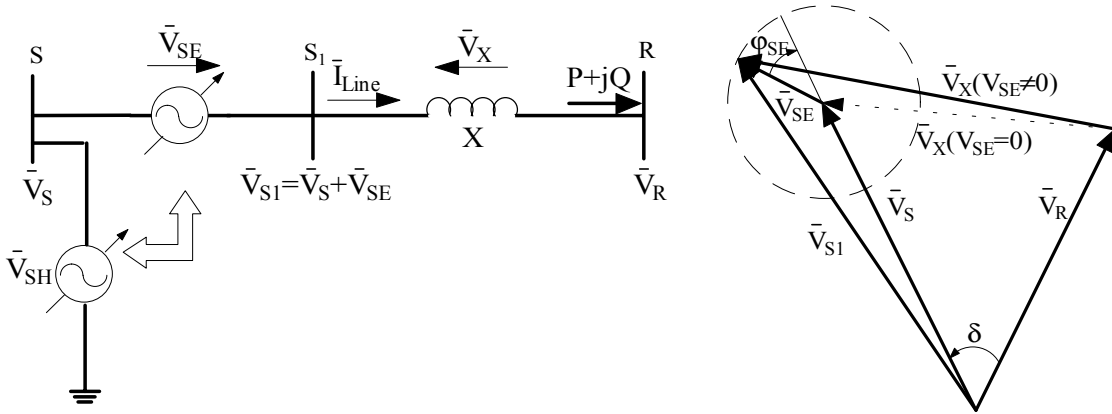


Fig. 3.7 Transmission line with UPFC

In this case, the complex power received at the receiving end of the line is given by

$$S = \bar{V}_R \bar{I}_{Line}^* = \bar{V}_R \left(\frac{\bar{V}_S + \bar{V}_{SE} - \bar{V}_R}{jX} \right)^* \quad (3.17)$$

where $\bar{V}_{SE} = V_{SE} \angle (\delta_S - \phi_{SE})$.

The complex conjugate of this complex power is

$$S^* = P - jQ = \bar{V}_R^* \left(\frac{\bar{V}_S + \bar{V}_{SE} - \bar{V}_R}{jX} \right) \quad (3.18)$$

Performing simple mathematical manipulations and separating real and imaginary components of (3.18) the following expressions for real and the reactive powers received at the receiving end of the line are

$$\begin{aligned} P &= \frac{V_S V_R}{X} \sin \delta + \frac{V_R V_{SE}}{X} \sin(\delta - \varphi_{SE}) = P_0(\delta) + P_{SE}(\delta, \varphi_{SE}) \\ Q &= -\frac{V_R^2}{X} + \frac{V_S V_R}{X} \cos \delta + \frac{V_R V_{SE}}{X} \cos(\delta - \varphi_{SE}) = Q_0(\delta) + Q_{SE}(\delta, \varphi_{SE}) \end{aligned} \quad (3.19)$$

For $V_{SE}=0$ the above equations are identical to equation (3.12) and the second equation of (3.13) that represent the real and reactive powers of the uncompensated system.

It was stated before that the UPFC series voltage magnitude can be controlled between 0 and V_{SEmax} , and its phase angle can be controlled between 0 and 360 degrees at any power angle δ . It can be seen from (3.19) that the real and reactive power received at bus R for the system with the UPFC installed can be controlled between

$$\begin{aligned} P_{\min}(\delta) &\leq P \leq P_{\max}(\delta) \\ Q_{\min}(\delta) &\leq Q \leq Q_{\max}(\delta) \end{aligned} \quad (3.20)$$

$$\begin{aligned} \text{where: } P_{\min}(\delta) &= P_0(\delta) - \frac{V_R V_{SEmax}}{X} & P_{\max}(\delta) &= P_0(\delta) + \frac{V_R V_{SEmax}}{X} \\ Q_{\min}(\delta) &= Q_0(\delta) - \frac{V_R V_{SEmax}}{X} & Q_{\max}(\delta) &= Q_0(\delta) + \frac{V_R V_{SEmax}}{X} \end{aligned}$$

Rotation of the series injected voltage phasor with RMS value of V_{SEmax} from 0 to 360° allows the real and the reactive power flow to be controlled within the boundary circle with a radius of $\frac{V_R V_{SEmax}}{X}$ and a center at $(P_0(\delta), Q_0(\delta))$. This circle is defined by the following equation

$$(P(\delta, \varphi_{SE}) - P_0(\delta))^2 + (Q(\delta, \varphi_{SE}) - Q_0(\delta))^2 = \left(\frac{V_R V_{SEmax}}{X} \right)^2 \quad (3.21)$$

Fig. 3.8 shows plots of the reactive power Q demanded at the receiving bus versus the transmitted real power P as a function of the series voltage magnitude V_{SE} and phase angle

ϕ_{SE} at four different power angles δ i.e. $\delta=0^\circ, 30^\circ, 60^\circ$ and 90° , with $V_S = V_R = V$, $\frac{V^2}{X}=1$ and $\frac{V_R V_{SEmax}}{X} = 0.5$ [3]. The capability of UPFC to independently control real and reactive power flow at any transmission angle is clearly illustrated in Fig. 3.8.

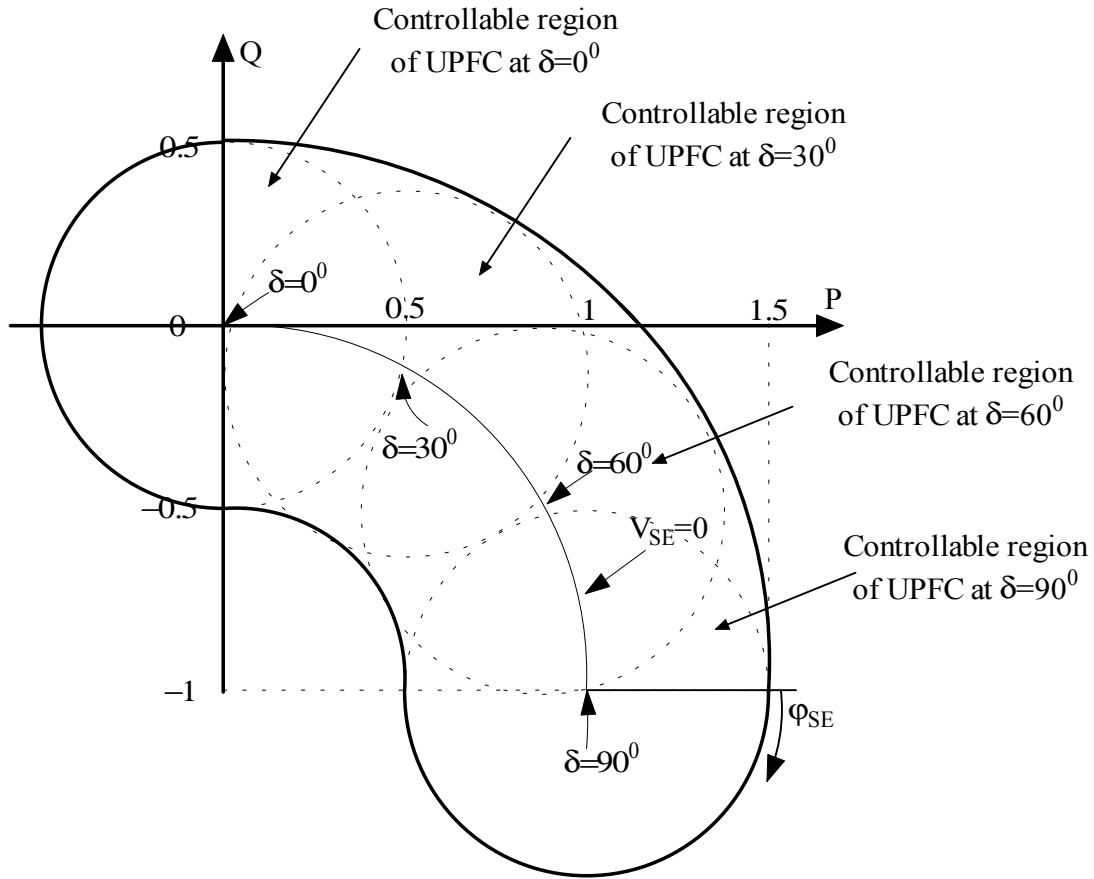


Fig. 3.8 P-Q relationship for simple two-bus system with a UPFC at $\delta=0^\circ, 30^\circ, 60^\circ$ and 90°

3.6 Comparison of the UPFC to Series Compensators and Phase Angle Regulators

In order to show superiority of UPFC over controlled series compensators and phase angle regulators when it comes to power flow control a comparison between their power flow control characteristics is briefly discussed in this section [3]. The power flow characteristics of controlled series compensators and phase angle regulators are analyzed using systems shown in Fig. 3.9 and Fig. 3.10.

Controlled series compensators: Thyristor-Switched Series Capacitor (TSSC), Gate-Controlled Series Capacitor (GCSC), Thyristor-Controlled Series Capacitor (TCSC) and Static Synchronous Series Compensator (SSSC) inject a series compensating voltage orthogonal to the line current. TSSC and GCSC provide controllable series capacitive impedance in the range of $0 < X < X_{Cmax}$. Therefore, they inject voltage with 90 degree lagging (capacitive) relationship with respect to the line current. TCSC and SSSC inject voltage V_q of maximum magnitude V_{qmax} that can have both 90 degree lagging (capacitive), or 90 degree leading (inductive) relationship with respect to the line current providing capacitive or inductive compensation.

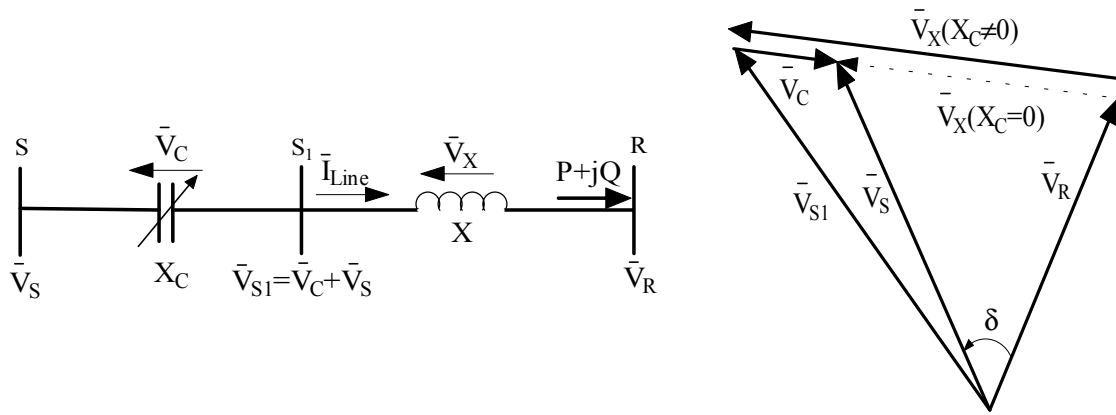


Fig. 3.9 Transmission line with controlled series capacitive compensation

The real and the reactive powers received at the receiving end of the line for the system with controlled series compensators are given by

$$P = \frac{V_S V_R}{X - X_q} \sin \delta$$

$$Q = \frac{V_S V_R}{X - X_q} \cos \delta - \frac{V_R^2}{X - X_q} \quad (3.22)$$

where $0 < X_q < X_{Cmax}$ for TSSC and GCSC and $-\frac{V_{qmax}}{I_{Line}} < X_q < \frac{V_{qmax}}{I_{Line}}$ for TCSC and SSSC.

Equation (3.22) is of the same form as equations for $P_0(\delta)$ and $Q_0(\delta)$ that describe the uncompensated system. Therefore, for a given value of X_q , the relationship between the real and reactive powers is a circle similar to that shown in Fig. 3.5. Each point on that circle defines P and Q values for a specific power angle δ . P-Q locus obtained with $X_q = 0$

represents the lower boundary curve and P-Q locus obtained with $X_q=X_{Cmax}$ represents the upper boundary curve for TSSC and GCSC. These two curves are shown in Fig. 3.11 as $(P-Q)_{Xq=0}$ and $(P-Q)_{Xqmax}$ respectively. Similarly, the lower and the upper boundary curves for SSSC and TCSC are obtained with $X_q = -\frac{V_{qmax}}{I}$ and $X_q = \frac{V_{qmax}}{I}$. They are identified as $(P-Q)_{-Vqmax}$ and $(P-Q)_{Vqmax}$ characteristics.

Ideal Phase Angle Regulator (PAR) can change the phase angle between buses where the insertion transformer is connected in the range $-\theta_{max} < \theta < \theta_{max}$ while keeping the magnitude of the phase-shifted voltage unchanged as shown in Fig. 3.10.

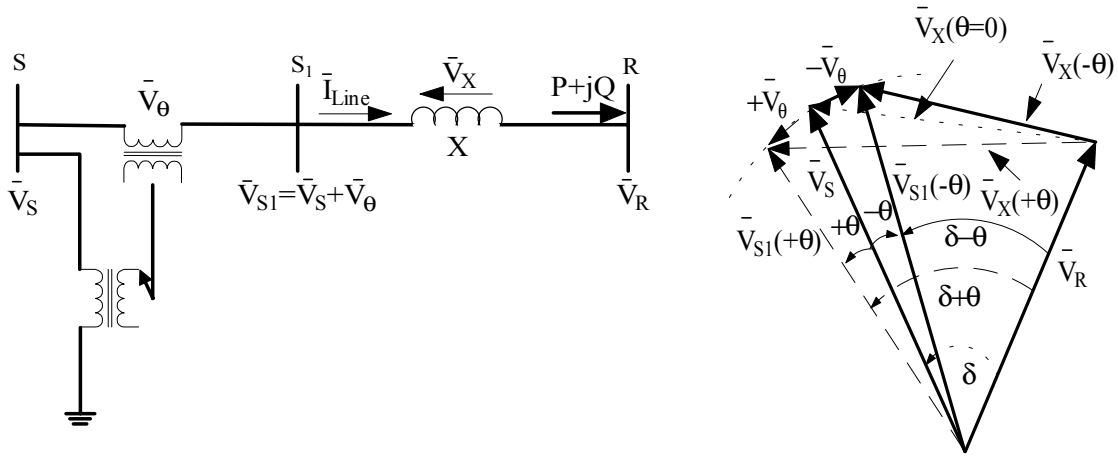


Fig. 3.10 Transmission line controlled with a Phase Angle Regulator

The real and reactive power attainable with PAR are given by

$$\begin{aligned}
 P &= \frac{V_S V_R}{X} \sin(\delta \pm \theta) \\
 Q &= \frac{V_S V_R}{X} \cos(\delta \pm \theta) - \frac{V_R^2}{X}
 \end{aligned}
 \tag{3.23}$$

Bold lines in Fig. 3.11 represent controllable region of TSSC/GCSC and solid hairline lines represent controllable region of SSSC/TCSC at $\delta=0^0, 30^0, 60^0$ and 90^0 . Fig. 3.12 shows attainable P and Q values with PAR at $\delta=0^0, 30^0, 60^0$ and 90^0 with θ varied in the range of $-30^0 < \theta < 30^0$. Both figures are plotted for $V_S = V_R = V$ and $\frac{V^2}{X} = 1$. The UPFC circular control region with radius of 0.5 is shown in both Fig. 3.11 and Fig. 3.12 [3].

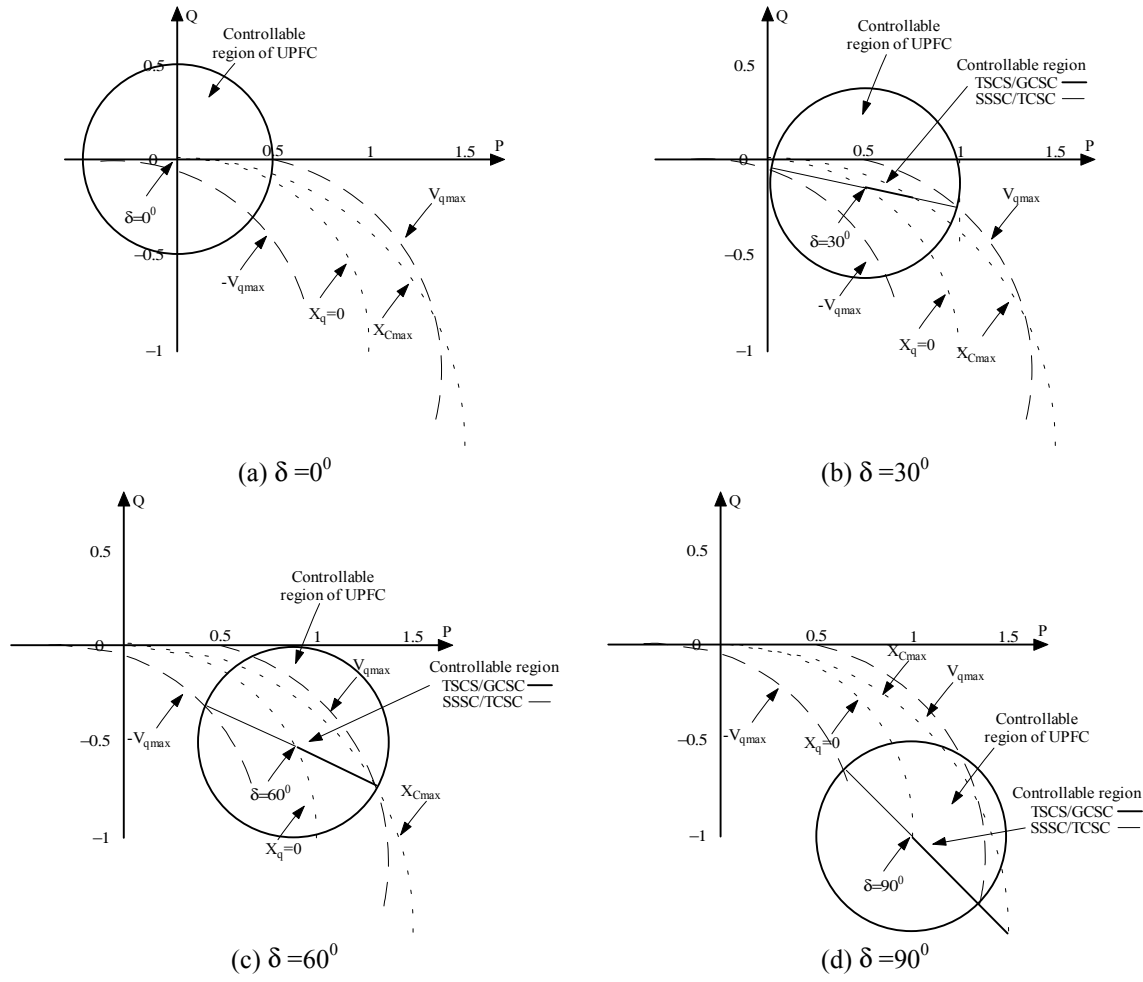


Fig. 3.11 P-Q relationship attainable with transmission line controlled with series compensators and a UPFC at (a) $\delta=0^\circ$, (b) 30° , (c) 60° and (d) 90°

Maximum increase in the transmitted real power that can be obtained with the controllable series compensators depends on the power angle δ . The bigger the power angle, the bigger the maximum increase in the transmitted real power. Controllable series compensators do not allow independent control of the reactive power demanded at the receiving end. The reactive power is determined by the transmitted real power. The PAR can change the real power by adjusting the phase shift angle θ . It cannot increase the maximum transmittable power. It also does not allow independent control of the reactive power. The UPFC can control both real and reactive power independently. It allows wider range (independent of power angle δ) for power control.

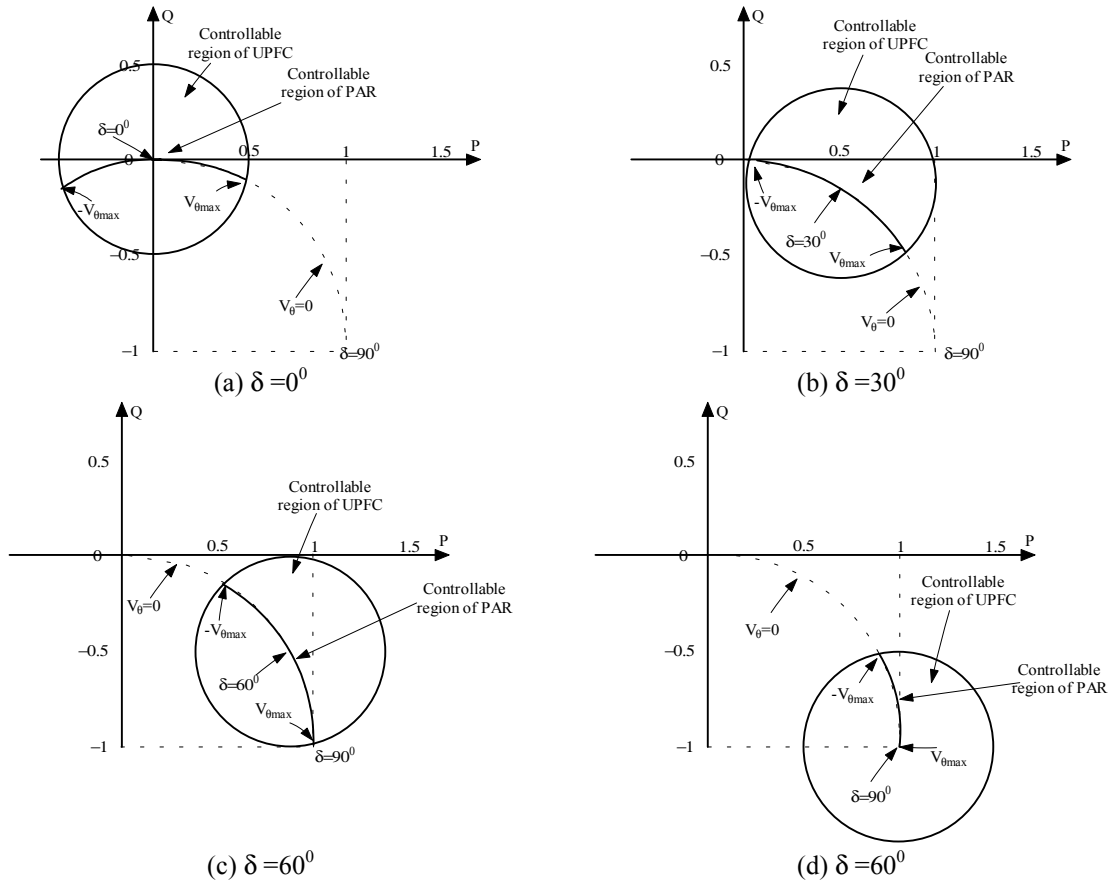


Fig. 3.12 P-Q relationship attainable with transmission line controlled with a PAR and a UPFC at (a) $\delta=0^\circ$, (b) 30° , (c) 60° and (d) 90°

Chapter 4

UPFC MODELING AND INTERFACING

In order to simulate a power system that contains a UPFC, the UPFC needs to be modeled for steady-state and dynamic operations. The UPFC model needs to be interfaced with the power system model. Hence, in this chapter modeling and interfacing of the UPFC with the power network are described. Linearized model of the power network with UPFC, useful for small signal analysis and damping controller design, will also be derived.

4.1 UPFC Load Flow (LF) Model

For steady-state operation, the DC link voltage remains constant at its pre-specified value. In the case of a lossless DC link the real power supplied to the shunt converter $P_{SH} = \text{Re}(\bar{V}_{SH} \bar{I}_{SH}^*)$ satisfies the real power demanded by the series converter

$$P_{SH} = \text{Re}(\bar{V}_{SE} \bar{I}_{Line}^*)$$

$$P_{SH} = P_{SE} \quad (4.1)$$

The LF model discussed here assumes that the UPFC is operated to keep (i) real and reactive power flows at the receiving bus and (ii) sending bus voltage magnitude at their pre-specified values [10]. In this case UPFC can be replaced by an “equivalent generator” at the sending bus (PV-type bus using load flow terminology) and a “load” at the receiving bus (PQ-type bus) as shown in Fig. 4.1.

To obtain the LF solution for the power network with the UPFC an iterative procedure is needed. Power demanded at the receiving bus is set to the desired real and reactive powers at that bus. The real power injected into a PV bus for conventional LF algorithm is kept constant and the reactive power is adjusted in order to achieve the pre-specified voltage magnitude. With UPFC, the real power injected into the sending bus is not known exactly. This real power injection is initialized to the value that equals the pre-specified real power flow at the receiving bus. During the iterative procedure the real power adjustment is done

in order to cover the losses of the shunt and series impedances and to force the sum of converters' interaction to become zero.

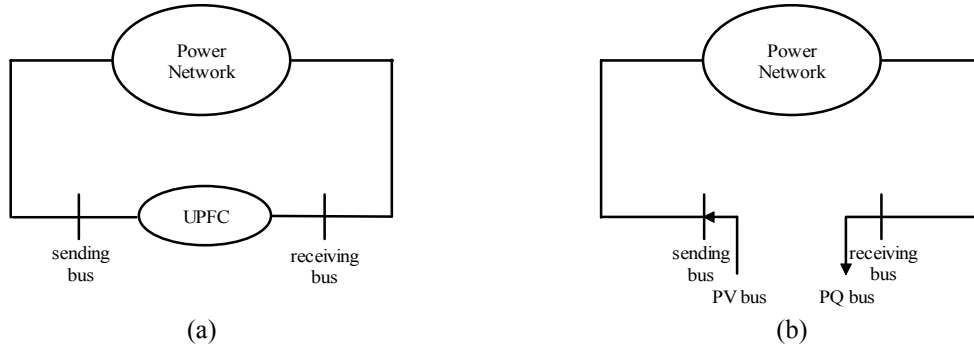


Fig. 4.1 Power network with a UPFC included (a) schematic (b) Load Flow Model

The algorithm in its graphical form is given in Fig. 4.2.

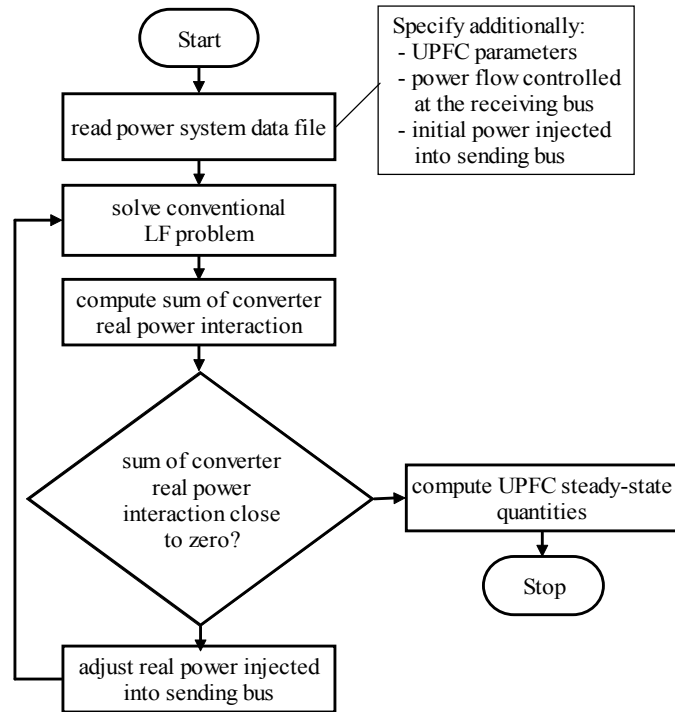


Fig. 4.2 Load flow algorithm

Necessary computations are shown bellow.

The complex power injected into sending bus is

$$\bar{S}_s = \bar{V}_s \bar{I}_s^* \quad (4.2)$$

Using the voltages and currents as assigned in Fig. 3.3

$$\begin{aligned}
\bar{V}_S &= \bar{V}_{SH} + \bar{V}_{Z_{SH}} \\
\bar{V}_{Z_{SH}} &= \bar{I}_{SH} Z_{SH} \\
\bar{I}_S &= -\bar{I}_{SH} - \bar{I}_{Line}
\end{aligned} \tag{4.3}$$

results in

$$\begin{aligned}
S_S &= (\bar{V}_{SH} + \bar{V}_{Z_{SH}})(-\bar{I}_{SH} - \bar{I}_{Line})^* = \\
&= -\bar{V}_{SH} \bar{I}_{SH}^* - \bar{V}_{Z_{SH}} \bar{I}_{SH}^* - \bar{V}_{SH} \bar{I}_{Line}^* - \bar{V}_{Z_{SH}} \bar{I}_{Line}^* = \\
&= -\bar{V}_{SH} \bar{I}_{SH}^* - Z_{SH} I_{SH}^2 - \bar{V}_{SH} \bar{I}_{Line}^* - Z_{SH} \bar{I}_{SH} \bar{I}_{Line}^*
\end{aligned} \tag{4.4}$$

Computing the line current by using the bus voltages and the power flow at the receiving bus as given by the load flow solution

$$\bar{I}_{Line} = -\frac{S_R^*}{\bar{V}_R} \tag{4.5}$$

allows to compute the series injected voltage and the series converter interaction with the power system

$$\begin{aligned}
\bar{V}_{SE} &= \bar{I}_{Line} Z_{SE} + \bar{V}_R - \bar{V}_S \\
P_{SE} &= \text{Re}(\bar{V}_{SE} \bar{I}_{Line}^*)
\end{aligned} \tag{4.6}$$

Taking the real part of (4.4) and using (4.1), the new injected real power at the sending bus becomes

$$P_S = -P_{SE} + \text{Re}(-Z_{SH} I_{SH}^2 - \bar{V}_{SH} \bar{I}_{Line}^* - Z_{SH} \bar{I}_{SH} \bar{I}_{Line}^*) \tag{4.7}$$

It can be seen from Fig. 4.2 that UPFC control parameters are computed directly after a conventional LF solution satisfying (4.1) is found. Neglecting transformer losses and initializing the real power injected into sending bus to the real power flow controlled on the line the convergence of the proposed LF algorithm is obtained within one step.

4.2 UPFC Dynamic Model

For transient stability studies, the DC link dynamics have to be taken into account and (4.1) can no longer be applied. The DC link capacitor will exchange energy with the system and its voltage will vary.

The power frequency dynamic model can be described by the following equation [20], [22]

$$CV_{DC} \frac{dV_{DC}}{dt} = (P_{SH} - P_{SE})S_B \quad (4.8)$$

Note that in the above equation the DC variables are expressed in MKSA units while the ac system variables are expressed as per unit quantities. S_B is the system side base power.

4.3 Interfacing the UPFC with the Power Network

The interface of the UPFC with the power network is shown in Fig. 4.3 [22]. In order to get the network solution (bus voltages and the currents) an iterative approach is used. The UPFC sending and receiving bus voltages \bar{V}_S and \bar{V}_R can be expressed as a function of generator internal voltages \bar{E}_G and the UPFC injection voltages \bar{V}_{SH} and \bar{V}_{SE} (equation (4.15)). Control output and (3.3) determine the UPFC injection voltage magnitudes V_{SH} and V_{SE} . However, the phase angles of the injected voltages, δ_{SH} and δ_{SE} , are unknown since they depend on the phase angle of the sending bus voltage, δ_S , which is the result of the network solution. Graphical form of the algorithm for interfacing the UPFC with the power network is shown in Fig. 4.4.

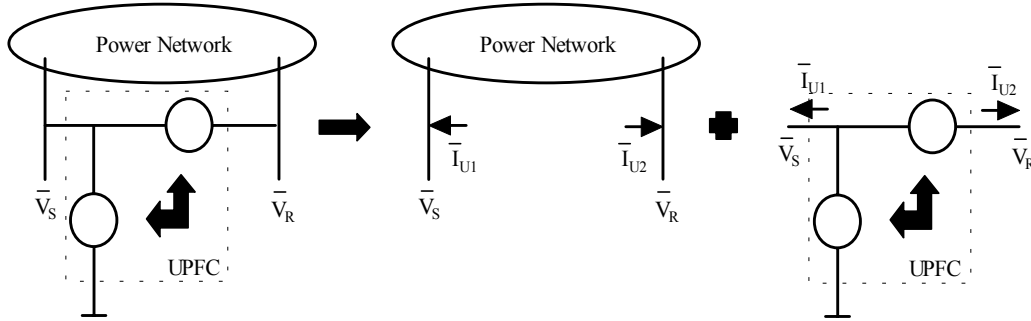


Fig. 4.3 Interface of the UPFC with power network

Necessary computations are shown below.

Reducing the bus admittance matrix to generator internal buses and UPFC terminal buses the following equation can be written

$$\begin{bmatrix} Y_{GG} & Y_{GU} \\ Y_{UG} & Y_{UU} \end{bmatrix} \begin{bmatrix} \bar{E}_G \\ \bar{V}_U \end{bmatrix} = \begin{bmatrix} \bar{I}_G \\ \bar{I}_U \end{bmatrix} \quad (4.9)$$

where:

Y_{GG} - reduced admittance matrix connecting the generator current injection to the internal generator voltages

Y_{GU} - admittance matrix component which gives the generator currents due to the voltages at UPFC buses

Y_{UG} - admittance matrix component which gives UPFC currents in terms of the generator internal voltages

Y_{UU} - admittance matrix connecting UPFC currents to the voltages at UPFC buses

\bar{E}_G - vector of generator internal bus voltages

\bar{V}_U - vector of UPFC ac bus voltages

\bar{I}_G - vector of generator current injections

\bar{I}_U - vector of UPFC currents injected to the power network.

The second equation of (4.9) is of the form

$$\bar{I}_U = Y_{UG} \bar{E}_G + Y_{UU} \bar{V}_U \quad (4.10)$$

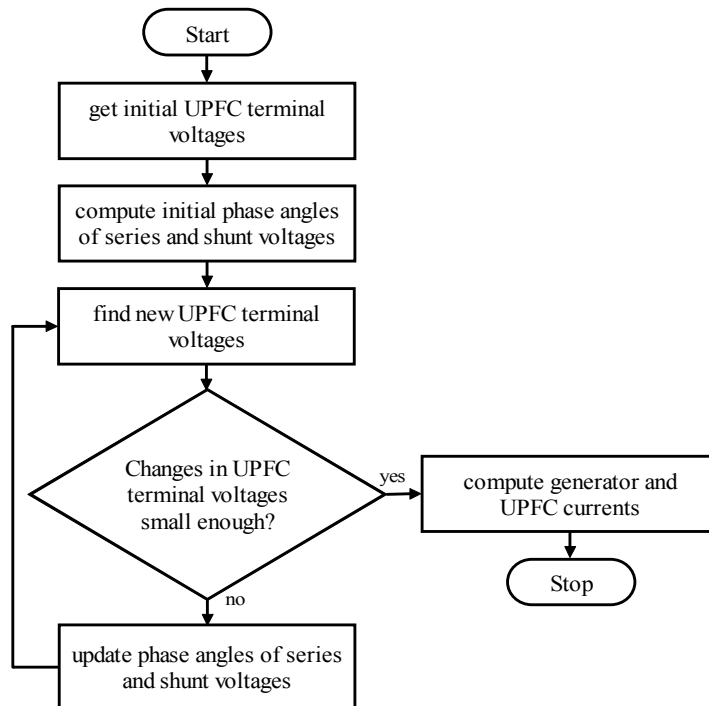


Fig. 4.4 Algorithm for interfacing the UPFC with the power network

Neglecting series and shunt transformer resistances the following equations can be written for the UPFC currents injected into the power network (see Fig. 3.3 and Fig. 4.3)

$$\bar{I}_{U1} = -\bar{I}_{SH} - \bar{I}_{Line} \quad (4.11)$$

$$\bar{I}_{U2} = \bar{I}_{Line}$$

$$\bar{I}_{SH} = \frac{\bar{V}_S - \bar{V}_{SH}}{jX_{SH}} \quad (4.12)$$

$$\bar{I}_{Line} = \frac{\bar{V}_{SE} + \bar{V}_S - \bar{V}_R}{jX_{SE}} \quad (4.13)$$

Combining the above equations the following equation can be obtained

$$\bar{I}_U = W_U \bar{V}_U + W_C \bar{V}_C \quad (4.14)$$

where:

$$W_C = \begin{bmatrix} \frac{1}{jX_{SH}} & -\frac{1}{jX_{SE}} \\ 0 & \frac{1}{jX_{SE}} \end{bmatrix} \quad W_U = \begin{bmatrix} -\frac{1}{jX_{SE}} & -\frac{1}{jX_{SH}} & \frac{1}{jX_{SE}} \\ \frac{1}{jX_{SE}} & & -\frac{1}{jX_{SE}} \end{bmatrix}$$

$$\bar{I}_U = \begin{bmatrix} \bar{I}_{U1} \\ \bar{I}_{U2} \end{bmatrix} \quad \bar{V}_U = \begin{bmatrix} \bar{V}_S \\ \bar{V}_R \end{bmatrix} \quad \bar{V}_C = \begin{bmatrix} \bar{V}_{SH} \\ \bar{V}_{SE} \end{bmatrix}$$

Equating (4.10) with (4.14) the following equation can be written

$$\bar{V}_U = (W_U - Y_{UU})^{-1} Y_{UG} \bar{E}_G - (W_U - Y_{UU})^{-1} W_C \bar{V}_C = L_G \bar{E}_G + L_C \bar{V}_C \quad (4.15)$$

Substitution of (4.15) into(4.9) gives

$$\begin{aligned} \bar{I}_G &= M_G \bar{E}_G + M_C \bar{V}_C \\ \bar{I}_U &= M_{G1} \bar{E}_G + M_{C1} \bar{V}_C \end{aligned} \quad (4.16)$$

where:

$$\begin{aligned} L_G &= (W_U - Y_{UU})^{-1} Y_{UG} & M_G &= Y_{GG} + Y_{GU} L_G & M_C &= Y_{GU} L_C \\ L_C &= -(W_U - Y_{UU})^{-1} W_C & M_{G1} &= Y_{UG} + Y_{UU} L_G & M_{C1} &= Y_{UU} L_C \end{aligned}$$

Defining

will be discussed in the following section. The results obtained using the two approaches will be compared and presented in the sixth chapter.

4.4.1 Basic terms and definitions

The state space representation of the linear continuous time system is given by

$$\begin{aligned}\dot{x}(t) &= Ax(t) + Bu(t) \\ y(t) &= Cx(t) + Du(t)\end{aligned}\tag{4.21}$$

where:

- $x(t)$ is the state of the system at time t
- $u(t)$ is the control input at time t
- $y(t)$ is the output of the system at time t
- A is the $n \times n$ plant matrix
- B is the $n \times m_u$ input matrix
- C is the $m_y \times n$ output matrix
- D is the $m_y \times m_u$ feed forward matrix

Eigenvalues of the matrix A , $\lambda_i = \alpha_i \pm j\beta_i$ $i=1..n$, are the roots of the characteristic polynomial

$$p(\lambda) = |\lambda I - A|\tag{4.22}$$

where:

I is an $n \times n$ identity matrix.

Complex eigenvalues always appear in pairs of complex conjugate numbers.

Definition 1 (stability in the sense of Lyapunov) [32]

The origin is a stable equilibrium point if for any given value $\epsilon > 0$ there exist a number $\delta(\epsilon, t_0)$ such that if $\|x(t_0)\| < \delta$ then the resultant motion $x(t)$ satisfies $\|x(t)\| < \epsilon$ for all $t > t_0$.

Definition 2 (asymptotical stability) [32]

The origin is an asymptotically stable equilibrium point if (i) it is stable and if in addition (ii) there exists a number $\delta'(t_0) > 0$ such that whenever $\|x(t_0)\| < \delta'(t_0)$ the resultant motion satisfies $\lim_{t \rightarrow \infty} \|x(t)\| = 0$.

Stability criteria for a linear system is given in Table 4.1 [32].

Table 4.1 Stability criteria for linear system

Unstable	If $\alpha_i > 0$ for any simple root or if $\alpha_i \geq 0$ for any repeated root
Stable i.s. Lyapunov	If $\alpha_i \leq 0$ for all simple roots and if $\alpha_i < 0$ for all repeated root
Asymptotically stable	If $\alpha_i < 0$ for all roots

4.4.2 Linearized Model Derivation

Consider n-machine power system. Using two axis model generator equations can be written as follows

$$\begin{aligned}
 \dot{E}'_d &= (T'_{q0})^{-1} (-E'_d + (X_q - X'_q)I_{gq}) \\
 \dot{E}'_q &= (T'_{d0})^{-1} (E_{fd} - E'_q + (X_d - X'_d)I_{gd}) \\
 \dot{\omega} &= \frac{1}{2} H^{-1} (T_m - T_e - D(\omega - 1)) \\
 \dot{\delta} &= \omega_B (\omega - 1) \\
 V_{gd} &= E'_d + X'_q I_{gq} \\
 V_{gq} &= E'_q - X'_d I_{gd} \\
 T_e &= V_{gq} I_{gq} + V_{gd} I_{gd}
 \end{aligned} \tag{4.23}$$

where:

$$\begin{aligned}
 E'_q &= [E'_{q1} \ E'_{q2} \ \dots \ E'_{qn}]^T & E'_d &= [E'_{d1} \ E'_{d2} \ \dots \ E'_{dn}]^T & E_{fd} &= [E_{fd1} \ E_{fd2} \ \dots \ E_{fdn}]^T \\
 V_{gq} &= [V_{gq1} \ V_{gq2} \ \dots \ V_{gqn}]^T & V_{gd} &= [V_{gd1} \ V_{gd2} \ \dots \ V_{gdn}]^T & I_{gq} &= [I_{gq1} \ I_{gq2} \ \dots \ I_{gqn}]^T \\
 I_{gd} &= [I_{gd1} \ I_{gd2} \ \dots \ I_{gdn}]^T & \delta &= [\delta_1 \ \delta_2 \ \dots \ \delta_n]^T & \omega &= [\omega_1 \ \omega_2 \ \dots \ \omega_n]^T \\
 H &= \text{diag}(H_i) & T'_{d0} &= \text{diag}(T'_{d0i}) & T'_{q0} &= \text{diag}(T'_{q0i}) \\
 D_{\text{damp}} &= \text{diag}(D_i) & X_q &= \text{diag}(x_{qi}) & X'_q &= \text{diag}(x'_{qi}) \\
 X_d &= \text{diag}(x_{di}) & X'_d &= \text{diag}(x'_{di})
 \end{aligned}$$

Linearizing (4.19) around the operating point and separating d and q components the following expressions for generator and UPFC currents can be obtained

$$\begin{aligned}
 \Delta I_{gd} &= D_1 \Delta E'_q + D_2 \Delta E'_d + D_3 \Delta \delta + D_4 \Delta m_{SH} + D_5 \Delta \phi_{SH} + D_6 \Delta m_{SE} + D_7 \Delta \phi_{SE} + D_8 \Delta V_{dc} \\
 \Delta I_{gq} &= Q_1 \Delta E'_q + Q_2 \Delta E'_d + Q_3 \Delta \delta + Q_4 \Delta m_{SH} + Q_5 \Delta \phi_{SH} + Q_6 \Delta m_{SE} + Q_7 \Delta \phi_{SE} + Q_8 \Delta V_{dc} \\
 \Delta I_{ud} &= D_{1u} \Delta E'_q + D_{2u} \Delta E'_d + D_{3u} \Delta \delta + D_{4u} \Delta m_{SH} + D_{5u} \Delta \phi_{SH} + D_{6u} \Delta m_{SE} + D_{7u} \Delta \phi_{SE} + D_{8u} \Delta V_{dc} \\
 \Delta I_{uq} &= Q_{1u} \Delta E'_q + Q_{2u} \Delta E'_d + Q_{3u} \Delta \delta + Q_{4u} \Delta m_{SH} + Q_{5u} \Delta \phi_{SH} + Q_{6u} \Delta m_{SE} + Q_{7u} \Delta \phi_{SE} + Q_{8u} \Delta V_{dc}
 \end{aligned} \tag{4.24}$$

where¹:

$$\begin{array}{cccc}
D_1 = \frac{\partial I_{gd}}{\partial E'_q} & D_2 = \frac{\partial I_{gd}}{\partial E'_d} & D_3 = \frac{\partial I_{gd}}{\partial \delta} & D_4 = \frac{\partial I_{gd}}{\partial m_{SH}} \\
D_5 = \frac{\partial I_{gd}}{\partial \varphi_{SH}} & D_6 = \frac{\partial I_{gd}}{\partial m_{SE}} & D_7 = \frac{\partial I_{gd}}{\partial \varphi_{SE}} & D_8 = \frac{\partial I_{gd}}{\partial V_{dc}} \\
Q_1 = \frac{\partial I_{gq}}{\partial E'_q} & Q_2 = \frac{\partial I_{gq}}{\partial E'_d} & Q_3 = \frac{\partial I_{gq}}{\partial \delta} & Q_4 = \frac{\partial I_{gq}}{\partial m_{SH}} \\
Q_5 = \frac{\partial I_{gq}}{\partial \varphi_{SH}} & Q_6 = \frac{\partial I_{gq}}{\partial m_{SE}} & Q_7 = \frac{\partial I_{gq}}{\partial \varphi_{SE}} & Q_8 = \frac{\partial I_{gq}}{\partial V_{dc}} \\
D_{1u} = \frac{\partial I_{ud}}{\partial E'_q} & D_{2u} = \frac{\partial I_{ud}}{\partial E'_d} & D_{3u} = \frac{\partial I_{ud}}{\partial \delta} & D_{4u} = \frac{\partial I_{ud}}{\partial m_{SH}} \\
D_{5u} = \frac{\partial I_{ud}}{\partial \varphi_{SH}} & D_{6u} = \frac{\partial I_{ud}}{\partial m_{SE}} & D_{7u} = \frac{\partial I_{ud}}{\partial \varphi_{SE}} & D_{8u} = \frac{\partial I_{ud}}{\partial V_{dc}} \\
Q_{1u} = \frac{\partial I_{uq}}{\partial E'_q} & Q_{2u} = \frac{\partial I_{uq}}{\partial E'_d} & Q_{3u} = \frac{\partial I_{uq}}{\partial \delta} & Q_{4u} = \frac{\partial I_{uq}}{\partial m_{SH}} \\
Q_{5u} = \frac{\partial I_{uq}}{\partial \varphi_{SH}} & Q_{6u} = \frac{\partial I_{uq}}{\partial m_{SE}} & Q_{7u} = \frac{\partial I_{uq}}{\partial \varphi_{SE}} & Q_{8u} = \frac{\partial I_{uq}}{\partial V_{dc}}
\end{array}$$

Linearizing (4.20) and substituting UPFC injected currents d and q components given by (4.24) the following equation can be written

$$\Delta V_{dc} = L_1 \Delta E'_q + L_2 \Delta E'_d + L_3 \Delta \delta + L_4 \Delta m_{SH} + L_5 \Delta \varphi_{SH} + L_6 \Delta m_{SE} + L_7 \Delta \varphi_{SE} + L_8 \Delta V_{dc} \quad (4.25)$$

where:

$$\begin{array}{ccc}
L_1 = K_1 Q_{u1} + K_2 D_{u1} & L_2 = K_1 Q_{u2} + K_2 D_{u2} & L_3 = K_1 Q_{u3} + K_2 D_{u3} \\
L_4 = K_1 Q_{u4} + K_2 D_{u4} + K_3 & L_5 = K_1 Q_{u5} + K_2 D_{u5} + K_4 & L_6 = K_1 Q_{u6} + K_2 D_{u6} + K_5 \\
L_7 = K_1 Q_{u7} + K_2 D_{u7} + K_6 & L_8 = K_1 Q_{u8} + K_2 D_{u8} & \\
K_1 = \frac{\partial V_{DC}}{\partial I_{ud}} & K_2 = \frac{\partial V_{DC}}{\partial I_{uq}} & K_3 = \frac{\partial V_{DC}}{\partial m_{SH}} \\
K_4 = \frac{\partial V_{DC}}{\partial \varphi_{SH}} & K_5 = \frac{\partial V_{DC}}{\partial m_{SE}} & K_6 = \frac{\partial V_{DC}}{\partial \varphi_{SE}}
\end{array}$$

Representing AVR by simplified first order transfer function ($\frac{E_{fdi}}{V_{ti}} = -\frac{K_{Ai}}{1+sT_{Ai}}$ $i = 1 \dots n$),

¹ D₁-D₈, Q₁-Q₈, D_{1u}-D_{8u}, Q_{1u}-Q_{8u}, K₁-K₆, are the Jacobean matrices of appropriate size

neglecting the function of governors ($T_m = 0$) and linearizing (4.23) the following equations can be obtained

$$\begin{aligned}
\Delta \dot{E}'_d &= M_1 \Delta E'_q + M_2 \Delta E'_d + M_3 \Delta \delta + M_4 \Delta m_{SH} + M_5 \Delta \varphi_{SH} + M_6 \Delta m_{SE} + M_7 \Delta \varphi_{SE} + M_8 \Delta V_{dc} \\
\Delta \dot{E}'_q &= N_1 \Delta E'_q + N_2 \Delta E'_d + N_3 \Delta \delta + N_4 \Delta m_{SH} + N_5 \Delta \varphi_{SH} + N_6 \Delta m_{SE} + N_7 \Delta \varphi_{SE} + N_8 \Delta V_{dc} \\
&\quad + N_9 \Delta E'_{fd} \\
\Delta \dot{\omega} &= W_1 \Delta E'_q + W_2 \Delta E'_d + W_3 \Delta \delta + W_4 \Delta m_{SH} + W_5 \Delta \varphi_{SH} + W_6 \Delta m_{SE} + W_7 \Delta \varphi_{SE} + W_8 \Delta V_{dc} \\
&\quad + W_9 \Delta \omega + W_{10} \Delta E'_{fd} \\
\Delta \dot{E}'_{fd} &= S_1 \Delta E'_q + S_2 \Delta E'_d + S_3 \Delta \delta + S_4 \Delta m_{SH} + S_5 \Delta \varphi_{SH} + S_6 \Delta m_{SE} + S_7 \Delta \varphi_{SE} + S_8 \Delta V_{dc} + S_9 \Delta E'_{fd} \\
\Delta V_t &= P_1 \Delta V_{gd} + P_2 \Delta V_{gq} = R_1 \Delta E'_q + R_2 \Delta E'_d + R_3 \Delta \delta + R_4 \Delta m_{SH} + R_5 \Delta \varphi_{SH} + R_6 \Delta m_{SE} + R_7 \Delta \varphi_{SE} \\
&\quad + R_8 \Delta V_{dc}
\end{aligned} \tag{4.26}$$

where:

$$\begin{aligned}
M_1 &= (T'_{q0})^{-1} (X_q - X'_q) Q_1 & M_2 &= (T'_{q0})^{-1} (-I + (X_q - X'_q) Q_2) & M_3 &= (T'_{q0})^{-1} (X_q - X'_q) Q_3 \\
M_4 &= (T'_{q0})^{-1} (X_q - X'_q) Q_4 & M_5 &= (T'_{q0})^{-1} (X_q - X'_q) Q_5 & M_6 &= (T'_{q0})^{-1} (X_q - X'_q) Q_6 \\
M_7 &= (T'_{q0})^{-1} (X_q - X'_q) Q_7 & M_8 &= (T'_{q0})^{-1} (X_q - X'_q) Q_8 & N_1 &= (T'_{d0})^{-1} (-I - (X_d - X'_d) D_1) \\
N_2 &= -(T'_{d0})^{-1} (X_d - X'_d) D_2 & N_3 &= -(T'_{d0})^{-1} (X_d - X'_d) D_3 & N_4 &= -(T'_{d0})^{-1} (X_d - X'_d) D_4 \\
N_5 &= -(T'_{d0})^{-1} (X_d - X'_d) D_5 & N_6 &= -(T'_{d0})^{-1} (X_d - X'_d) D_6 & N_7 &= -(T'_{d0})^{-1} (X_d - X'_d) D_7 \\
N_8 &= -(T'_{d0})^{-1} (X_d - X'_d) D_8 & N_9 &= (T'_{d0})^{-1} & W_1 &= -\frac{1}{2} (H)^{-1} (I_{gq}^0 + U_1 Q_1 + U_2 D_1) \\
W_2 &= -\frac{1}{2} (H)^{-1} (I_{gd}^0 + U_1 Q_2 + U_2 D_2) & W_3 &= -\frac{1}{2} (H)^{-1} (U_1 Q_3 + U_2 D_3) & W_4 &= -\frac{1}{2} (H)^{-1} (U_1 Q_4 + U_2 D_4) \\
W_5 &= -\frac{1}{2} (H)^{-1} (U_1 Q_5 + U_2 D_5) & W_6 &= -\frac{1}{2} (H)^{-1} (U_1 Q_6 + U_2 D_6) & W_7 &= -\frac{1}{2} (H)^{-1} (U_1 Q_7 + U_2 D_7) \\
W_8 &= -\frac{1}{2} (H)^{-1} (U_1 Q_8 + U_2 D_8) & W_9 &= -\frac{1}{2} (H)^{-1} D_{damp} & W_{10} &= -\frac{1}{2} (H)^{-1} \\
U_1 &= (I_{gd}^0 X'_d + V_{gq}^0) & U_2 &= (-I_{gq}^0 X'_d + V_{gd}^0) & I_{gd}^0 &= \text{diag}(I_{gd})|_{x_0, u_0} \\
I_{gq}^0 &= \text{diag}(I_{gq})|_{x_0, u_0} & V_{gd}^0 &= \text{diag}(V_{gd})|_{x_0, u_0} & V_{gq}^0 &= \text{diag}(V_{gq})|_{x_0, u_0} \\
R_1 &= P_1 X'_d Q_1 + P_2 (I - X'_d D_1) & R_2 &= P_1 (I + X'_d Q_2) - P_2 X'_d D_2 & R_3 &= P_1 X'_d Q_3 - P_2 X'_d D_3 \\
R_4 &= P_1 X'_d Q_4 - P_2 X'_d D_4 & R_5 &= P_1 X'_d Q_5 - P_2 X'_d D_5 & R_6 &= P_1 X'_d Q_6 - P_2 X'_d D_6 \\
R_7 &= P_1 X'_d Q_7 - P_2 X'_d D_7 & R_8 &= P_1 X'_d Q_8 - P_2 X'_d D_8 & P_1 &= \text{diag}\left(\frac{V_{gdi}}{V_{ti}}\right)|_{x_0, u_0} \\
P_2 &= \text{diag}\left(\frac{V_{gqi}}{V_{ti}}\right)|_{x_0, u_0} & S_1 &= -(T_A)^{-1} K_A R_1 & S_2 &= -(T_A)^{-1} K_A R_2 \\
S_3 &= -(T_A)^{-1} K_A R_3 & S_4 &= -(T_A)^{-1} K_A R_4 & S_5 &= -(T_A)^{-1} K_A R_5 \\
S_6 &= -(T_A)^{-1} K_A R_6 & S_7 &= -(T_A)^{-1} K_A R_7 & S_8 &= -(T_A)^{-1} K_A R_8 \\
S_9 &= -(T_A)^{-1} & T_A &= \text{diag}(T_{Ai}) & K_A &= \text{diag}(K_{Ai})
\end{aligned}$$

Linearized power system with UPFC included can now be written in the matrix form

$$\begin{bmatrix} \Delta \dot{E}'_q \\ \Delta \dot{E}'_d \\ \Delta \dot{\delta} \\ \Delta \dot{\omega} \\ \Delta \dot{V}_{DC} \\ \Delta \dot{E}'_{fd} \end{bmatrix} = \begin{bmatrix} N_1 & N_2 & N_3 & 0 & N_8 & N_9 \\ M_1 & M_2 & M_3 & 0 & M_8 & 0 \\ 0 & 0 & 0 & \omega_B I & 0 & 0 \\ W_1 & W_2 & W_3 & W_9 & W_8 & W_{10} \\ L_1 & L_2 & L_3 & 0 & L_8 & 0 \\ S_1 & S_2 & S_3 & 0 & S_8 & S_9 \end{bmatrix} \begin{bmatrix} \Delta E'_q \\ \Delta E'_d \\ \Delta \delta \\ \Delta \omega \\ \Delta V_{DC} \\ \Delta E'_{fd} \end{bmatrix} + \begin{bmatrix} N_6 & N_7 & N_4 & N_5 \\ M_6 & M_7 & M_4 & M_5 \\ 0 & 0 & 0 & 0 \\ W_6 & W_7 & W_4 & W_5 \\ L_6 & L_7 & L_4 & L_5 \\ S_6 & S_7 & S_4 & S_5 \end{bmatrix} \begin{bmatrix} \Delta m_{SE} \\ \Delta \phi_{SE} \\ \Delta m_{SH} \\ \Delta \phi_{SH} \end{bmatrix} \quad (4.27)$$

Note: The equations for linearization of the simple two-machine/UPFC power system can be found in the m-file given in Appendix C.

4.5 Linearization of a Power System with the PST and Modal Analysis

The m-files added to the PST form the state matrices of a power system model including a UPFC with the DC-link voltage as state. The basic control of the UPFC based on PI-controllers for the real and reactive line power flow, the sending bus voltage, and the DC-link voltage, as well as a double-stage lead-lag compensator with a washout can be included in the linearization process.

4.5.1 Description

The process of finding the state matrices and modal analysis is based on the following steps:

- select a data file (power system can include any number of busses, generators, generator controls (exciters, governors, and PSS), and one UPFC with its basic controls and one damping controller)
- perform a load flow
- form a linearized model by perturbing each state and input signal in turn
- form the minimum realization by choosing one generator (angle) as reference
- perform a modal analysis of the system (i.e. identify critical eigenvalues, frequency, damping ratio, etc.).

4.5.2 Method

Each state x_i ($i = 1..n$) and input signal u_i ($i = 1..m_u$) are perturbed in turn by a small value (small percentage of the load flow solution value) and the rate of change of the states

is computed. The entries in the system matrix corresponding to the perturbed i^{th} state are the entries in the i^{th} column and are calculated as

$$A_{1..n,i} = \frac{\Delta \dot{x}_{1..n}}{\Delta x_i} \quad (4.28)$$

where:

A is the $n \times n$ state matrix
 $\Delta \dot{x}_{1..n}$ is the computed rate of change in all states
 Δx_i is the applied change in the i^{th} state variable

The entries in the output matrix are found by perturbing the i^{th} state and computing the rate of the changes in the m_y output variables as

$$C_{1..m_y,i} = \frac{\Delta y_{1..m_y}}{\Delta x_i} \quad (4.29)$$

where:

C is the $m_y \times n$ output matrix
 $\Delta y_{1..m_y}$ is the computed change in the m_y output variables
 Δx_i is the applied change in the i^{th} state variable

The entries in the input matrix are found by perturbing the i^{th} input and computing the rate of the changes in the states as

$$B_{1..n,i} = \frac{\Delta \dot{x}_{1..n}}{\Delta u_i} \quad (4.30)$$

where:

B is the $n \times m_u$ input matrix
 $\Delta \dot{x}_{1..n}$ is the computed rate of change in all states
 Δu_i is the applied change in the i^{th} input channel

The entries in the feed forward matrix are found by perturbing the i^{th} input and computing the changes in the m_y output variables as

$$D_{1..m_y,i} = \frac{\Delta y_{1..m_y}}{\Delta u_i} \quad (4.31)$$

where:

D is the $m_y \times m_u$ feed forward matrix
 $\Delta y_{1..m_y}$ is the computed rate of change in all states
 Δu_i is the applied change in the i^{th} input channel

4.5.3 States, Input and Output Signals

The possible signals for in- and outputs of a generator are

inputs	exciter reference voltage
	turbine/governor power reference
outputs	generator speed
	generator electrical torque
	generator electrical power

The possible UPFC states are

states	Number of states	Comments
V_{DC}	1	UPFC with DC-link voltage as state without controller applied
$V_{DC}, m_{SH}, \phi_{SH}, V_p, V_q$ or $V_{DC}, m_{SH}, \phi_{SH}, m_{SE}, \phi_{SE}$	5	UPFC with DC-link voltage as state and its basic controls in form of PI-controllers for real and reactive line power flow, sending bus voltage and DC-link voltage added
$V_{DC}, m_{SH}, \phi_{SH}, V_p, V_q$, upfc1 - washout state variable, upfc2 - 1 st lead-lag state, upfc3 - 2 nd lead-lag-state	8	UPFC with DC-link voltage as state and its basic controls in form of PI-controllers for real and reactive line power flow, sending bus voltage and DC-link voltage added plus three states for the damping controller double-stage lead-lag controller with washout

The possibilities to form the linearized model including a UPFC are

	variables/channels	Comments
inputs	$m_{SH}, \phi_{SH}, m_{SE}, \phi_{SE}$ or $m_{SH}, \phi_{SH}, V_p, V_q$	UPFC with DC-link voltage as state without controller applied
	$P_{line}^{ref}, Q_{line}^{ref}, V_S ^{ref}, V_{DC}^{ref}$	UPFC with DC-link voltage as state with basic control in form of PI-controllers for real and reactive line power flow, sending bus voltage and DC-link voltage added
outputs	real line power flow	
	reactive line power flow	
	sending bus voltage	
	DC-link voltage	

4.5.4 Minimum realization

In the absence of an infinite bus the relative rotor angles instead of the absolute rotor angles are required as state variables. Therefore, a reference machine is chosen to compute the relative machine angles and to reduce the state matrices by the entries corresponding to the reference machine. The reduction is done with the following two steps:

- A and B matrix: subtract the row of the reference machine angle from the rows belonging to the other generator angles
- A, B, C, D matrix: eliminate the rows and columns belonging to the reference machine angle.

The order of the system is therefore reduced by one and the new states belonging to the machine angles are measures with respect to the reference machine.

Chapter 5

CONTROLLER DESIGN

To operate the UPFC in the automatic control mode discussed in the third chapter, and also to use the UPFC to enhance power system stability and damp low frequency oscillations, two control designs need to be performed. A primary control design, referred to as the *UPFC basic control design*, involves simultaneous control of (i) real and reactive power flow on the transmission line, (ii) sending bus voltage magnitude, and (iii) DC voltage magnitude. A secondary control design, referred to as the *damping controller design*, is a supplementary control loop that is designed to improve transient stability of the entire electric power system. The two control designs are described in this chapter.

5.1 Basic control

The UPFC basic control design consists of four separate control loops grouped into a *series control scheme*, whose objective is to control real and reactive power flow on the line, and a *shunt control scheme*, whose objective is the control of the sending bus voltage magnitude and the DC voltage magnitude.

5.1.1 Series control scheme

This scheme has two control loops, one for the tracking of the real power flow at the receiving bus of the line, and the second performs the same task for the reactive power flow. Specifically, the objective is to track these real and reactive power flows following step changes and eliminate steady-state tracking errors. This is obtained by the appropriate selection of the voltage drop between the sending and the receiving buses, which is denoted \bar{V}_{PQ} (see Fig 3.3). This voltage can be decomposed into the following two quantities which affect the tracked powers, namely:

- V_P = voltage component orthogonal to the sending bus voltage (it affects primarily the real power flow on the transmission line)
- V_Q = component in phase with the sending bus voltage (it affects mainly the reactive power flow on the transmission line).

These quantities are in phasor diagram Fig. 5.1 [22].

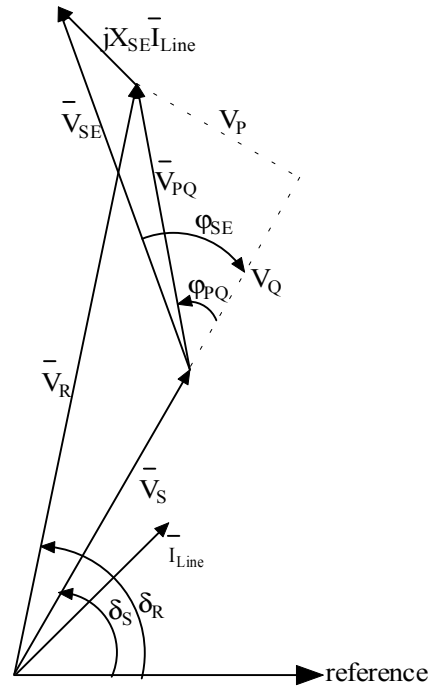


Fig. 5.1 Phasor diagram

Both voltages, V_P and V_Q , are obtained by designing classic PI (proportional-integral) controllers as illustrated in Fig. 5.2. The integral controller will guarantee error free steady-state control of the real and reactive line power flows.

After the V_P and V_Q components have been found the injected series voltage can be computed as

$$\begin{aligned}
 V_{PQ} &= \sqrt{V_P^2 + V_Q^2} \\
 \phi_{PQ} &= \text{tg}^{-1} \frac{V_P}{V_Q} \\
 \bar{V}_{PQ} &= V_{PQ} \angle (\delta_S + \phi_{PQ}) \\
 \bar{V}_{SE} &= \bar{V}_{PQ} + jX_{SE}\bar{I}_{Line}
 \end{aligned} \tag{5.1}$$

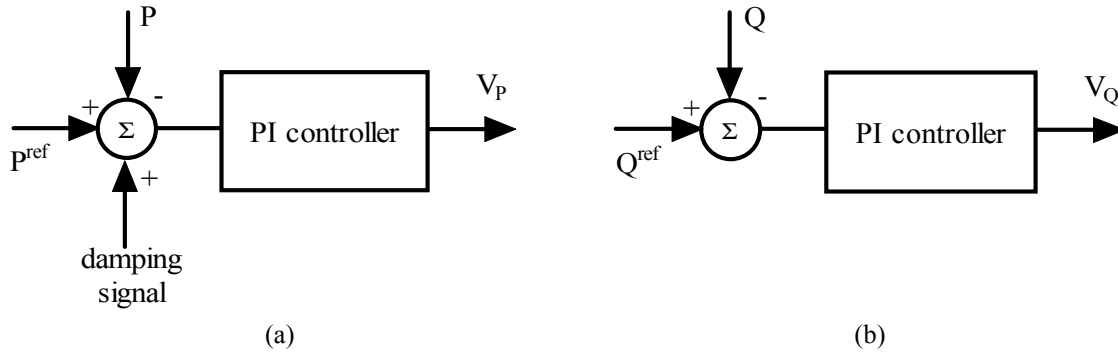


Fig. 5.2 Series control scheme-automatic power flow mode

From (3.3) and (3.4) series converter amplitude modulation index and the firing angle can be computed as

$$m_{SE} = \frac{2\sqrt{2}n_{SE} V_{SE} V_B}{V_{DC}} \quad (5.2)$$

$$\varphi_{SE} = \delta_S - \delta_{SE}$$

5.1.2 Shunt control scheme

This control scheme also has two loops that are designed to maintain the magnitude of the sending bus voltage and the DC link voltage at their pre-specified values.

The magnitude of the injected shunt voltage (equation (3.3)) affects the reactive power flow in the shunt branch, which in turn affects the sending bus voltage magnitude. The angle between the sending bus voltage and the injected shunt voltage, φ_{SH} (equation (3.4)), affects the real power flow in the shunt branch. It can be used to control the power flow to the DC link and therefore the DC link voltage.

This is achieved by using two separate PI controllers as shown in Fig. 5.3 [21], [22].

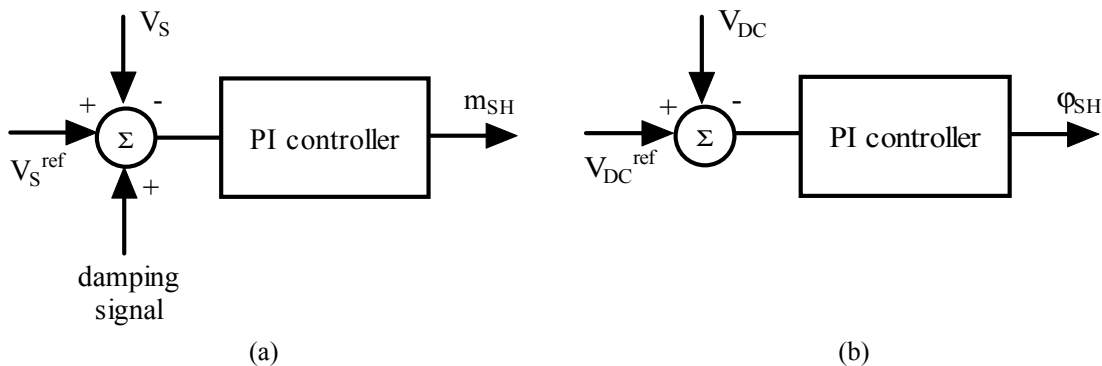


Fig. 5.3 Shunt control scheme

5.2 Damping Controller Design

Low frequency oscillations occur frequently due to disturbances such as changes in loading conditions or a loss of a transmission line or a generator unit. These conditions need to be controlled to maintain system stability. Several control devices, such as power system stabilizers, are used to enhance power system stability. Recently [18], [19], [22], it has shown that oscillations can be damped by introducing a supplementary signal, based on the real power flow along the transmission line, to the series converter side through the modulation of the active power flow reference signal (Fig. 5.2(a)), or to the shunt converter side through the modulation of voltage magnitude reference signal (Fig. 5.3(a)). The damping controllers used so far were of lead-lag type with the transfer function similar to the one shown in Fig. 5.4.

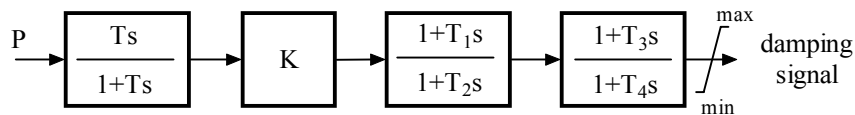


Fig. 5.4 Lead –lag controller structure

The damping controller design in this section is based on the fuzzy logic. A brief introduction to fuzzy set theory, basics of fuzzy control design, and its application to UPFC damping controller design are given next.

5.2.1 Introduction

Fuzzy control is based on fuzzy logic theory. There is no systematic design procedure in fuzzy control. The important advantage of fuzzy control design is that mathematical model of the system is not required.

Fuzzy controllers are rule-based controllers. The rules are given in the “if-then” format. The “if-side” is called condition and the “then-side” is called conclusion. The rules may use several variables both in condition and conclusion of the rules. Therefore, the fuzzy controllers can be applied both to nonlinear multi-input-multi-output (MIMO) and single-input-single-output (SISO) problems.

Control rules can be found based on:

- Expert experience and control engineering knowledge
- Learning (i.e. neural networks)

Some basic definitions and terms [26] are now given:

Fuzzy set: Let X be a collection of objects, then a fuzzy set A in X is defined as

$$A = \{(x, \mu_A(x)) \mid x \in X\} \quad (5.3)$$

$\mu_A(x)$ is called the membership function of x in A . It usually takes values in the interval $[0, 1]$. The numerical interval X relevant for the description of a fuzzy variable is called Universe of Discourse.

Operations on fuzzy sets:

Let A and B be two fuzzy sets with membership functions $\mu_A(x)$ and $\mu_B(x)$.

The AND operator or intersection of two fuzzy sets A and B is a fuzzy set C whose membership function $\mu_C(x)$ is defined as

$$\mu_C(x) = \min\{\mu_A(x), \mu_B(x)\}, x \in X \quad (5.4)$$

The OR operator or union of two fuzzy sets A and B is a fuzzy set C whose membership function $\mu_C(x)$ is defined as

$$\mu_C(x) = \max\{\mu_A(x), \mu_B(x)\}, x \in X \quad (5.5)$$

5.2.2 Structure of a Fuzzy Controller

A fuzzy controller structure is shown in Fig. 5.5 [31]. The controller is placed between preprocessing and post-processing blocks.

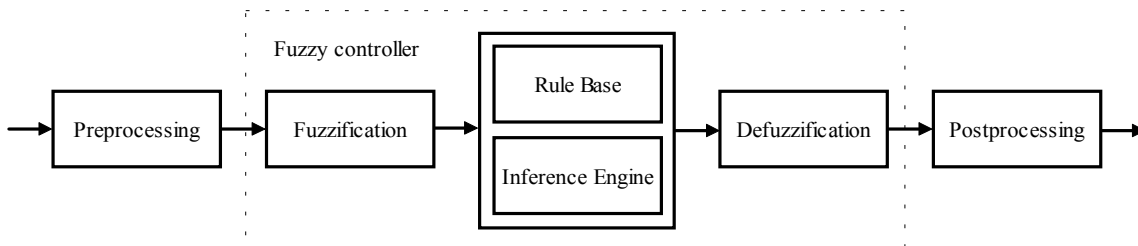


Fig. 5.5 Fuzzy controller structure

The preprocessing block conditions the inputs, usually crisp measurements, before they enter the controller.

First step in fuzzy controller design is to choose appropriate input and output signals of the controller.

Second step is to choose linguistic variables that will describe all input and output variables.

Third step is to define membership functions for fuzzy sets. Membership functions can be of different shape i.e. triangular, trapezoidal, Gaussian functions etc.

Fourth step is to define fuzzy rules. For two-input one-output system each control rule R_i will be of the following form:

IF input (1) is A_{i1} AND input (2) is A_{i2} THEN output is B_i

Fifth step is to join rules by using Inference engine. The most often used inference engines are *Mamdani Max- Min and Max-Product*.

The Max-Product Inference procedure can be summarized as:

- For the i^{th} rule
 - Obtain the minimum between the input membership functions by using the AND operator
 - Re-scale the output membership function by the obtained minimum to get the output membership function due to the i^{th} rule
- Repeat the same procedure for all rules
- Find the maximum between output membership functions obtained from each rule by using the OR operator. This gives the final output membership function due to all rules.

Graphical technique of Mamdani (Max-Product) Inference is shown in Fig. 5.6.

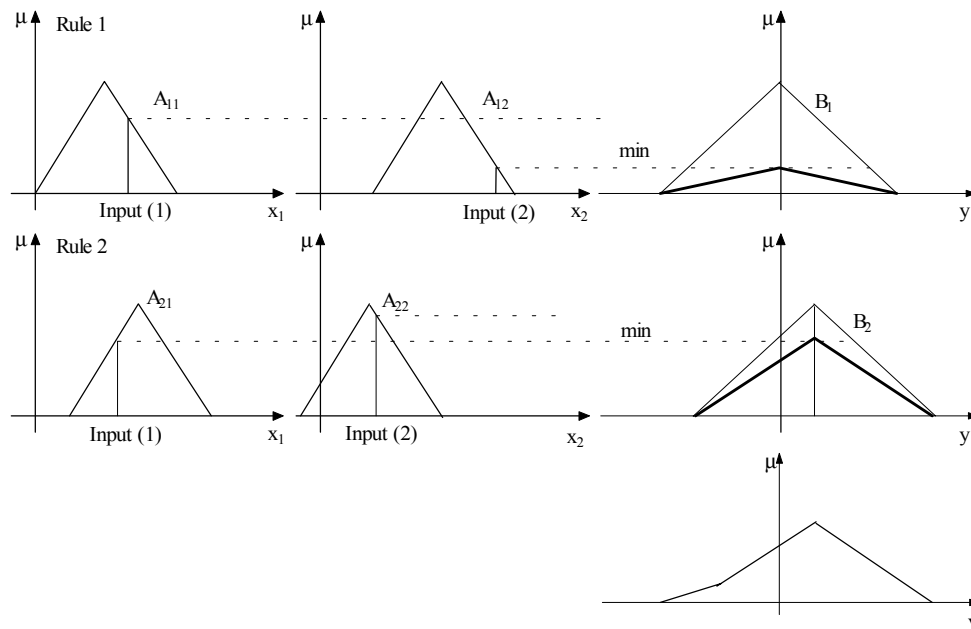


Fig. 5.6 Mamdani Max-Product Inference

Graphical technique of Mamdani Max-Min Inference shown in Fig. 5.7 can be explained in similar matter.

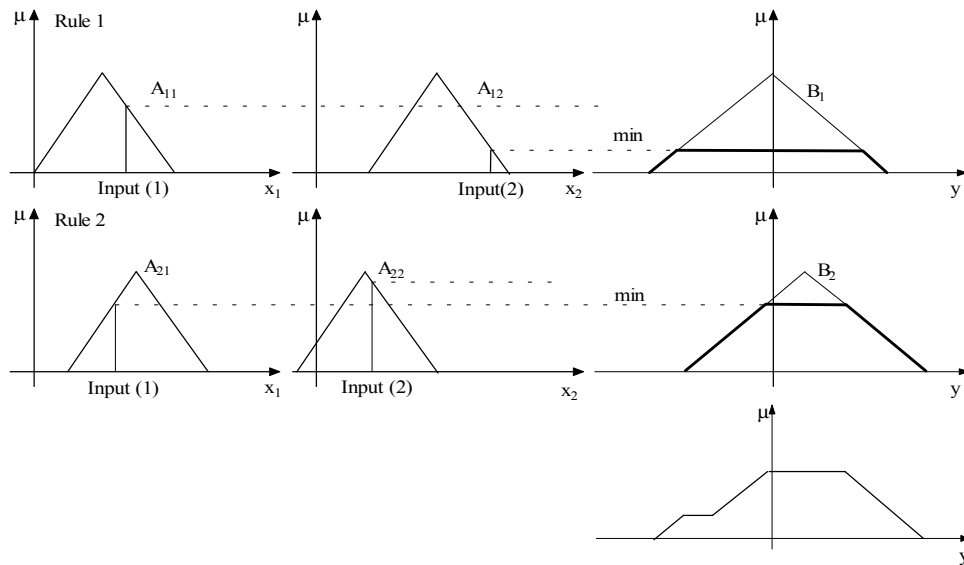


Fig. 5.7 Mamdani (Max-Min) Inference

Sixth step is defuzzification.

The resulting fuzzy set must be converted to a number. This operation is called defuzzification. The most often used defuzzification method is the centroid method or Center of area as shown in Fig. 5.8.

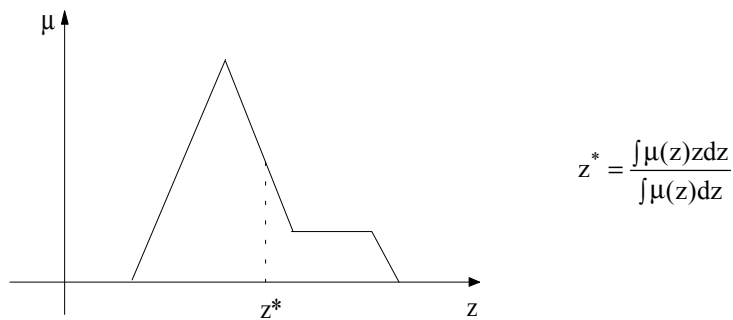


Fig. 5.8 Centroid method

Post-processing

The post-processing block often contains an output gain that can be tuned.

5.2.3 Fuzzy Logic UPFC Damping Controller

Input signals to the controller, power flow deviation from the steady-state value ΔP and its integral ΔE , are derived from the real power flow signal at the UPFC site. They have to be driven back to zero for a new steady-state by the damping controller [24,25]. The choice of the input signals parallels work done on PSSs and SVCs [24]-[29]. The process of finding ΔP and ΔE signals requires signal conditioning, involving removal of the offset components and integration (Fig. 5.9).



Fig. 5.9 Obtaining the input signals for fuzzy controller

The inputs are described by the following linguistic variables: P (positive), NZ (near zero), and N (negative). The output is described by five linguistic variables P (positive), PS (positive small), NZ (near zero), NS (negative small), and N (negative). Gaussian functions are used as membership functions for both inputs, and triangular membership functions are used for output (Fig. 5.10). Damping signal is controller output. Fuzzy rules used are given in Table 5.1.

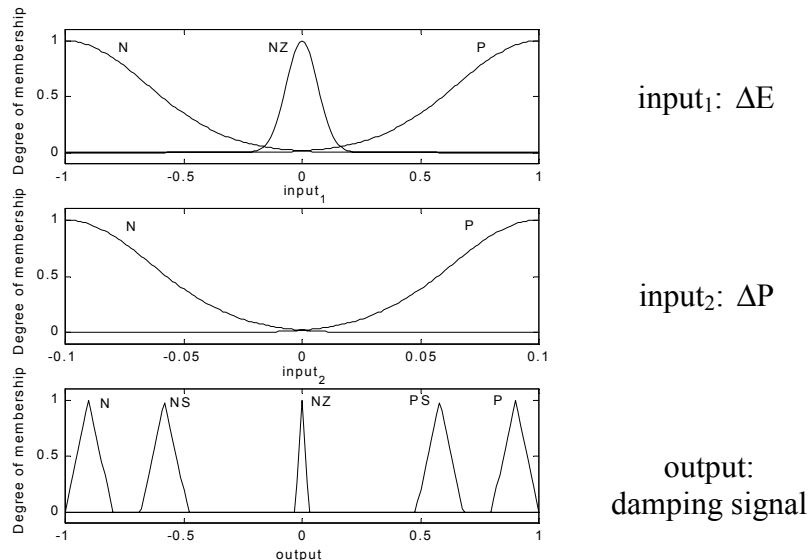


Fig. 5.10 Fuzzy Logic Controller input and output variables

Table 5.1 Fuzzy rules

if ΔE is NZ then damping signal is NZ
if ΔE is P then damping signal is P
if ΔE is N then damping signal is N
if ΔE is NZ and ΔP is P then damping signal is NS
if ΔE is NZ and ΔP is N then damping signal is PS

Chapter 6

CASE STUDY

6.1 Test System

To assess the UPFC's capabilities through simulation a software tool is needed. The PST has several power devices but not the UPFC. A UPFC module that consists of four components: a steady state model, a dynamic model with its basic and damping controllers, an interfacing algorithm, and a linearized model as explained in the previous chapters were integrated within the PST. To demonstrate the proposed tools a two-area-four-generator test system as shown in Fig. 6.1 is used.

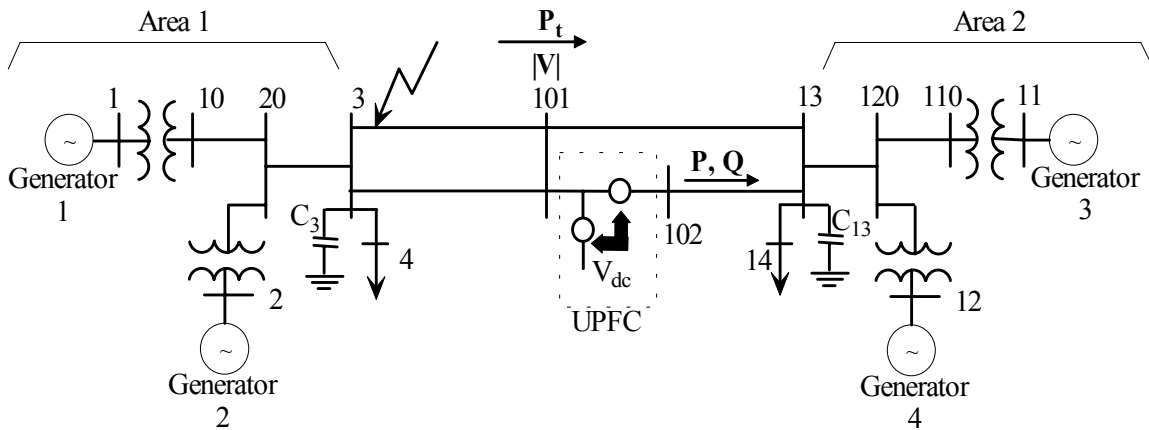


Fig. 6.1 Two-area-four-generator test system

Two areas are identical to one another and interconnected with two parallel 230-km tie-lines that carry about 400MW from area 1 (generators 1 and 2) to area 2 (generators 3 and 4) during normal operating conditions. The UPFC is placed at the beginning of the lower parallel line between the buses 101 and 13 in order to control the power flow through that line as well as to regulate voltage level at bus 101. The test system and the UPFC data are given in Appendix A.

6.2 Load Flow

To initialize the simulation load flow program lfdemo is executed. Solved load flow and the UPFC steady state quantities for the case when UPFC is operated to control line power flow at $1.6-0.15j$ pu at the receiving bus and to regulate the sending bus voltage at 1pu are given in Appendix B. Series and shunt transformer reactances are set to 0.01 pu.

It can be seen from the Table B.1 that LF algorithm has converged within the third step. The remaining deviation of the series and shunt converter real power interaction is 1.576×10^{-5} , which is less than a specified tolerance of 10^{-4} (Table B.1). The injected real power at the sending bus is -1.654 pu. The load at the receiving bus is -1.6 pu and therefore the injection to the receiving bus is 1.6 pu. The difference between the real power injected into the sending bus and the load at the receiving bus is caused by the losses of series and shunt transformers as shown in Table B.2 ($0.029+0.025=0.054$).

6.3 Linearized Model

In order to verify the linearized model discussed in the fourth chapter simple two-machine system with UPFC as shown in Fig. 6.2 was considered. Equations derived following the approach discussed in the fourth chapter for linearization of this system can be found in the m-file given in Appendix C.

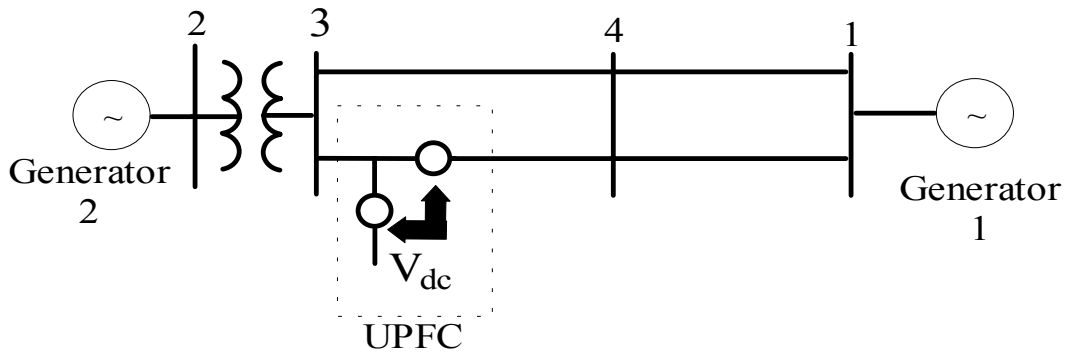


Fig. 6.2 Two-machine/UPFC system

Table 6.1 and Table 6.2 show the system state and input matrices, and Table 6.3 shows the eigenvalues obtained using the approaches described previously. The results are almost identical, verifying the numerical approach of the PST.

Table 6.1 System state matrices and eigenvalues using the derived equations and the PST

A-matrix (derived equations):							
0.000	0.009	0.017	0.009	0.000	0.004	-0.008	0.000
0.000	-0.170	0.000	-0.010	0.000	0.019	0.012	0.000
0.000	0.001	-3.347	-0.383	0.000	-0.231	0.347	0.000
-376.991	0.000	0.000	0.000	376.991	0.000	0.000	0.000
0.000	-0.004	-0.008	-0.049	0.000	-0.012	0.047	0.000
0.000	0.019	-0.012	-0.029	0.000	-0.238	0.000	0.000
0.000	0.230	0.348	2.119	0.000	0.003	-4.617	0.000
0.000	-32138.264	-58977.168	276037.870	0.000	55162.026	-263067.485	-0.012
A-matrix (PST):							
0.000	0.009	0.017	0.009	0.000	0.004	-0.008	0.000
0.000	-0.170	0.000	-0.010	0.000	0.019	0.012	0.000
0.000	0.001	-3.347	-0.383	0.000	-0.231	0.347	0.000
-376.991	0.000	0.000	0.000	376.991	0.000	0.000	0.000
0.000	-0.004	-0.008	-0.049	0.000	-0.012	0.047	0.000
0.000	0.019	-0.012	-0.029	0.000	-0.238	0.000	0.000
0.000	0.230	0.348	2.119	0.000	0.003	-4.617	0.000
-0.001	-32632.017	-60178.111	281309.844	-0.001	56154.767	-268098.827	-0.014

Table 6.2 Input matrices of the power system using the derived equations and the PST

B-matrix (derived equations):			
0.005	0.000	0.003	-0.010
-0.006	0.002	0.029	0.009
-0.195	-0.025	-0.222	0.416
0.000	0.000	0.000	0.000
-0.003	0.000	-0.004	-0.040
0.000	-0.001	0.121	-0.018
0.112	-0.001	0.435	1.746
-14023.269	-2661.280	3260.730	341274.372
B-matrix (PST):			
0.005	0.000	0.003	-0.010
-0.006	0.002	0.029	0.009
-0.195	-0.025	-0.222	0.416
0.000	0.000	0.000	0.000
-0.003	0.000	-0.004	-0.040
0.000	-0.001	0.121	-0.018
0.112	-0.001	0.435	1.746
-14371.130	-2670.800	3258.697	335732.601

Table 6.3 Eigenvalues for two-machine/UPFC system

eigenvalues using the derived equations:	eigenvalues using the PST:
-0.3678 + 4.3534i	-0.3621 + 4.3603i
-0.3678 - 4.3534i	-0.3621 - 4.3603i
-3.5040	-3.5083
-3.0043	-2.9998
-0.0000	-0.0000
-0.4156 + 0.0634i	-0.4203 + 0.0225i
-0.4156 - 0.0634i	-0.4203 - 0.0225i
-0.3097	-0.3144

Table 6.4 States and input signals of the linearized power system

states		inputs	
1	ω_1	1	m_{SE}
2	E_{q1}		
3	E_{d1}	2	ϕ_{SE}
4	δ_{21}		
5	ω_2	3	m_{SH}
6	E_{q2}		
7	E_{d2}	4	ϕ_{SH}
8	V_{DC}		

6.4 Nonlinear Simulations and Modal Analysis

In this section test system is used and two cases are considered:

- UPFC performance when the real and reactive power references are changed
- UPFC performance when the fault is applied.

6.4.1 Tracking Real and Reactive Powers Reference Values

The objective is to keep the sending bus voltage at the pre-specified value and to

1. keep the reactive power constant while tracking the step changes in the real power (UPFC is initially operated to control the real power flow at 1.6 pu; at time 0.5 s real power flow reference is raised to 1.8 pu and at time 3.5 s is dropped to 1.3 pu; at time 7.5 s system returns to the initial operating condition as shown in Fig. 6.3(a))
2. keep the real power constant while tracking the step changes in the reactive power (at time 0.5 s reactive power flow reference is changed from -0.15 pu to -0.2 pu, at time 3.5 s reference is set to 0.2 pu, and at time 7.5 s system returns to the initial operating condition as shown in Fig. 6.4(a)).

Results depicted in Fig. 6.3 and Fig. 6.4 show that the UPFC responses almost instantaneously to changes in real and reactive power flow reference values. For both cases sending bus voltage is regulated at 1 pu as shown in Fig. 6.3(b) and Fig. Fig. 6.4(b). Plots also show that UPFC is able to independently control real and reactive power flow. This is accomplished by injecting the voltage of appropriate magnitude and phase angle as shown in Fig. 6.3(c)-(d) and Fig. 6.4(c)-(d).

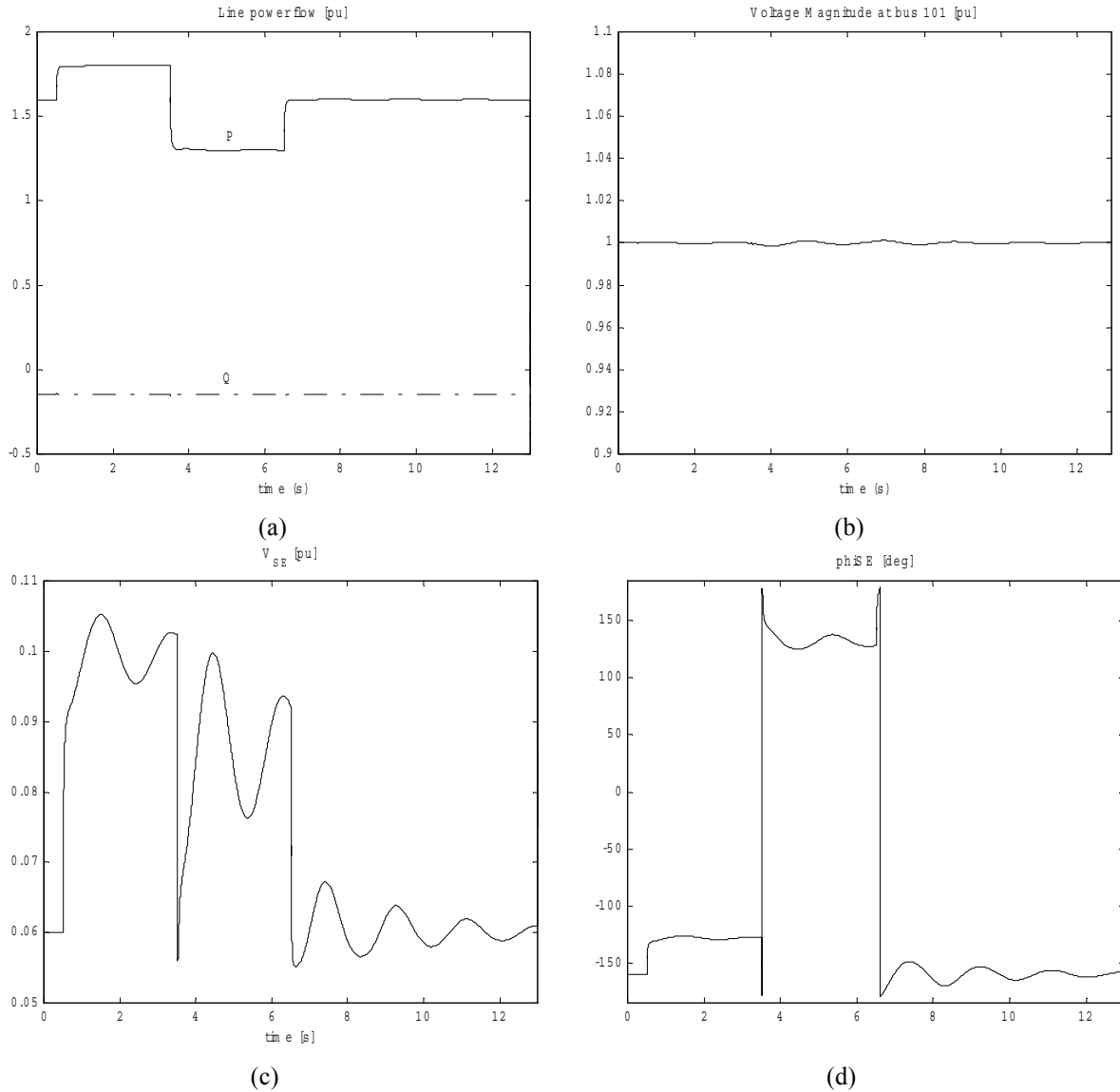


Fig. 6.3 Changing real power reference value

6.4.2 Operation Under the Fault Condition

In this section test system response to a 100 ms three-phase fault applied in area 1, at bus 3 is examined. The fault is cleared by removing one line between the fault bus and bus 101. Four different cases are considered:

- test system with exciters and governors as only controls
- test system with power system stabilizers (PSS)
- test system with the PSS and the UPFC operated in the automatic power flow control mode

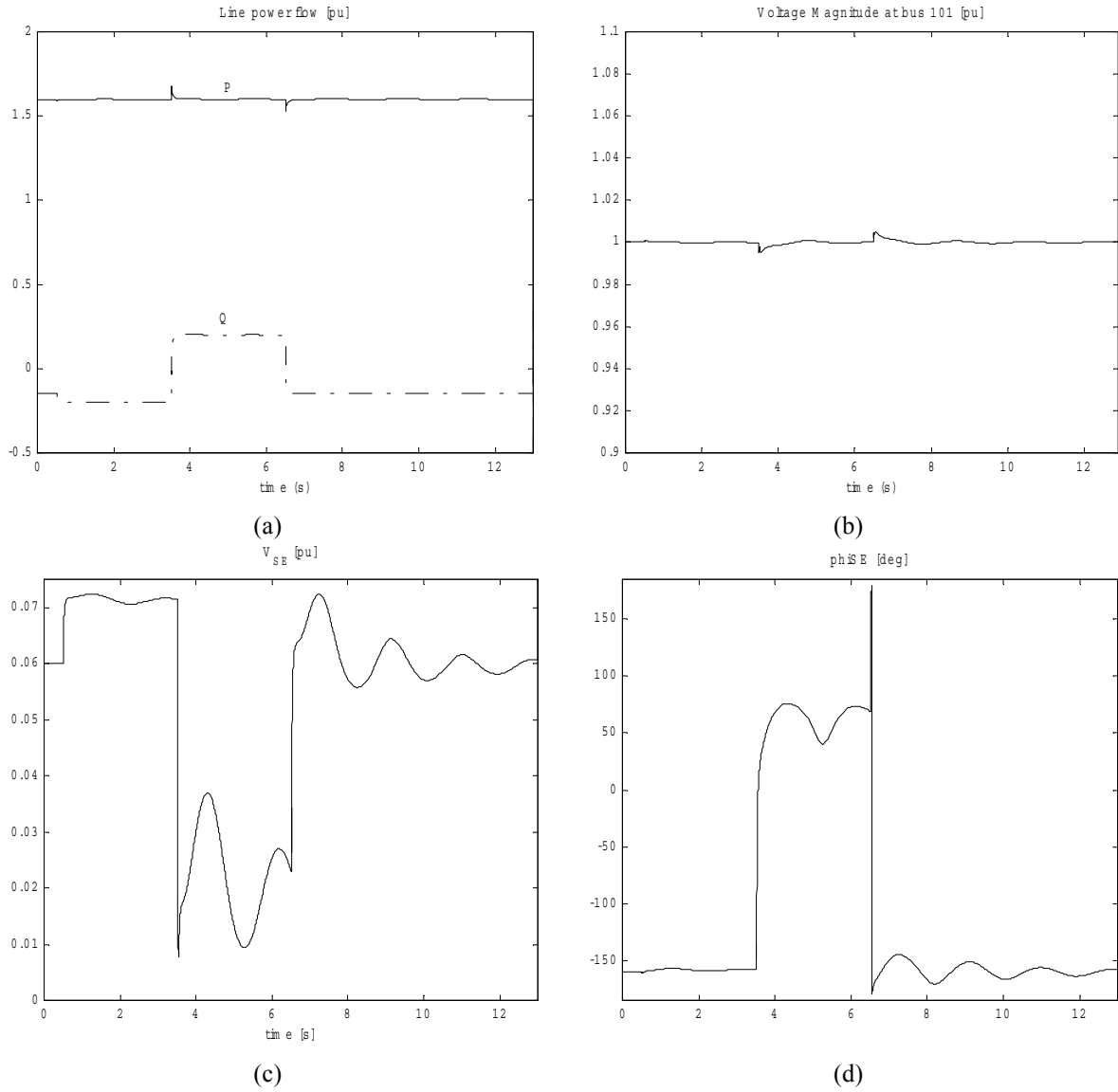


Fig. 6.4 Changing reactive power reference value

- test system with the PSS and the UPFC operated in the damping control mode.

Modal analysis was performed for all cases.

1) Test system with exciters and governors as only controls

The dominant eigenvalues for this case are shown in Table 6.5 and nonlinear simulation in Fig. 6.5. The system is unstable since complex conjugate pair $0.1643 + 3.3985i$, further on referred to as critical mode, has positive real part.

Table 6.5 Dominant eigenvalues for the test system with exciters and governors as only controls

Eigenvalues	frequency	damping ratio
19: -0.4694 + (7.3601)i	1.171	0.064
20: -0.4694 + (-7.3601)i	1.171	0.064
21: -0.5536 + (6.8778)i	1.095	0.080
22: -0.5536 + (-6.8778)i	1.095	0.080
27: 0.1643 + (3.3985)i	0.541	-0.048
28: 0.1643 + (-3.3985)i	0.541	-0.048
34: -0.2495 + (0.6615)i	0.105	0.353
35: -0.2495 + (-0.6615)i	0.105	0.353

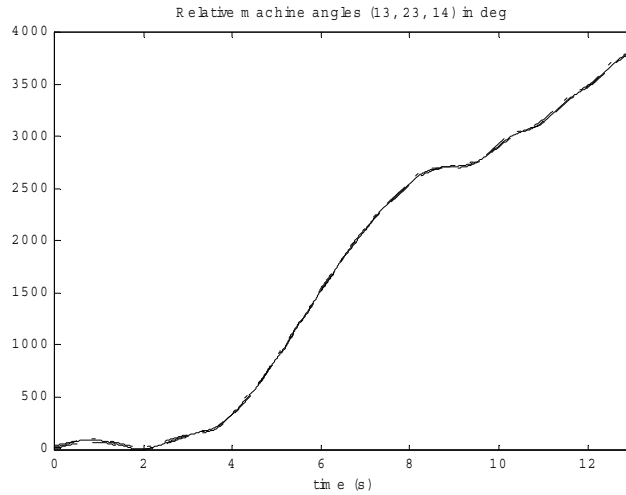


Fig. 6.5 Test system with PSS: Nonlinear simulation

2) Test system with PSS

Adding the PSS stabilizes the power system. The critical mode is moved to the left (Table 6.6). Nonlinear simulation results shown in Fig. 6.6 confirm this result.

Table 6.6 Dominant eigenvalues for the test system with the PSS

Eigenvalues	frequency	damping ratio
23: -0.8470 + (7.1124)i	1.132	0.118
24: -0.8470 + (-7.1124)i	1.132	0.118
25: -1.3300 + (7.1312)i	1.135	0.183
26: -1.3300 + (-7.1312)i	1.135	0.183
31: -0.2834 + (3.3608)i	0.535	0.084
32: -0.2834 + (-3.3608)i	0.535	0.084
46: -0.2395 + (0.5596)i	0.089	0.393
47: -0.2395 + (-0.5596)i	0.089	0.393

3) Test system with the UPFC operated in the automatic power flow control mode

The UPFC is operated to control the sending bus voltage at 1 pu and to regulate the line power flow at:

- a) 1.97-0.15j pu
- b) 1.60-0.15j pu
- c) 2.50-0.15j pu.

Table 6.7 shows dominant eigenvalues for cases 3a, 3b and 3c. It has been found that the UPFC with its basic controls interacts negatively with the PSS. The same result has been reported in [19].

Table 6.7 Dominant eigenvalues for the test system with the PSS and the UPFC operated in the automatic power control mode

Case 3a		
Eigenvalues	frequency	damping ratio
26: -1.0571 +(10.0563)i	1.601	0.105
27: -1.0571 +(-10.0563)i	1.601	0.105
28: -1.4059 +(7.1234)i	1.134	0.194
29: -1.4059 +(-7.1234)i	1.134	0.194
30: -0.6999 +(6.4889)i	1.033	0.107
31: -0.6999 +(-6.4889)i	1.033	0.107
36: -0.2208 +(3.5507)i	0.565	0.062
37: -0.2208 +(-3.5507)i	0.565	0.062
50: -0.2205 +(0.5764)i	0.092	0.357
51: -0.2205 +(-0.5764)i	0.092	0.357
Case 3b		
Eigenvalues	frequency	damping ratio
26: -1.1238 +(9.9533)i	1.584	0.112
27: -1.1238 +(-9.9533)i	1.584	0.112
28: -1.4066 +(7.1242)i	1.134	0.194
29: -1.4066 +(-7.1242)i	1.134	0.194
30: -0.7105 +(6.4586)i	1.028	0.109
31: -0.7105 +(-6.4586)i	1.028	0.109
36: -0.2140 +(3.5842)i	0.570	0.060
37: -0.2140 +(-3.5842)i	0.570	0.060
50: -0.2202 +(0.5748)i	0.091	0.358
51: -0.2202 +(-0.5748)i	0.091	0.358
Case 3c		
Eigenvalues	frequency	damping ratio
26: -0.9527 +(10.1341)i	1.613	0.094
27: -0.9527 +(-10.1341)i	1.613	0.094
28: -1.3996 +(7.1155)i	1.132	0.193
29: -1.3996 +(-7.1155)i	1.132	0.193
30: -0.6873 +(6.5128)i	1.037	0.105
31: -0.6873 +(-6.5128)i	1.037	0.105
36: -0.2277 +(3.4912)i	0.556	0.065
37: -0.2277 +(-3.4912)i	0.556	0.065
51: -0.2223 +(0.5809)i	0.092	0.357
52: -0.2223 +(-0.5809)i	0.092	0.357

Fig. 6.6 shows comparison of the simulation results for the test system with the PSS and the test system with the PSS and the UPFC (case 3a). During the steady-state operation each interconnecting tie line carries 1.97 pu from area 1 to area 2. It can be seen from Fig. 6.6(a)

that the line power flow for the test system without the UPFC oscillates long after the fault is cleared while the desired power flow conditions are reached quickly after the fault is cleared for the test system with the UPFC. For the test system without the UPFC bus 101 voltage is 0.92 pu which is below accepted limits. Therefore, the UPFC is operated to keep bus 101 voltage at 1 pu (Fig. 6.6(b)). The power angle swings for the test system with UPFC are better damped though it can be seen from Fig. 6.6(c) that constant power flow has negative effect on the system first swing transient. The same result can be found in [22]. The dc capacitor voltage fluctuation during the transient is less than 1% of its rated value 22 kV (Fig. 6.6(d)) which is acceptable for this application.

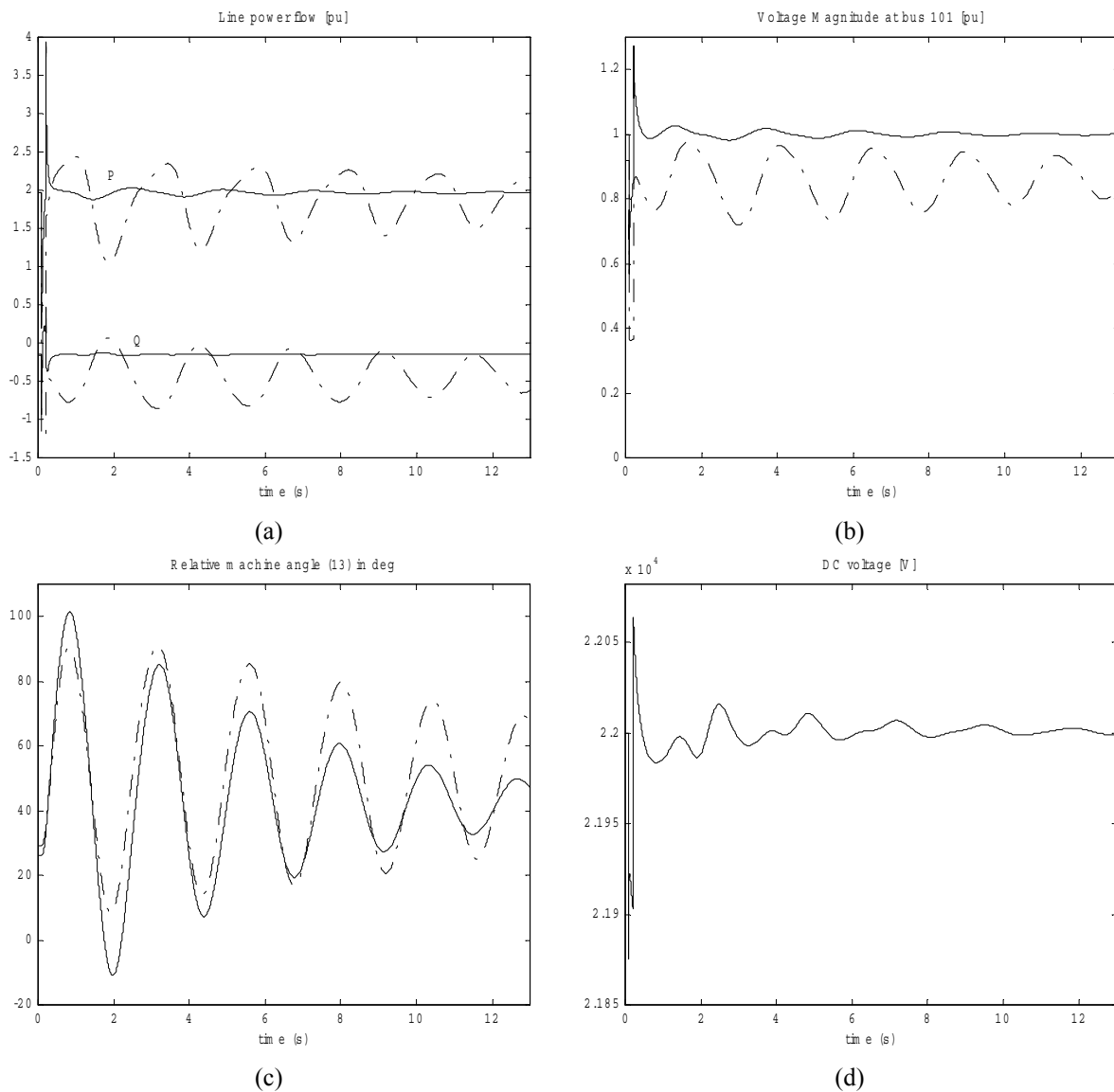


Fig. 6.6 Nonlinear simulation results: dashed lines-system with PSS; solid lines-system with PSS/UPFC

Power line flow and the sending bus voltage magnitude for cases 3b and 3c are shown in Fig. 6.7 and Fig. 6.8. These plots clearly show that the UPFC is capable of forcing a given power flow through the line and regulating the bus voltage under the dynamic conditions.

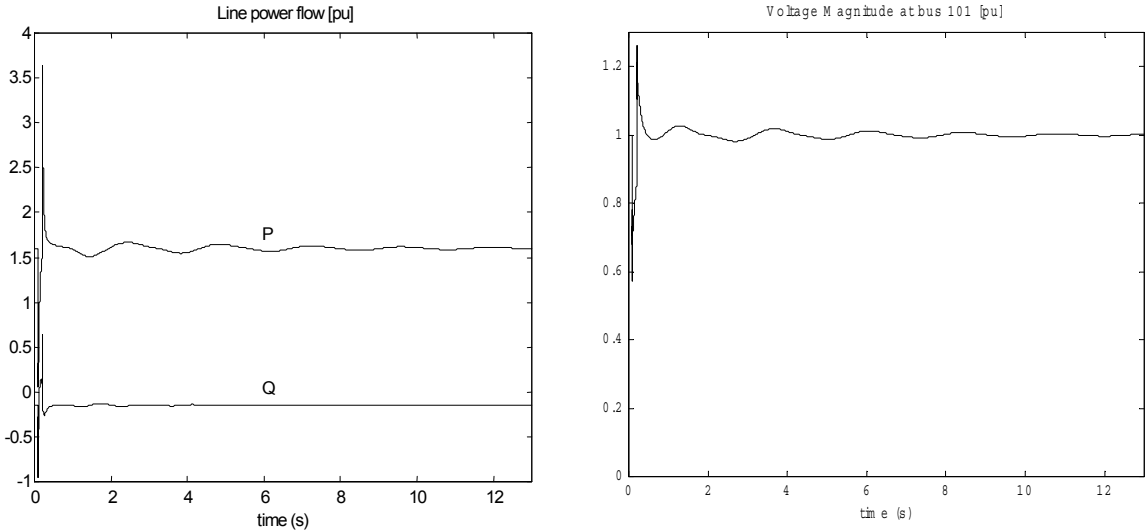


Fig. 6.7 Case 3 b: Nonlinear simulation results

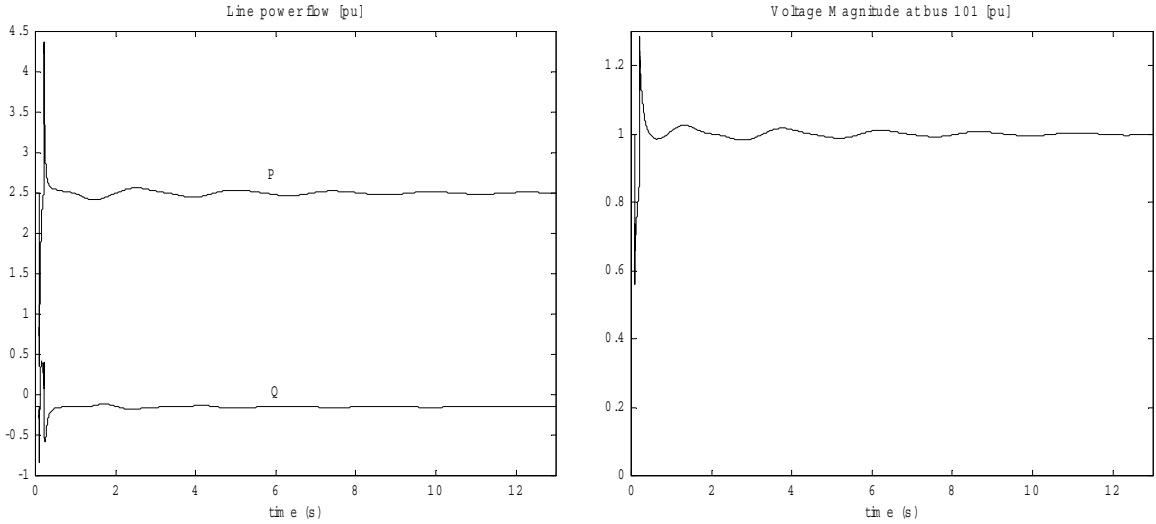


Fig. 6.8 Case 3 c: Nonlinear simulation results

4) Test system with the UPFC operated in the power oscillation damping control mode

In order to improve the power oscillation damping the UPFC is operated in the automatic power flow mode but with added damping control. To show the robustness of the proposed control scheme, based on fuzzy logic, discussed in the Chapter 5 different operating conditions were simulated. The real power that each interconnecting tie-line carries during pre-fault operating conditions, from area 1 to area 2, is given in Table 6.8.

Table 6.8 Operating conditions (values are in MW)

case	line 101 - 13	line 102 - 13	load bus 4	load bus 14
(a)	232	160	976	1767
(b)	24	160	1176	1567
(c)	143	250	976	1767
(d)	-232	-160	1767	976

The fuzzy damping controller is applied to the series converter side. The inputs to the controller are derived from the total real power flow P_t at the UPFC sending bus as shown in Fig. 6.1. The Max-Product inference engine was used and the centroid defuzzification method was applied. The results obtained with fuzzy controller are compared with those obtained with the lead-lag controller applied at the shunt converter side. Both, fuzzy and lead-lag damping controllers were designed for the first operating condition (case (a) in Table 6.8). Controller parameters are given in the Appendix A.

Table 6.9 shows dominant eigenvalues for the first operating condition. The critical eigenvalue is moved further to the left and the system becomes more stable.

Table 6.9 Dominant eigenvalues for the test system with the PSS and the UPFC operated in the power oscillation damping control mode

Eigenvalues	frequency	damping ratio
28: -1.3036 +(10.2216)i	1.627	0.127
29: -1.3036 +(-10.2216)i	1.627	0.127
30: -1.4126 +(7.0987)i	1.130	0.195
31: -1.4126 +(-7.0987)i	1.130	0.195
32: -1.0015 +(6.3031)i	1.003	0.157
33: -1.0015 +(-6.3031)i	1.003	0.157
38: -0.5546 +(3.7612)i	0.599	0.146
39: -0.5546 +(-3.7612)i	0.599	0.146
52: -0.2198 +(0.5770)i	0.092	0.356
53: -0.2198 +(-0.5770)i	0.092	0.356

Nonlinear simulation results show that the supplementary control signal greatly enhances the damping of all machines, and therefore system becomes more stable. Due to the similarities of the results only relative machine angle δ_{13} is depicted in Fig. 6.9. It can be

seen that the fuzzy damping controller performs better for different operating conditions than the conventional controller.

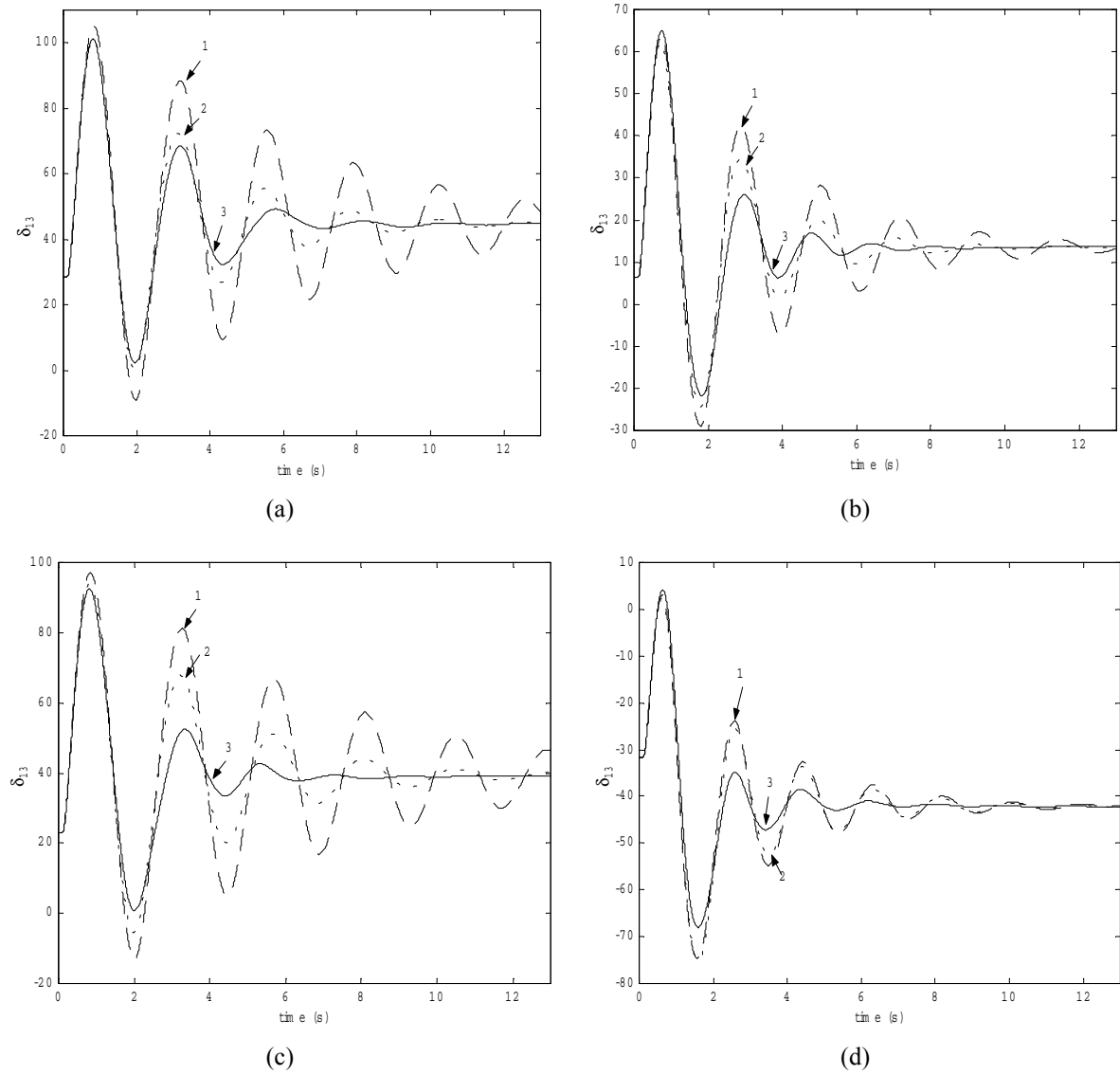


Fig. 6.9 Relative machine angle δ_{13} in degrees for operating conditions (a)-(d): 1 without damping controller ;2 lead-lag damping controller; 3 fuzzy damping controller

Chapter 7

CONCLUSION

This thesis deals with the FACTS device known as the Unified Power Flow Controller that is used to maintain and improve power system operation and stability. It presents UPFC steady-state, dynamic and linearized models, algorithm for interfacing the UPFC with the power network and UPFC basic and damping controller design.

To demonstrate various advantages of having the UPFC in the power system two-area-four-generator test system was simulated using the Power System Toolbox (PST). Since PST does not come with the UPFC included the software was modified in order to incorporate the proposed tools. The main advantage of the PST over other simulation packages is that its open frame allows new device models to be included simply by inserting a few new functions within the existing steady-state, transient stability and small signal analysis programs. Further on, conventional as well as intelligent control schemes can be applied easily. The trade off is the simulation time. The simulation time is function of the number of the time steps. Adding the new devices and increasing the system size increases the simulation time leading to the quite time consuming simulations.

To start the simulation MATLAB script file `s_simu` is called. It allows user to select the data file and the load flow (LF) analysis is performed. The convergence of the proposed LF algorithm depends on the convergence of the existing conventional LF algorithm and the initial guess for the real power injected into the sending bus. During the iterative procedure the real power injected into sending bus is adjusted in each step in order to cover the losses of the shunt and series impedances and to force the sum of converters' interaction to become zero. When transformer's losses are included convergence is usually obtained with the third LF solution. Neglecting the transformer's losses convergence is found within the first step.

Once the LF solution is found the non-linear simulation is performed. The simulation results demonstrate the validity of the proposed fundamental frequency model and the UPFC network-interfacing algorithm.

In order to operate the UPFC in the automatic control mode and to use the UPFC to damp low frequency oscillations two control designs: the UPFC basic control design and the damping controller design, were performed. It has been shown that the UPFC with its basic controllers is capable of controlling independently real and reactive power flow through the transmission line both in steady state and dynamic conditions. This feature cannot be accomplished with the mechanical and other FACTS devices. It has also been shown that UPFC can be used for voltage support and for improvement of transient stability of the entire electric power through a supplementary control loop. The proposed supplementary control based on the fuzzy logic is effective in damping power oscillations. The controller is decentralized since it requires only local measurement – the tie-line power flow at the UPFC location. Simulation results have shown that controller exhibits good damping characteristics for different operating conditions and compared to the conventional controller shows superior performance.

The results obtained in this thesis can be further improved by:

- Taking into consideration the effect of different input signals such as line current, difference in sending and receiving bus voltages phase angles, etc, on the damping controller performance
- Modifying s_simu program to include more than one UPFC
- Coordinating the UPFC with mechanical and other FACTS controllers.

REFERENCES

- [1] Anderson, P. M., Fouad, A.A., *Power System Control and Stability*, Iowa State University Press, 1977
- [2] Kundur, P., *Power System stability and Control*, McGraw-Hill Inc., 1994
- [3] Hingorani, N.G, Gyugyi,L., *Understanding FACTS Devices*, IEEE Press 2000
- [4] Hingorani, N.G., 'Flexible AC Transmission', *IEEE Spectrum*, April 1993, p. 40-44
- [5] Gyugyi, L., 'Dynamic Compensation of AC Transmission Lines by Solid-state Synchronous Voltage Sources', *IEEE*, 1993, p. 904-911
- [6] Edris, A. Mehraban, A.S., Rahman, M., Gyugyi, L., Arabi, S., Rietman, T., 'Controlling the Flow of Real and Reactive Power', *IEEE Computer Application in Power*, January 1998, p. 20-25
- [7] Gyugyi, L., 'A Unified Power Flow Control Concept for Flexible AC Transmission Systems', *IEE Proceedings-C*, Vol. 139, No. 4, July 1992, p. 323-331
- [8] Gyugyi, L., Schauder, C.D., Williams, S.L., Rietman, T.R., Torgerson, D.R., Edris, A., 'The Unified Power Flow Controller: A New Approach to Power Transmission Control', *IEEE Transactions on Power Delivery*, Vol. 10, No. 2, April 1995, p. 1085-1093
- [9] Noroozian, M., Angquist, L., Ghandhari, M., Andersson, G., 'Use of UPFC for Optimal Power Flow Control', *IEEE Transactions on Power Delivery*, Vol. 12, No. 4, October 1997, p. 1629-1634
- [10] Nabavi-Niaki, A., Iravani, M.R., 'Steady-state and Dynamic Models of Unified Power Flow Controller (UPFC) for Power System Studies', *IEEE Transactions of Power Systems*, Vol. 11, No. 4, November 1996, p. 1937-1943
- [11] Fuerte-Esquivel, C.R., Acha, E., 'Unified Power Flow Controller: A Critical Comparison of Newton-Raphson UPFC algorithms in Power Flow Studies', *IEE Proceedings Generation Transmission Distribution*, Vol. 144, No. 5, September 1997, p. 437-444
- [12] Fuerte-Esquivel, C.R., Acha, E., 'Newton-Raphson Algorithm for reliable Solution of Large Power Networks with Embedded FACTS Devices', *IEE Proceedings Generation Transmission Distribution*, Vol. 143, No. 5, September 1996, p. 447-454

- [13] Ambriz-Perez, H., Acha, E., Fuerte-Esquivel, C.R, De la Torre, A., 'Incorporation of a UPFC Model in an Optimal Power Flow Using Newton's Method', *IEE Proceedings Generation Transmission Distribution*, Vol. 145, No. 3, May 1998, p. 336-344
- [14] Schauder, C., Metha, H., 'Vector Analysis and Control of Advanced Static VAR Compensators', *IEE Proceedings-C*, Vol. 140, No. 4, July 1993, p. 299-306
- [15] Papic, I., Zunko, P., Povh, D., Weinhold, M., 'Basic Control of Unified Power Flow Controller', , *IEEE Transactions of Power Systems*, Vol. 12, No. 4, November 1997, p. 1734-1739
- [16] Smith, K.S., Ran, L., Penman, J., 'Dynamic Modeling of a Unified Power Flow Controller', *IEE Proceedings Generation Transmission Distribution*, Vol. 144, No. 1, January 1997, p. 7-12
- [17] Padiyar, K.R., Kulkarni, A.M., 'Control Design and Simulation of Unified Power Flow Controller', *IEEE Transactions on Power Delivery*, Vol. 13, No. 4, October 1997, p. 1348-1354
- [18] Wang, H.F., 'Damping Function of Unified Power Flow Controller', *IEE Proceedings Generation Transmission Distribution*, Vol. 146, No. 1, January 1999, p. 81-87
- [19] Wang, H.F., 'Applications of Modelling UPFC into Multi-machine Power Systems', *IEE Proceedings Generation Transmission Distribution*, Vol. 146, No. 3, May 1999, p. 306-312
- [20] Uzunovic, E., Canizares, C.A., Reeve, J., 'Fundamental Frequency Model of Unified Power Flow Controller', *North American Power Symposium*, NAPS, Cleveland, Ohio, October 1998
- [21] Uzunovic, E., Canizares, C.A., Reeve, J., 'EMTP Studies of UPFC Power Oscillation Damping', *Proceedings of the North American Power Symposium (NAPS)*, San Luis Obispo, CA, October 1999, pp. 405-410
- [22] Huang, Z., Ni, Y., Shen, C.M., Wu, F.F., Chen, S., Zhang, B., 'Application of Unified Power Flow Controller in Interconnected Power Systems -- Modeling, Interface, Control Strategy and Case Study', *IEEE Power Engineering Society Summer Meeting*, 1999
- [23] *Dynamic Tutorial and Functions*, Power System Toolbox Version 2.0, Cherry Tree Scientific Software, Ontario, Canada
- [24] Hiyama, T, Hubbi, W., Ortmeyer, Th., 'Fuzzy Logic Control Scheme with Variable Gain for Static Var Compensator to Enhance Power System Stability', *IEEE Transactions on Power Systems*, Vol. 14, No. 1, February 1999, pp. 186-191

- [25] Hiyama, T, 'Fuzzy Logic Switching of Thyristor Controlled Braking Resistor Considering Coordination with SVC', *IEEE Transactions on Power Delivery*, Vol. 10, No. 4, October 1995, pp. 2020-2026
- [26] Y.Y.Hsu, C.H.Cheng, 'Design of Fuzzy Power System Stabilizers for Multimachine Power Systems', *IEE Proceedings*, Vol. 137, Pt. C No. 3, May 1990, pp 233_238,
- [27] Hoang P., Tomsovic K., 'Design and Analysis of an Adaptive Fuzzy Power System Stabilizers', *IEEE Transactions on Energy Conversion*, Vol . 11, No. 2, June 1996
- [28] Toliyat H. A., Sadeh J., Ghazi R., 'Design of Augmented Fuzzy Logic Power System Stabilizers to Enhance Power Systems Stability', *IEEE Transactions on Energy Conversion*, Vol. 11, No. 1, March 1996
- [29] Cheng,S., Malik, O.P., Hope, G.S., 'Self Tuning Stabilizers for a Multimachine Power System', *IEE Proceedings*, Part C, No. 4, 1986, pp. 176-185
- [30] Kothari, M.L., Nanda, J., Bhattacharya, K., 'Design of Variable Structure power System Stabilizers with Desired Eigenvalues in the Sliding Mode', *IEE Proceedings*, Part C, Vol 140, No. 4, July 1993
- [31] Jantzen, J., 'Design of Fuzzy Controllers', Techn. Report No. 98-E 864 (design), Technical University of Denmark, Department of automation, 19. August 1998
- [32] Brogan, W.L., *Modern Control Theory*, Prentice Hall, 1985
- [33] Mohan N, Undeland T.M., Robbins, W.P., *Power Electronics: Converters, Applications and Design*, John Wiley & Sons, Inc.,1995

APPENDIX A

Test System and UPFC Data

PST - data file for the Two-area-four-machine/UPFC power system

```

%
% Two Area Test Case
% (two area - four machines)
% displaying results:1 no UPFC;2 UPFC + damping controller; 3 UPFC + fuzzy; 4 UPFC (step response
controller inputs);5 UPFC
disp_flag = 2;
% bus data format
% bus:
% col1 number
% col2 voltage magnitude(pu)
% col3 voltage angle(degree)
% col4 p_gen(pu)
% col5 q_gen(pu),
% col6 p_load(pu)
% col7 q_load(pu)
% col8 G shunt(pu)
% col9 B shunt(pu)
% col10 bus_type
%     bus_type - 1, swing bus
%               - 2, generator bus (PV bus)
%               - 3, load bus (PQ bus)
% col11 q_gen_max(pu)
% col12 q_gen_min(pu)
% col13 v_rated (kV)
% col14 v_max pu
% col15 v_min pu

% operating condition 1 (power flow on UPFC controlled line 1.6-0.15j)
bus = [ 1 1.03 0. 7.00 1.85 0.00 0.00 0.00 0.00 1 99.0 -99.0 22.0 1.1 .9;
        2 1.01 -9.7 7.00 2.35 0.00 0.00 0.00 0.00 2 5.0 -2.0 22.0 1.1 .9;
        3 0.9781 -6.1 0.00 2.00 0.00 0.00 0.00 0.00 3 0.0 0.0 500.0 1.5 .9;
        4 0.95 -10 0.00 0.00 9.76 1.00 0.00 0.00 3 0.0 0.0 115.0 1.05 .95;
        10 1.0103 12.1 0.00 0.00 0.00 0.00 0.00 0.00 3 0.0 0.0 230.0 1.5 .5;
        11 1.03 -6.8 7.19 1.76 0.00 0.00 0.00 0.00 2 5.0 -2.0 22.0 1.1 .9;
        12 1.01 -16.9 7.00 2.02 0.00 0.00 0.00 0.00 2 5.0 -2.0 22.0 1.1 .9;
        13 0.9899 -31.8 0.00 3.50 0.00 0.00 0.00 0.00 3 0.0 0.0 500.0 1.5 .9;
        14 0.95 -38 0.00 0.00 17.67 1.00 0.00 0.00 3 0.0 0.0 115.0 1.05 .95;
        20 0.9876 2.1 0.00 0.00 0.00 0.00 0.00 0.00 3 0.0 0.0 230.0 1.5 .9;
        101 1 -19.3 -1.6 8.00 0.00 0.00 0.00 0.00 2 99.0 -99.0 500.0 1.5 .9;
        102 1.05 -19.3 0.00 0.00 -1.6 .15 0.00 0.00 3 99.0 -99.0 500.0 1.5 .9;
        110 1.0125 -13.4 0.00 0.00 0.00 0.00 0.00 0.00 3 0.0 0.0 230.0 1.5 .9;
        120 0.9938 -23.6 0.00 0.00 0.00 0.00 0.00 0.00 3 0.0 0.0 230.0 1.5 .9 ];

% operating condition 2 (change in loads on buses 4 and 14)
bus = [ 1 1.03 0. 7.00 1.85 0.00 0.00 0.00 0.00 1 99.0 -99.0 22.0 1.1 .9;
        2 1.01 -9.7 7.00 2.35 0.00 0.00 0.00 0.00 2 5.0 -2.0 22.0 1.1 .9;
        3 0.9781 -6.1 0.00 2.00 0.00 0.00 0.00 0.00 3 0.0 0.0 500.0 1.5 .9;
        4 0.95 -10 0.00 0.00 11.76 1.00 0.00 0.00 3 0.0 0.0 115.0 1.05 .95;
        10 1.0103 12.1 0.00 0.00 0.00 0.00 0.00 0.00 3 0.0 0.0 230.0 1.5 .9;
        11 1.03 -6.8 7.19 1.76 0.00 0.00 0.00 0.00 2 5.0 -2.0 22.0 1.1 .9;
        12 1.01 -16.9 7.00 2.02 0.00 0.00 0.00 0.00 2 5.0 -2.0 22.0 1.1 .9;
        13 0.9899 -31.8 0.00 3.50 0.00 0.00 0.00 0.00 3 0.0 0.0 500.0 1.5 .9;
        14 0.95 -38 0.00 0.00 15.67 1.00 0.00 0.00 3 0.0 0.0 115.0 1.05 .95;
        20 0.9876 2.1 0.00 0.00 0.00 0.00 0.00 0.00 3 0.0 0.0 230.0 1.5 .9;
        101 1 -19.3 -1.6 8.00 0.00 0.00 0.00 0.00 2 99.0 -99.0 500.0 1.5 .9;
        102 1.05 -19.3 0.00 0.00 -1.6 .15 0.00 0.00 3 99.0 -99.0 500.0 1.5 .9;
        110 1.0125 -13.4 0.00 0.00 0.00 0.00 0.00 0.00 3 0.0 0.0 230.0 1.5 .9;
        120 0.9938 -23.6 0.00 0.00 0.00 0.00 0.00 0.00 3 0.0 0.0 230.0 1.5 .9 ]; %

operating condition 3 (:power flow on UPFC controlled line -1.6+0.15j)
bus = [ 1 1.03 0. 7.00 1.85 0.00 0.00 0.00 0.00 1 99.0 -99.0 22.0 1.1 .9;
        2 1.01 0 7.00 2.35 0.00 0.00 0.00 0.00 2 5.0 -2.0 22.0 1.1 .9;
        3 0.9781 0 0.00 2.00 0.00 0.00 0.00 0.00 3 0.0 0.0 500.0 1.5 .9;
        4 0.95 0 0.00 0.00 17.67 1.00 0.00 0.00 3 0.0 0.0 115.0 1.05 .95;
        10 1.0103 0 0.00 0.00 0.00 0.00 0.00 0.00 3 0.0 0.0 230.0 1.5 .9;
        11 1.03 0 7.19 1.76 0.00 0.00 0.00 0.00 2 5.0 -2.0 22.0 1.1 .9;

```

```

12 1.01 0 7.00 2.02 0.00 0.00 0.00 0.00 2 5.0 -2.0 22.0 1.1 .9;
13 0.9899 0 0.00 3.50 0.00 0.00 0.00 0.00 3 0.0 0.0 500.0 1.5 .9;
14 0.95 0 0.00 0.00 9.76 1.00 0.00 0.00 3 0.0 0.0 115.0 1.05 .95;
20 0.9876 0 0.00 0.00 0.00 0.00 0.00 0.00 3 0.0 0.0 230.0 1.5 .9;
101 1 0 1.6 8.00 0.00 0.00 0.00 0.00 2 99.0 -99.0 500.0 1.5 .9;
102 1.05 0 0.00 0.00 1.6 -.15 0.00 0.00 3 99.0 -99.0 500.0 1.5 .9;
110 1.0125 0 0.00 0.00 0.00 0.00 0.00 0.00 3 0.0 0.0 230.0 1.5 .9;
120 0.9938 0 0.00 0.00 0.00 0.00 0.00 0.00 3 0.0 0.0 230.0 1.5 .9 ];
% operating condition 4(power flow on UPFC controlled line 2.5-0.15j)
bus = [1 1.03 0 7.00 1.85 0.00 0.00 0.00 0.00 1 99.0 -99.0 22.0 1.1 .9;
2 1.01 -9.7 7.00 2.35 0.00 0.00 0.00 0.00 2 5.0 -2.0 22.0 1.1 .9;
3 0.9781 -6.1 0.00 2.00 0.00 0.00 0.00 0.00 3 0.0 0.0 500.0 1.5 .9;
4 0.95 -10 0.00 0.00 9.76 1.00 0.00 0.00 3 0.0 0.0 115.0 1.05 .95;
10 1.0103 12.1 0.00 0.00 0.00 0.00 0.00 0.00 3 0.0 0.0 230.0 1.5 .5;
11 1.03 -6.8 7.19 1.76 0.00 0.00 0.00 0.00 2 5.0 -2.0 22.0 1.1 .9;
12 1.01 -16.9 7.00 2.02 0.00 0.00 0.00 0.00 2 5.0 -2.0 22.0 1.1 .9;
13 0.9899 -31.8 0.00 3.50 0.00 0.00 0.00 0.00 3 0.0 0.0 500.0 1.5 .9;
14 0.95 -38 0.00 0.00 17.67 1.00 0.00 0.00 3 0.0 0.0 115.0 1.05 .95;
20 0.9876 2.1 0.00 0.00 0.00 0.00 0.00 0.00 3 0.0 0.0 230.0 1.5 .9;
101 1 -19.3 -2.5 8.00 0.00 0.00 0.00 0.00 2 99.0 -99.0 500.0 1.5 .9;
102 1.05 -19.3 0.00 0.00 -2.5 .15 0.00 0.00 3 99.0 -99.0 500.0 1.5 .9;
110 1.0125 -13.4 0.00 0.00 0.00 0.00 0.00 0.00 3 0.0 0.0 230.0 1.5 .9;
120 0.9938 -23.6 0.00 0.00 0.00 0.00 0.00 0.00 3 0.0 0.0 230.0 1.5 .9 ];
% operating condition 5 (power flow on UPFC controlled line 1.97-0.15j)
bus = [1 1.03 0 7.00 1.85 0.00 0.00 0.00 0.00 1 99.0 -99.0 22.0 1.1 .9;
2 1.01 -9.7 7.00 2.35 0.00 0.00 0.00 0.00 2 5.0 -2.0 22.0 1.1 .9;
3 0.9781 -6.1 0.00 2.00 0.00 0.00 0.00 0.00 3 0.0 0.0 500.0 1.5 .9;
4 0.95 -10 0.00 0.00 9.76 1.00 0.00 0.00 3 0.0 0.0 115.0 1.05 .95;
10 1.0103 12.1 0.00 0.00 0.00 0.00 0.00 0.00 3 0.0 0.0 230.0 1.5 .5;
11 1.03 -6.8 7.19 1.76 0.00 0.00 0.00 0.00 2 5.0 -2.0 22.0 1.1 .9;
12 1.01 -16.9 7.00 2.02 0.00 0.00 0.00 0.00 2 5.0 -2.0 22.0 1.1 .9;
13 0.9899 -31.8 0.00 3.50 0.00 0.00 0.00 0.00 3 0.0 0.0 500.0 1.5 .9;
14 0.95 -38 0.00 0.00 17.67 1.00 0.00 0.00 3 0.0 0.0 115.0 1.05 .95;
20 0.9876 2.1 0.00 0.00 0.00 0.00 0.00 0.00 3 0.0 0.0 230.0 1.5 .9;
101 1 -19.3 -1.97 8.00 0.00 0.00 0.00 0.00 2 99.0 -99.0 500.0 1.5 .9;
102 1.05 -19.3 0.00 0.00 -1.97 .15 0.00 0.00 3 99.0 -99.0 500.0 1.5 .9;
110 1.0125 -13.4 0.00 0.00 0.00 0.00 0.00 0.00 3 0.0 0.0 230.0 1.5 .9;
120 0.9938 -23.6 0.00 0.00 0.00 0.00 0.00 0.00 3 0.0 0.0 230.0 1.5 .9 ];
% line data format
% line: from bus, to bus, resistance(pu), reactance(pu),
% line charging(pu), tap ratio, tap phase, tapmax, tapmin, tapsize
line = [...
1 10 0.0 0.0167 0.00 1.0 0.0 0.0 0.0;
2 20 0.0 0.0167 0.00 1.0 0.0 0.0 0.0;
3 4 0.0 0.005 0.00 1.0 0.1.2 0.8 0.05;
3 20 0.001 0.0100 0.0175 1.0 0.0 0.0 0.0;
3 101 0.011 0.110 0.1925 1.0 0.0 0.0 0.0;
3 101 0.011 0.110 0.1925 1.0 0.0 0.0 0.0;
10 20 0.0025 0.025 0.0437 1.0 0.0 0.0 0.0;
11 110 0.0 0.0167 0.0 1.0 0.0 0.0 0.0;
12 120 0.0 0.0167 0.0 1.0 0.0 0.0 0.0;
13 14 0.0 0.005 0.00 1.0 0.1.2 0.8 0.05;
13 101 0.011 0.11 0.1925 1.0 0.0 0.0 0.0;
13 102 0.011 0.11 0.1925 1.0 0.0 0.0 0.0;
13 120 0.001 0.01 0.0175 1.0 0.0 0.0 0.0;
110 120 0.0025 0.025 0.0437 1.0 0.0 0.0 0.0];
% Machine data format
% Machine data format
% 1. machine number,
% 2. bus number,
% 3. base mva,
% 4. leakage reactance x_l(pu),
% 5. resistance r_a(pu),
% 6. d-axis synchronous reactance x_d(pu),
% 7. d-axis transient reactance x'_d(pu),
% 8. d-axis subtransient reactance x''_d(pu),
% 9. d-axis open-circuit time constant T'_do(sec),
% 10. d-axis open-circuit subtransient time constant
% T''_do(sec),
% 11. q-axis synchronous reactance x_q(pu),
% 12. q-axis transient reactance x'_q(pu),
% 13. q-axis subtransient reactance x''_q(pu),
% 14. q-axis open-circuit time constant T'_go(sec),
% 15. q-axis open circuit subtransient time constant
% T''_go(sec),
% 16. inertia constant H(sec),
% 17. damping coefficient d_o(pu),
% 18. damping coefficient d_l(pu),
% 19. bus number

```

```

%
% note: all the following machines use sub-transient model
mac_con = [...
1 1 900 0.200 0.0025 1.8 0.30 0.25 8.00 0.03 1.7 0.55 0.25 0.4 0.05 6.5 0 0 1;
2 2 900 0.200 0.0025 1.8 0.30 0.25 8.00 0.03 1.7 0.55 0.25 0.4 0.05 6.5 0 0 2;
3 11 900 0.200 0.0025 1.8 0.30 0.25 8.00 0.03 1.7 0.55 0.25 0.4 0.05 6.175 0 0 11;
4 12 900 0.200 0.0025 1.8 0.30 0.25 8.00 0.03 1.7 0.55 0.25 0.4 0.05 6.175 0 0 12];

% exciter configuration
exc_con = [...
1 1 0.01 46.0 0.06 0.00 0.0 1.00 -0.9 0.0 0.46 3.10 0.330 2.30 0.100 0.10 1.00 0.00 0.0 0.00;
3 2 0.01 7.04 1.00 6.67 1.0 10.00 -10.0 0.2 -0.2 200.00 4.370 20.00 4.830 0.09 1.10 8.63 1.0 6.53;
0 3 0.01 200.0 0.00 0.00 0.0 5.00 -5.0 0.0 0.0 0.00 0.000 0.00 0.000 0.00 0.00 0.00 0.0 0.00;
2 4 0.01 300.0 0.01 0.00 0.0 4.95 -4.9 1.0 1.33 3.05 0.279 2.29 0.117 0.10 0.675 0.00 0.0 0.00;

% pss on exciter 2 and 3
pss_con = [...
1 2 300.0 20.0 0.1 0.02 0.1 0.02 0.2 -0.05;
1 3 300.0 20.0 0.06 0.04 0.08 0.04 0.2 -0.05];

% governor model
% tg_con matrix format
% column data unit
% 1 turbine model number (=1)
% 2 machine number
% 3 speed set point wf pu
% 4 steady state gain 1/R pu
% 5 maximum power order Tmax pu on generator base
% 6 servo time constant Ts sec
% 7 governor time constant Tc sec
% 8 transient gain time constant T3 sec
% 9 HP section time constant T4 sec
% 10 reheater time constant T5 sec
tg_con = [...
1 1 1 25.0 1.0 0.1 0.5 0.0 1.25 5.0;
1 2 1 25.0 1.0 0.1 0.5 0.0 1.25 5.0;
1 3 1 25.0 1.0 0.1 0.5 0.0 1.25 5.0;
1 4 1 25.0 1.0 0.1 0.5 0.0 1.25 5.0];

% non-conforming load
% col 1 bus number
% col 2 fraction const real power load
% col 3 fraction const reactive power load
% col 4 fraction const real current load
% col 5 fraction const reactive current load
load_con = [...
101 0 0 0 0;
102 0 0 0 0];

% upfc_con
% 1 - upfc number
% 2 - sending bus
% 3 - receiving bus
% 4 - shunt transformer resistance
% 5 - shunt transformer reactance
% 6 - series transformer resistance
% 7 - series transformer reactance
% 8 - shunt transformer turn ratio (n_sh)
% 9 - series transformer turn ratio (n_se)
% 10 - DC voltage (reference)
% 11 - capacitance (C)
% 12 - base voltage (Vb)
% 13 - 0
% 14 - 0
% 15 - line reactance
% 16 - number of UPFC states
% 1 - Vdc only
% 2 - Vdc, Vp1, Vq1, Upfc_PI_Vs, Upfc_PI_dc
% 17 - mode
% 1 - nonlinear simulation
% 1 - linearising
% 3 - input response
% 18 - way of forming A,B,C (upfc_con==1)
% 1 - state Vdc only: A=a_mat, B=[upfc], C=[upfc]
% 2 - state Vdc and expand system by PI-controllers (B,C based on UPFC)
% 3 - state Vdc and expand system by PI-controllers (B,C based on TG, EXC, UPFC)
% 4 - upfc_con == 1, closed loop approach
%

upfc_con = [ 1 101 102 0 .00025/5 0 .05 .0295 .088 22000 .055 220e3 0 0 .11 2 1 4];
upfc_con(5) = upfc_con(5) / upfc_con(8)^2;

```

```

% UPFC lead lag damping controller
% 1 - upfc damping controller type (1 - speed input, 2 - power input)
% 2 - machine number
% 3 - gain K
% 4 - washout time constant T
% 5 - lead time constant T1
% 6 - lag time constant T2
% 7 - lead time constant T3
% 8 - lag time constant T4
% 9 - maximum output limit
% 10 - minimum output limit
% 11 - UPFC number
% 12 - gain kf PT1 filter
% 13 - time constant Tf PT1 filter
% 14 - 1 - placed on shunt, 2 - placed on series
%upfc_damp = [2 1 15 10 0.02 0.01 0.02 0.01 0.25 -0.25 1 1 0 1]

%UPFC fuzzy damping controller
% col 1 upfc number
% col 2 maximum real power signal Pmax(pu)
% col 3 minimum real power signal Pmin(pu)
% col 4 scaling factor for output
% col 5 scaling factor for input 1
% col 6 scaling factor for input 2
% col 7 dP washout filter time constant
% col 8 dE washout filter time constant
% col 9 upfc dP-value controlled by:
%
% 1 = fuzzy logic controller based on real power flow,
% col 10 1:placed on shunt; 2:placed on series
% col 11 bus no. for line power measurement (0 = not used)
%upfcF_con1 = [1 1.00 -1.00 0.9 1 0.25 1.7 1. 1 2 13];

% upfc_ctrl
% 1 - controller type
% 0 - no controller
% 1 - P type
% 2 - PT1 type
% 3 - I type
% 4 - Basic control:
% series:
% 1. line P/Q (pq-mode using PI), or
% 2. series compensation (PT1)
% 3. Vr/Vs (PI)
% 4. angle between Vr and Vs
% shunt:
% - Vs and Vdc using PI-controllers
% 5 - shunt current controller
% 6 - decoupled line P/Q and Vs/Vdc using PIs
% 7 - LQ regulator for line P/Q and LQR for Vs/Vdc (using PIs to get reference values)
% 2 - Vs_ref
% 3 - Vs_flag
% 0 - Vs not controlled
% 1 - Vs controlled
% 4 - P_ref
% 5 - Q_ref
% 6 - constant K_PI_dc
% 7 - time constant T_PI_dc
% 8 - constant K_PI_Vs
% 9 - time constant T_PI_Vs
% 10 - constant k_PT1_Vp1
% 11 - time constant T_PT1_Vp1
% 12 - constant k_PT1_Vq1
% 13 - time constant T_PT1_Vq1
% 14 - time constant T_Vp2
% 15 - time constant T_Vq2
% 16 - prop. constant K ref
% 17 - prop. constant k_PI_V3
% 18 - time constant T_PI_V3
% 19 - n_ref (Vr/Vs)
% 20 - constant K_PI_V4
% 21 - time constant T_PI_V4
% 22 - alpha_ref (thetaR - thetaS) [deg]
%% OC 1 2
upfc_ctrl = [4 1 1 1.60 -.15 8 .3 1. .05 .1 .1 .1 .1 .001 0.02 0.4 1 1 1 1 100 .005];
% OC 3
upfc_ctrl = [4 1 1 -1.60 .15 8 .3 1. .05 .1 .1 .1 .1 .001 0.02 0.4 1 1 1 1 100 .005];
% OC 4
upfc_ctrl = [4 1 1 2.50 -.15 8 .3 1. .05 .1 .1 .1 .1 .001 0.02 0.4 1 1 1 1 100 .005];

```

```

% OC 5
%upfc_ctrl = [4 1 1 1.97 -.15 8 .3 1. .05 .1 .1 .1 .1 .001 0.02 0.4 1 1 1 1 100 .005];

% upfc_weight (if controller type 4 is used) to determine active mode
% 1 - weight on Vp1, Vq1 (line P/Q)
% 2 - weight on Vp2, Vq2 (series compensation)
% 3 - weight on Vp3=0, Vq3 (Vr/Vs)
% 4 - weight on Vp4, Vq3=0 (angle(Vr)-angle(Vs))
upfc_weight = [1 0 0 0];

% changing P/Q reference values
% upfc_sim: each row contains time/Pref and time/Qref pair
% col 1: time Pref is applied
% col 2: Pref to be applied
% col 3: time Qref is applied
% col 4: Qref to be applied
% col 5: time nref is applied nref=|Vr|/|Vs|
% col 6: nref to be applied
% col 7: time alpha is applied alpha_ref=ang(Vr)-ang(Vs)
% col 8: alpha to be applied
% last row: time > Tend of simulation
upfc_sim = ...
[0.1 1.8 4.5 -.2 0 0 0 0;
 1.5 1.3 6.0 .2 0 0 0 0;
 3.0 1.6 20 0 0 0 0 0;
 20. 1.6 0 0 0 0 0 0;
 20 0 0 0 0 0 0 0];

%Switching file defines the simulation control
% row 1 col1 simulation start time (s) (cols 2 to 6 zeros)
% col7 initial time step (s)
% row 2 col1 fault application time (s)
% col2 bus number at which fault is applied
% col3 bus number defining far end of faulted line
% col4 zero sequence impedance in pu on system base
% col5 negative sequence impedance in pu on system base
% col6 type of fault - 0 three phase
% - 1 line to ground
% - 2 line-to-line to ground
% - 3 line-to-line
% - 4 loss of line with no fault
% - 5 loss of load at bus
% col7 time step for fault period (s)
% row 3 col1 near end fault clearing time (s) (cols 2 to 6 zeros)
% col7 time step for second part of fault (s)
% row 4 col1 far end fault clearing time (s) (cols 2 to 6 zeros)
% col7 time step for fault cleared simulation (s)
% row 5 col1 time to change step length (s)
% col7 time step (s)
% row n col1 finishing time (s) (n indicates that intermediate rows may be inserted)
% FAULT simulation
sw_con = [...
0 0 0 0 0 0 0.01; % sets initial time step
.1 3 101 0 0 0 0.0005; % apply three phase fault at bus 3, on line 3-101
.20 0 0 0 0 0 0.00001; % clear fault at bus 3
.20001 0 0 0 0 0 0.0005; % clear remote end
1.5 0 0 0 0 0 0.001; % change time step
10.0 0 0 0 0 0 0.002; % change time step
13. 0 0 0 0 0 0.0001; % end

```

APPENDIX B

Load Flow Solution

Table B.1 and Table B.2 show solved load flow and the UPFC steady state quantities for two-area/UPFC test system for the case when UPFC is operated to control line power flow at 1.6-0.15j pu at the receiving bus and to regulate the sending bus voltage at 1pu. Series and shunt transformer reactances are set to 0.01 pu.

Table B.1 Load flow solution

LOAD-FLOW STUDY							
REPORT OF POWER FLOW CALCULATIONS							
SWING BUS	: BUS 1						
NUMBER OF ITERATIONS	: 2						
SOLUTION TIME	: 0 sec.						
TOTAL TIME	: 0.11 sec.						
TOTAL REAL POWER LOSSES	: 0.866219.						
TOTAL REACTIVE POWER LOSSES:	13.426.						
				GENERATION		LOAD	
BUS	VOLTS	ANGLE	REAL	REACTIVE	REAL	REACTIVE	
1.0000	1.0300	0	7.1603	1.7847	0	0	
2.0000	1.0100	-10.1268	7.0000	2.0942	0	0	
3.0000	0.9691	-25.3159	0	2.0000	-0.0000	0.0000	
4.0000	0.9625	-28.3149	0	0	9.7600	1.0000	
10.0000	1.0078	-6.6151	0	0	0.0000	0.0000	
11.0000	1.0300	-28.2791	7.1900	1.9906	0	0	
12.0000	1.0100	-38.5345	7.0000	2.5715	0	0	
13.0000	0.9551	-53.9507	0	3.5000	0.0000	0.0000	
14.0000	0.9965	-59.0099	0	0	17.6700	1.0000	
20.0000	0.9822	-16.8942	0	0	-0.0000	-0.0000	
101.0000	1.0000	-38.8167	-1.6541	1.6350	0	0	
102.0000	0.9480	-42.6972	0	0	-1.6000	0.1500	
110.0000	1.0045	-34.9434	0	0	-0.0000	-0.0000	
120.0000	0.9744	-45.3566	0	0	-0.0000	-0.0000	
LINE FLOWS							
LINE	FROM BUS	TO BUS	REAL	REACTIVE			
1.0000	1.0000	10.0000	7.1603	1.7847			
2.0000	2.0000	20.0000	7.0000	2.0942			
3.0000	3.0000	4.0000	9.7600	1.5195			
4.0000	3.0000	20.0000	-13.8269	1.1262			
5.0000	3.0000	101.0000	2.0335	-0.3228			
6.0000	3.0000	101.0000	2.0335	-0.3228			
7.0000	10.0000	20.0000	7.1603	0.9275			
8.0000	11.0000	110.0000	7.1900	1.9906			
9.0000	12.0000	120.0000	7.0000	2.5715			
10.0000	13.0000	14.0000	17.6700	2.5772			
11.0000	13.0000	101.0000	-2.2533	0.0491			
12.0000	13.0000	102.0000	-1.5686	0.2895			
13.0000	13.0000	120.0000	-13.8481	0.5841			
14.0000	110.0000	120.0000	7.1900	1.1145			
1.0000	10.0000	1.0000	-7.1603	-0.9275			
2.0000	20.0000	2.0000	-7.0000	-1.2202			
3.0000	4.0000	3.0000	-9.7600	-1.0000			
4.0000	20.0000	3.0000	14.0319	0.9067			
5.0000	101.0000	3.0000	-1.9844	0.6269			
6.0000	101.0000	3.0000	-1.9844	0.6269			
7.0000	20.0000	10.0000	-7.0319	0.3135			
8.0000	110.0000	11.0000	-7.1900	-1.1145			
9.0000	120.0000	12.0000	-7.0000	-1.6611			
10.0000	14.0000	13.0000	-17.6700	-1.0000			
11.0000	101.0000	13.0000	2.3147	0.3813			
12.0000	102.0000	13.0000	1.6000	-0.1500			
13.0000	120.0000	13.0000	14.0587	1.5056			
14.0000	120.0000	110.0000	-7.0587	0.1555			
Load Flow after 3 steps, remaining Psh-Pse = 1.576e-005.							

Table B.2 UPFC steady-state quantities

```
UPFC data (calculated):  
  
bus voltage Vs:  
real(f) = 0.779 [pu] imag(f) = -0.627 [pu] |f| = 1.000 [pu] arg(f) = -38.817 [deg]  
bus voltage Vr:  
real(f) = 0.697 [pu] imag(f) = -0.643 [pu] |f| = 0.948 [pu] arg(f) = -42.697 [deg]  
Flow on the line (as specified in the load flow data):  
From Receiving to Sending bus (1 phase) :  
real(f) = -1.600 [pu] imag(f) = 0.150 [pu] |f| = 1.607 [pu] arg(f) = 174.644 [deg]  
Total power injection at Sending bus (1 phase):  
real(f) = -1.654 [pu] imag(f) = 1.635 [pu] |f| = 2.326 [pu] arg(f) = 135.332 [deg]  
Line current from sending to receiving bus :  
real(f) = 1.348 [pu] imag(f) = -1.028 [pu] |f| = 1.695 [pu] arg(f) = -37.341 [deg]  
Total current at sending bus :  
real(f) = 2.314 [pu] imag(f) = 0.237 [pu] |f| = 2.326 [pu] arg(f) = 5.851 [deg]  
Current into shunt converter :  
real(f) = 0.966 [pu] imag(f) = 1.265 [pu] |f| = 1.592 [pu] arg(f) = 52.6333 [deg]  
Voltage drops due to impedances:  
series:  
real(f) = 0.065 [pu] imag(f) = 0.057 [pu] |f| = 0.086 [pu] arg(f) = 41.349 [deg]  
shunt:  
real(f) = 0.063 [pu] imag(f) = -0.068 [pu] |f| = 0.093 [pu] arg(f) = -47.229 [deg]  
Losses due to impedances:  
series:  
real(f) = 0.029 [pu] imag(f) = 0.144 [pu] |f| = 0.147 [pu] arg(f) = 78.690 [deg]  
shunt:  
real(f) = 0.025 [pu] imag(f) = 0.146 [pu] |f| = 0.148 [pu] arg(f) = 80.127 [deg]  
Injected voltages:  
series :  
real(f) = -0.01755 [pu] imag(f) = 0.04109 [pu] |f| = 0.04469 [pu] arg(f) = 113.131 [deg]  
shunt :  
real(f) = 0.84220 [pu] imag(f) = -0.69498 [pu] |f| = 1.09192 [pu] arg(f) = -39.529 [deg]  
Converter consumption:  
series :  
real(f) = 0.06592 [pu] imag(f) = -0.03734 [pu] |f| = 0.076 [pu] arg(f) = -29.528 [deg]  
shunt :  
real(f) = -0.06593 [pu] imag(f) = -1.73694 [pu] |f| = 1.738 [pu] arg(f) = -92.174 [deg]
```

APPENDIX C

Two-machine/UPFC power system: Linearized Model

Equations for this system are derived following the approach discussed in the fourth chapter. They are given in the m-file shown bellow.

```
% Case Study: Two machine/UPFC power system
% PST data file: Linearized power system d2a_upfcSM1
% note: run s_simul to get initial values
jay = sqrt(-1);
%
Vb = 230e3;
Sb = 100e6;
%
% Machine data format
% Machine data format
% 1. machine number,
% 2. bus number,
% 3. base mva,
% 4. leakage reactance x_l(pu),
% 5. resistance r_a(pu),
% 6. d-axis synchronous reactance x_d(pu),
% 7. d-axis transient reactance x'_d(pu),
% 8. d-axis subtransient reactance x''_d(pu),
% 9. d-axis open-circuit time constant T'_do(sec),
% 10. d-axis open-circuit subtransient time constant
%     T''_do(sec),
% 11. q-axis synchronous reactance x_q(pu),
% 12. q-axis transient reactance x'_q(pu),
% 13. q-axis subtransient reactance x''_q(pu),
% 14. q-axis open-circuit time constant T'_qo(sec),
% 15. q-axis open circuit subtransient time constant
%     T''_qo(sec),
% 16. inertia constant H(sec),
% 17. damping coefficient d_o(pu),
% 18. damping coefficient d_l(pu),
% 19. bus number
%
% note: all the following machines use sub-transient model
%1 2 3 4 5 6 7 8 9 10 1 2 3 4 5 6 7 8 9
mac_con = [ ...
1 1 900 0.200 0.0025 1.8 0.30 0.0 8.00 0.03 1.7 0.30 0.0 0.4 0.05 6.5 0 0 1;
2 2 900 0.200 0.0025 1.8 0.30 0.0 8.00 0.03 1.7 0.30 0.0 0.4 0.05 6.5 0 0 2];
% 1 - upfc number
% 2 - sending bus
% 3 - receiving bus
% 4 - shunt transformer resistance
% 5 - shunt transformer reactance
% 6 - series transformer resistance
% 7 - series transformer reactance
% 8 - shunt transformer turn ratio (n_sh)
% 9 - series transformer turn ratio (n_se)
% 10 - DC voltage (reference)
% 11 - capacitance (C)
% 12 - base voltage (Vb)
% 13 -
% 14 -
% 15 - line reactance
% 16 - number of UPFC states
% 1 - Vdc only
% 2 - Vdc, Vp1, Vq1, Upfc_PI_Vs, Upfc_PI_dc
% 17 - mode
% 1 - nonlinear simulation
% 2 - linearising
% 3 - input response
% 18 - way of forming A,B,C (upfc_con==1)
% 1 - state Vdc only: A=a_mat, B=[upfc], C=[upfc]
% 2 - state Vdc and expand system by PI-controllers (B,C based on UPFC)
% 3 - state Vdc and expand system by PI-controllers (B,C based on TG, EXC, UPFC)
% 4 - upfc_con == 1, closed loop approach (2nd)
% x - upfc_con == 2, closed loop approach (1st)
```

```

upfc_con = [ 1 3 4 0 .00025/.05^2 0 .05 .05 .25 31000 .055 230e3 .2 .2 .11 1 2 1];
xSH = upfc_con(5);
xSE = upfc_con(7);
% transform generator data to system base
SM1 = basmva./mac_con(1,3);
SM2 = basmva./mac_con(2,3);
Tq0 = [mac_con(1,14) 0; 0 mac_con(2,14)];
Td0 = [mac_con(1,9) 0; 0 mac_con(2,9)];
Xqgp = [(mac_con(1,11)- mac_con(1,12))*SM1 0; 0 (mac_con(2,11)- mac_con(2,12))*SM2];
Xdgp = [(mac_con(1,6) - mac_con(1,7))*SM1 0; 0 (mac_con(2,6) - mac_con(2,7))*SM2];
Xqdp = [(mac_con(1,12)- mac_con(1,7))*SM1 0; 0 (mac_con(2,12)- mac_con(2,7))*SM2];
H = [mac_con(1,16)/SM1 0; 0 mac_con(2,16)/SM2 ];
wb = 2*pi*60;
Da = [mac_con(1,17) 0; 0 mac_con(2,17)];
Xgp = diag([mac_con(1,12)*SM1, mac_con(2,12)*SM2]);
Xdp = diag([mac_con(1,7)*SM1, mac_con(2,7)*SM2]);
r = diag([mac_con(1,5)*SM1, mac_con(2,5)*SM2]);
% exciter (not used)
exc_con = [1 2 0.01 20.0 .06 0 0 1.0 -0.9 0.0 0.46 3.1 0.33 2.3 0.1 0.1 2.0 0 0 0];
Ta = diag([1e10 exc_con(5)]);
Ka = diag([0 exc_con(4)]);
% Y bus
% reduced Y-bus as computed by s_simul
Ygg = Y_gprf;
Ygu = Y_gncprf;
Yug = Y_ncgprf;
Yuu = Y_ncprf;
%
Ybusred = [Ygg Ygu; Yug Yuu];
% Y matrices for upfc
Wu = [jay*(1/xSH+1/xSE) -jay/xSE;
      -jay/xSE jay/xSE];
Wc = [-jay/xSH jay/xSE;
      0 -jay/xSE];

Lg = inv(Wu-Yuu)*Yug;
Lc = -inv(Wu-Yuu)*Wc;
Mg = Ygg+Ygu*Lg;
Mc = Ygu*Lc;
Mg1 = Yug+Yuu*Lg;
Mcl = Yuu*Lc;
% form Y bus for internal gen. voltages and UPFC VSC voltages
Y = [Mg Mc; Mg1 Mcl];
Ym = abs(Y);
Ya = angle(Y);
%
% LF solution
%
Vsh0 = V_SH(1);
Vse0 = V_SE(1);
mSH0 = mSH(1); mSE0 = mSE(1);
phisH0 = phiSH(1); phise0 = phiSE(1);

Vsh0dq = [-imag(Vsh0); real(Vsh0) ];
Vse0dq = [-imag(Vse0); real(Vse0) ];
%
bus_v0 = bus_v(:,1);
dS0 = angle(bus_v0(bus_int(upfc_con(:,2))));
dSH0 = dS0 - phisH0;
dSE0 = dS0 - phise0;
%
Epd0 = eqprime(:,1);
Epd0 = edprime(:,1);
%
dG0 = mac_ang(:,1);
d120 = dG0(1) - dG0(2);
%
Iupfc_se0 = Iupfc_se(:,1);
Iupfc_sh0 = Iupfc_sh(:,1);

Iu10 = -Iupfc_se0 - Iupfc_sh0;
Iu20 = Iupfc_se0;
Iuq0 = [ real(Iu10); real(Iu20)];
Iud0 = [-imag(Iu10); -imag(Iu20)];
%
Igg0 = curq(:,1);
Igd0 = curd(:,1);
Vd0 = Xdp*Igg0+Epd0-r*Igd0;
Vq0 = -Xdp*Igd0+Epd0-r*Igg0;
Vt0 = sqrt(Vd0.^2 + Vq0.^2);
P1 = diag(Vd0./Vt0);

```

```

P2 = diag(Vq0./Vt0);
%
Vdc0 = upfc_con(10);
nSH = upfc_con(8);
nSE = upfc_con(9);
%
% matrices
%
Q1 = [Ym(1,1)*cos(Ya(1,1)) Ym(1,2)*cos(Ya(1,2)-d120);Ym(2,1)*cos(Ya(2,1)+d120) Ym(2,2)*cos(Ya(2,2))];
D1 = [-Ym(1,1)*sin(Ya(1,1)) -Ym(1,2)*sin(Ya(1,2)-d120);-Ym(2,1)*sin(Ya(2,1)+d120) -Ym(2,2)*sin(Ya(2,2))];
%
Q2 = -D1;
D2 = Q1;
%
Q3(1,1) = Ym(1,2)*(-cos(Ya(1,2)-d120)*Epd0(2)+sin(Ya(1,2)-d120)*Epc0(2))+...
-Ym(1,3)*cos(Ya(1,3)-dG0(1))*Vsh0dq(1)+Ym(1,3)*sin(Ya(1,3)-dG0(1))*Vsh0dq(2)+...
-Ym(1,4)*cos(Ya(1,4)-dG0(1))*Vse0dq(1)+Ym(1,4)*sin(Ya(1,4)-dG0(1))*Vse0dq(2);
Q3(2,2) = Ym(2,1)*(-cos(Ya(2,1)+d120)*Epd0(1)+sin(Ya(2,1)+d120)*Epc0(1))+...
-Ym(2,3)*cos(Ya(2,3)-dG0(2))*Vsh0dq(1)+Ym(2,3)*sin(Ya(2,3)-dG0(2))*Vsh0dq(2)+...
-Ym(2,4)*cos(Ya(2,4)-dG0(2))*Vse0dq(1)+Ym(2,4)*sin(Ya(2,4)-dG0(2))*Vse0dq(2);
Q3(1,2) = -Ym(1,2)*(-cos(Ya(1,2)-d120)*Epd0(2)+sin(Ya(1,2)-d120)*Epc0(2));
Q3(2,1) = -Ym(2,1)*(-cos(Ya(2,1)+d120)*Epd0(1)+sin(Ya(2,1)+d120)*Epc0(1));
%
D3(1,1) = Ym(1,2)*(cos(Ya(1,2)-d120)*Epc0(2)+sin(Ya(1,2)-d120)*Epd0(2))+...
Ym(1,3)*cos(Ya(1,3)-dG0(1))*Vsh0dq(2)+Ym(1,3)*sin(Ya(1,3)-dG0(1))*Vsh0dq(1)+...
Ym(1,4)*cos(Ya(1,4)-dG0(1))*Vse0dq(2)+Ym(1,4)*sin(Ya(1,4)-dG0(1))*Vse0dq(1);
D3(2,2) = Ym(2,1)*(cos(Ya(2,1)+d120)*Epc0(1)+sin(Ya(2,1)+d120)*Epd0(1))+...
Ym(2,3)*cos(Ya(2,3)-dG0(2))*Vsh0dq(2)+Ym(2,3)*sin(Ya(2,3)-dG0(2))*Vsh0dq(1)+...
Ym(2,4)*cos(Ya(2,4)-dG0(2))*Vse0dq(2)+Ym(2,4)*sin(Ya(2,4)-dG0(2))*Vse0dq(1);
D3(1,2) = -Ym(1,2)*(cos(Ya(1,2)-d120)*Epc0(2)+sin(Ya(1,2)-d120)*Epd0(2));
D3(2,1) = -Ym(2,1)*(cos(Ya(2,1)+d120)*Epc0(1)+sin(Ya(2,1)+d120)*Epd0(1));
%
Q4 = 1/2/nSH/Vb * [-Ym(1,3)*sin(Ya(1,3)-dG0(1))*Vdc0*sin(dSH0)+Ym(1,3)*cos(Ya(1,3)-dG0(1))*Vdc0*cos(dSH0);
-Ym(2,3)*sin(Ya(2,3)-dG0(2))*Vdc0*sin(dSH0)+Ym(2,3)*cos(Ya(2,3)-
dG0(2))*Vdc0*cos(dSH0)];
%
D4 = 1/2/nSH/Vb * [-Ym(1,3)*cos(Ya(1,3)-dG0(1))*Vdc0*sin(dSH0)-Ym(1,3)*sin(Ya(1,3)-dG0(1))*Vdc0*cos(dSH0);
-Ym(2,3)*cos(Ya(2,3)-dG0(2))*Vdc0*sin(dSH0)-Ym(2,3)*sin(Ya(2,3)-
dG0(2))*Vdc0*cos(dSH0)];
%
Q5 = -1/2/nSH/Vb * [-Ym(1,3)*sin(Ya(1,3)-dG0(1))*Vdc0*cos(dSH0)*mSH0-Ym(1,3)*cos(Ya(1,3)-
dG0(1))*mSH0*Vdc0*sin(dSH0);
-Ym(2,3)*sin(Ya(2,3)-dG0(2))*Vdc0*cos(dSH0)*mSH0-Ym(2,3)*cos(Ya(2,3)-
dG0(2))*mSH0*Vdc0*sin(dSH0)];
%
D5 = -1/2/nSH/Vb * [-Ym(1,3)*cos(Ya(1,3)-dG0(1))*Vdc0*cos(dSH0)*mSH0+Ym(1,3)*sin(Ya(1,3)-
dG0(1))*mSH0*Vdc0*sin(dSH0);
-Ym(2,3)*cos(Ya(2,3)-dG0(2))*Vdc0*cos(dSH0)*mSH0+Ym(2,3)*sin(Ya(2,3)-
dG0(2))*mSH0*Vdc0*sin(dSH0)];
%
Q6 = 1/2/nSE/Vb * [-Ym(1,4)*sin(Ya(1,4)-dG0(1))*Vdc0*sin(dSE0)+Ym(1,4)*cos(Ya(1,4)-dG0(1))*Vdc0*cos(dSE0);
-Ym(2,4)*sin(Ya(2,4)-dG0(2))*Vdc0*sin(dSE0)+Ym(2,4)*cos(Ya(2,4)-
dG0(2))*Vdc0*cos(dSE0)];
%
D6 = 1/2/nSE/Vb * [-Ym(1,4)*cos(Ya(1,4)-dG0(1))*Vdc0*sin(dSE0)-Ym(1,4)*sin(Ya(1,4)-dG0(1))*Vdc0*cos(dSE0);
-Ym(2,4)*cos(Ya(2,4)-dG0(2))*Vdc0*sin(dSE0)-Ym(2,4)*sin(Ya(2,4)-
dG0(2))*Vdc0*cos(dSE0)];
%
Q7 = -1/2/nSE/Vb * [-Ym(1,4)*sin(Ya(1,4)-dG0(1))*Vdc0*cos(dSE0)*mSE0-Ym(1,4)*cos(Ya(1,4)-
dG0(1))*mSE0*Vdc0*sin(dSE0);
-Ym(2,4)*sin(Ya(2,4)-dG0(2))*Vdc0*cos(dSE0)*mSE0-Ym(2,4)*cos(Ya(2,4)-
dG0(2))*mSE0*Vdc0*sin(dSE0)];
%
D7 = -1/2/nSE/Vb * [-Ym(1,4)*cos(Ya(1,4)-dG0(1))*Vdc0*cos(dSE0)*mSE0+Ym(1,4)*sin(Ya(1,4)-
dG0(1))*mSE0*Vdc0*sin(dSE0);
-Ym(2,4)*cos(Ya(2,4)-dG0(2))*Vdc0*cos(dSE0)*mSE0+Ym(2,4)*sin(Ya(2,4)-
dG0(2))*mSE0*Vdc0*sin(dSE0)];
%
Q8 = [1/2/nSH/Vb * (-Ym(1,3)*sin(Ya(1,3)-dG0(1))*sin(dSH0)*mSH0+Ym(1,3)*cos(Ya(1,3)-
dG0(1))*mSH0*cos(dSH0))+...
1/2/nSE/Vb * (-Ym(1,4)*sin(Ya(1,4)-dG0(1))*sin(dSE0)*mSE0+Ym(1,4)*cos(Ya(1,4)-
dG0(1))*mSE0*cos(dSE0));
1/2/nSH/Vb * (-Ym(2,3)*sin(Ya(2,3)-dG0(2))*sin(dSH0)*mSH0+Ym(2,3)*cos(Ya(2,3)-

```

```

dG0(2))*mSH0*cos(dSH0))+...
1/2/nSE/Vb * (-Ym(2,4)*sin(Ya(2,4)-dG0(2))*sin(dSE0)*mSE0+Ym(2,4)*cos(Ya(2,4)-
dG0(2))*mSE0*cos(dSE0));
%
D8 = [1/2/nSH/Vb * (-Ym(1,3)*cos(Ya(1,3)-dG0(1))*sin(dSH0)*mSH0-Ym(1,3)*sin(Ya(1,3)-
dG0(1))*mSH0*cos(dSH0))+
1/2/nSE/Vb * (-Ym(1,4)*cos(Ya(1,4)-dG0(1))*sin(dSE0)*mSE0-Ym(1,4)*sin(Ya(1,4)-
dG0(1))*mSE0*cos(dSE0));
1/2/nSH/Vb * (-Ym(2,3)*cos(Ya(2,3)-dG0(2))*sin(dSH0)*mSH0-Ym(2,3)*sin(Ya(2,3)-
dG0(2))*mSH0*cos(dSH0))+...
1/2/nSE/Vb * (-Ym(2,4)*cos(Ya(2,4)-dG0(2))*sin(dSE0)*mSE0-Ym(2,4)*sin(Ya(2,4)-
dG0(2))*mSE0*cos(dSE0));
%
Qu1 = [ Ym(3,1)*cos(Ya(3,1)+dG0(1)) Ym(3,2)*cos(Ya(3,2)+dG0(2)); Ym(4,1)*cos(Ya(4,1)+dG0(1))
Ym(4,2)*cos(Ya(4,2)+dG0(2))];
Du1 = [-Ym(3,1)*sin(Ya(3,1)+dG0(1)) -Ym(3,2)*sin(Ya(3,2)+dG0(2));-Ym(4,1)*sin(Ya(4,1)+dG0(1)) -
Ym(4,2)*sin(Ya(4,2)+dG0(2))];
%
Qu2 = -Du1;
Du2 = Qu1;
%
Du3(1,1) = Ym(3,1)*(-cos(Ya(3,1)+dG0(1))*Epd0(1)-sin(Ya(3,1)+dG0(1))*Epd0(1));
Du3(2,1) = Ym(4,1)*(-cos(Ya(4,1)+dG0(1))*Epd0(1)-sin(Ya(4,1)+dG0(1))*Epd0(1));
Du3(1,2) = Ym(3,2)*(-cos(Ya(3,2)+dG0(2))*Epd0(2)-sin(Ya(3,2)+dG0(2))*Epd0(2));
Du3(2,2) = Ym(4,2)*(-cos(Ya(4,2)+dG0(2))*Epd0(2)-sin(Ya(4,2)+dG0(2))*Epd0(2));
%
Qu3(1,1) = Ym(3,1)*(cos(Ya(3,1)+dG0(1))*Epd0(1)-sin(Ya(3,1)+dG0(1))*Epd0(1));
Qu3(2,1) = Ym(4,1)*(cos(Ya(4,1)+dG0(1))*Epd0(1)-sin(Ya(4,1)+dG0(1))*Epd0(1));
Qu3(1,2) = Ym(3,2)*(cos(Ya(3,2)+dG0(2))*Epd0(2)-sin(Ya(3,2)+dG0(2))*Epd0(2));
Qu3(2,2) = Ym(4,2)*(cos(Ya(4,2)+dG0(2))*Epd0(2)-sin(Ya(4,2)+dG0(2))*Epd0(2));
%
Qu4 = 1/2/nSH/Vb * [-Ym(3,3)*sin(Ya(3,3))*Vdc0*sin(dSH0)+Ym(3,3)*cos(Ya(3,3))*Vdc0*cos(dSH0);
-Ym(4,3)*sin(Ya(4,3))*Vdc0*sin(dSH0)+Ym(4,3)*cos(Ya(4,3))*Vdc0*cos(dSH0)];
%
Du4 = 1/2/nSH/Vb * [-Ym(3,3)*cos(Ya(3,3))*Vdc0*sin(dSH0)-Ym(3,3)*sin(Ya(3,3))*Vdc0*cos(dSH0);
-Ym(4,3)*cos(Ya(4,3))*Vdc0*sin(dSH0)-Ym(4,3)*sin(Ya(4,3))*Vdc0*cos(dSH0)];
%
Qu5 = -1/2/nSH/Vb * [Ym(3,3)*Vdc0*mSH0*(-sin(Ya(3,3))*cos(dSH0)-cos(Ya(3,3))*sin(dSH0));
Ym(4,3)*Vdc0*mSH0*(-sin(Ya(4,3))*cos(dSH0)-cos(Ya(4,3))*sin(dSH0))];
%
Du5 = -1/2/nSH/Vb * [Ym(3,3)*Vdc0*mSH0*(-cos(Ya(3,3))*cos(dSH0)+sin(Ya(3,3))*sin(dSH0));
Ym(4,3)*Vdc0*mSH0*(-cos(Ya(4,3))*cos(dSH0)+sin(Ya(4,3))*sin(dSH0))];
%
Qu6 = 1/2/nSE/Vb * [Ym(3,4)*Vdc0*(-sin(Ya(3,4))*sin(dSE0)+cos(Ya(3,4))*cos(dSE0));
Ym(4,4)*Vdc0*(-sin(Ya(4,4))*sin(dSE0)+cos(Ya(4,4))*cos(dSE0))];
%
Du6 = 1/2/nSE/Vb * [Ym(3,4)*Vdc0*(-cos(Ya(3,4))*sin(dSE0)-sin(Ya(3,4))*cos(dSE0));
Ym(4,4)*Vdc0*(-cos(Ya(4,4))*sin(dSE0)-sin(Ya(4,4))*cos(dSE0))];
%
Qu7 = -1/2/nSE/Vb * [Ym(3,4)*Vdc0*mSE0*(-sin(Ya(3,4))*cos(dSE0)-cos(Ya(3,4))*sin(dSE0));
Ym(4,4)*Vdc0*mSE0*(-sin(Ya(4,4))*cos(dSE0)-cos(Ya(4,4))*sin(dSE0))];
%
Du7 = -1/2/nSE/Vb * [Ym(3,4)*Vdc0*mSE0*(-cos(Ya(3,4))*cos(dSE0)+sin(Ya(3,4))*sin(dSE0));
Ym(4,4)*Vdc0*mSE0*(-cos(Ya(4,4))*cos(dSE0)+sin(Ya(4,4))*sin(dSE0))];
%
Qu8 = [1/2/nSH/Vb*(Ym(3,3)*mSH0*(-sin(Ya(3,3))*sin(dSH0)+cos(Ya(3,3))*cos(dSH0)))+...
1/2/nSE/Vb*(Ym(3,4)*mSE0*(-sin(Ya(3,4))*sin(dSE0)+cos(Ya(3,4))*cos(dSE0)))+...
1/2/nSH/Vb*(Ym(4,3)*mSH0*(-sin(Ya(4,3))*sin(dSH0)+cos(Ya(4,3))*cos(dSH0)))+...
1/2/nSE/Vb*(Ym(4,4)*mSE0*(-sin(Ya(4,4))*sin(dSE0)+cos(Ya(4,4))*cos(dSE0)))]];
%
Du8 = [1/2/nSH/Vb*(Ym(3,3)*mSH0*(-cos(Ya(3,3))*sin(dSH0)-sin(Ya(3,3))*cos(dSH0)))+...
1/2/nSE/Vb*(Ym(3,4)*mSE0*(-cos(Ya(3,4))*sin(dSE0)-sin(Ya(3,4))*cos(dSE0)))+...
1/2/nSH/Vb*(Ym(4,3)*mSH0*(-cos(Ya(4,3))*sin(dSH0)-sin(Ya(4,3))*cos(dSH0)))+...
1/2/nSE/Vb*(Ym(4,4)*mSE0*(-cos(Ya(4,4))*sin(dSE0)-sin(Ya(4,4))*cos(dSE0)))]];
%
K1 = (1/upfc_con(11))*Sb*[-mSH0*cos(dSH0)/2/nSH/Vb -mSH0*cos(dSH0)/2/nSH/Vb-mSE0*cos(dSE0)/2/nSE/Vb];
K2 = (1/upfc_con(11))*Sb*[ mSH0*sin(dSH0)/2/nSH/Vb mSH0*sin(dSH0)/2/nSH/Vb+mSE0*sin(dSE0)/2/nSE/Vb];
K3 = (1/upfc_con(11))*Sb*[sin(dSH0)/2/nSH/Vb*(Iud0(1)+Iud0(2))-cos(dSH0)/2/nSH/Vb*(Iuq0(1)+Iuq0(2))];
K4 = -
(1/upfc_con(11))*Sb*[mSH0*cos(dSH0)/2/nSH/Vb*(Iud0(1)+Iud0(2))+mSH0*sin(dSH0)/2/nSH/Vb*(Iuq0(1)+Iuq0(2))];
K5 = (1/upfc_con(11))*Sb*[sin(dSE0)/2/nSE/Vb*Iud0(2)-cos(dSE0)/2/nSE/Vb*Iuq0(2)];
K6 = -(1/upfc_con(11))*Sb*[mSE0*cos(dSE0)/2/nSE/Vb*Iud0(2)+mSE0*sin(dSE0)/2/nSE/Vb*Iuq0(2)];
%
M1 = inv(Tq0)*Xqqp*Q1;
M2 = -inv(Tq0)+inv(Tq0)*Xqqp*Q2;
M3 = inv(Tq0)*Xqqp*Q3;
M4 = inv(Tq0)*Xqqp*Q4;
M5 = inv(Tq0)*Xqqp*Q5;
M6 = inv(Tq0)*Xqqp*Q6;
M7 = inv(Tq0)*Xqqp*Q7;

```

```

M8 = inv(Tq0)*Xqqp*Q8;
%
N1 = -inv(Td0)-inv(Td0)*Xddp*D1;
N2 = -inv(Td0)*Xddp*D2;
N3 = -inv(Td0)*Xddp*D3;
N4 = -inv(Td0)*Xddp*D4;
N5 = -inv(Td0)*Xddp*D5;
N6 = -inv(Td0)*Xddp*D6;
N7 = -inv(Td0)*Xddp*D7;
N8 = -inv(Td0)*Xddp*D8;
N9 = inv(Td0);
%
U1 = -diag(Igq0)*r+diag(Igd0)*Xdp+diag(Vq0);
U2 = -diag(Igd0)*r-diag(Igq0)*Xdp+diag(Vd0);
W1 = -1/2*inv(H)*(diag(Igq0)+U1*Q1+U2*D1);
W2 = -1/2*inv(H)*(diag(Igd0)+U1*Q2+U2*D2);
W3 = -1/2*inv(H)*(U1*Q3+U2*D3);
W4 = -1/2*inv(H)*(U1*Q4+U2*D4);
W5 = -1/2*inv(H)*(U1*Q5+U2*D5);
W6 = -1/2*inv(H)*(U1*Q6+U2*D6);
W7 = -1/2*inv(H)*(U1*Q7+U2*D7);
W8 = -1/2*inv(H)*(U1*Q8+U2*D8);
W9 = -1/2*inv(H)*Da;
W10 = 1/2*inv(H);
%
L1 = K1*Qu1+K2*Du1;
L2 = K1*Qu2+K2*Du2;
L3 = K1*Qu3+K2*Du3;
L4 = K1*Qu4+K2*Du4+K3;
L5 = K1*Qu5+K2*Du5+K4;
L6 = K1*Qu6+K2*Du6+K5;
L7 = K1*Qu7+K2*Du7+K6;
L8 = K1*Qu8+K2*Du8;
%
R1 = P1*(-r*D1+Xqp*Q1)+P2*(eye(2,2)-Xdp*D1-r*Q1);
R2 = P1*(eye(2,2)-r*D2+Xqp*Q2)+P2*(-Xdp*D2-r*Q2);
R3 = P1*(-r*D3+Xqp*Q3)+P2*(-Xdp*D3-r*Q3);
R4 = P1*(-r*D4+Xqp*Q4)+P2*(-Xdp*D4-r*Q4);
R5 = P1*(-r*D5+Xqp*Q5)+P2*(-Xdp*D5-r*Q5);
R6 = P1*(-r*D6+Xqp*Q6)+P2*(-Xdp*D6-r*Q6);
R7 = P1*(-r*D7+Xqp*Q7)+P2*(-Xdp*D7-r*Q7);
R8 = P1*(-r*D8+Xqp*Q8)+P2*(-Xdp*D8-r*Q8);
%
S1 = -inv(Ta)*Ka*R1;
S2 = -inv(Ta)*Ka*R2;
S3 = -inv(Ta)*Ka*R3;
S4 = -inv(Ta)*Ka*R4;
S5 = -inv(Ta)*Ka*R5;
S6 = -inv(Ta)*Ka*R6;
S7 = -inv(Ta)*Ka*R7;
S8 = -inv(Ta)*Ka*R8;
S9 = -inv(Ta);
%
A = [ N1          N2          N3          zeros(2,2)    N8          N9(:,2);
      M1          M2          M3          zeros(2,2)    M8          zeros(2,1);
      zeros(2,2) zeros(2,2)  zeros(2,2)  wb*eye(2,2)  zeros(2,1) zeros(2,1);
      W1          W2          W3          W9          W8          zeros(2,1);
      L1          L2          L3          zeros(1,2)    L8          zeros(1,1);
      S1(2,:)     S2(2,:)     S3(2,:)     zeros(1,2)    zeros(1,1) S9(2,2)];
% form minimum system
d1 = 5; d2 = 6;
A2 = A;
A2(d2,:) = (A2(d2,:) - A2(d1,:));
[nr,nc]=size(A2);
A1 = [A2(1:d1-1,1:d1-1) A2(1:d1-1,d1+1:nc);
      A2(d1+1:nr,1:d1-1) A2(d1+1:nr,d1+1:nc)];
A3 = cutM(A1,9); % take out exciter state
%
B = [N6          N7          N4          N5;
     M6          M7          M4          M5;
     zeros(2,1)  zeros(2,1)  zeros(2,1)  zeros(2,1);
     W6          W7          W4          W5;
     L6          L7          L4          L5;
     S6          S7          S4          S5];

B1 = B(1:9,:); % take out exciter
d1 = 5; d2 = 6;
B2 = B1;
B2(d2,:) = (B2(d2,:) - B2(d1,:));
[nr,nc]=size(B2);
B3 = [B2(1:d1-1,1:d1-1) B2(1:d1-1,d1+1:nc);

```

```

        B2(dl+1:nr,1:d1-1) B2(dl+1:nr,d1+1:nc)];
% swap col/rows to get numbering of states as in the PST
Ifrom = [1 6 4 4];
Ito   = [6 2 7 5];
An = A3;
for aa=1:length(Ifrom),
    An = exM(An,Ifrom(aa),Ito(aa));
end
Ifrom = [1 1 4 4];
Ito   = [2 6 7 5];
% swap rows to get numbering of inputs as in the PST
Bn = B3;
for aa=1:length(Ifrom),
    Bn = exMr(Bn,Ifrom(aa),Ito(aa));
end

```

PST - data file for the Two-machine/UPFC power system:

```

% Two machine/UPFC test system
% subtransient generator models
% dc exciters turbine/governor;
% bus data format
% col1 number
% col2 voltage magnitude(pu)
% col3 voltage angle(degree)
% col4 p_gen(pu)
% col5 q_gen(pu),
% col6 p_load(pu)
% col7 q_load(pu)
% col8 G shunt(pu)
% col9 B shunt(pu)
% col10 bus_type
%      bus_type - 1, swing bus
%                - 2, generator bus (PV bus)
%                - 3, load bus (PQ bus)
% col11 q_gen_max(pu)
% col12 q_gen_min(pu)
% col13 v_rated (kV)
% col14 v_max pu
% col15 v_min pu
bus = [...
1 1.      0 0      0.00 0.00 0.00 0.00 0.00 1  5.0 -5.0 22.0  1.1 .9;
2 1.03    6.1 .8    0.00 0.00 0.00 0.00 0.00 2  5.0 -5.0 230.0 1.5 .5;
3 1.03    6.1 -.80  0.15 0.00 0.00 0.00 0.00 2  5.0 -5.0 230.0 1.5 .5;
4 1.01    3    0.00 0.00 -.8  -.15 0.00 0.00 3  0.0  0.0 115.0 1.05 .95];
% line data format
% line: from bus, to bus, resistance(pu), reactance(pu),
%       line charging(pu), tap ratio, tap phase, tapmax, tapmin, tapsize
line = [...
2 3 0.0  0.07  0.00  1.0 0. 0. 0. 0.;
1 4 0.0  0.65  0.00  1.0 0. 0. 0. 0.;
1 4 0.0  0.65  0.00  1.0 0. 0. 0. 0.;
3 4 100  100   0.00  1.0 0. 0. 0. 0.]; % high impedance line to obtain LF solution
% Machine data format
% Machine data format
% 1. machine number,
% 2. bus number,
% 3. base mva,
% 4. leakage reactance x_l(pu),
% 5. resistance r_a(pu),
% 6. d-axis synchronous reactance x_d(pu),
% 7. d-axis transient reactance x'_d(pu),
% 8. d-axis subtransient reactance x''_d(pu),
% 9. d-axis open-circuit time constant T'_do(sec),
% 10. d-axis open-circuit subtransient time constant T''_do(sec),
% 11. q-axis synchronous reactance x_q(pu),
% 12. q-axis transient reactance x'_q(pu),
% 13. q-axis subtransient reactance x''_q(pu),
% 14. q-axis open-circuit time constant T'_qo(sec),
% 15. q-axis open circuit subtransient time constant
%     T''_qo(sec),
% 16. inertia constant H(sec),
% 17. damping coefficient d_o(pu),
% 18. damping coefficient d_l(pu),
% 19. bus number
%
% note: all the following machines use transient model
mac_con = [ ...

```

```

1 1 900 0.200 0.0025 1.8 0.30 0.0 8.00 0.03 1.7 0.3 0.0 0.4 0.05 6.5 0 0 1;
2 2 900 0.200 0.0025 1.8 0.30 0.0 8.00 0.03 1.7 0.3 0.0 0.4 0.05 6.5 0 0 2];
% non-conforming load
% col 1 bus number
% col 2 fraction const real power load
% col 3 fraction const reactive power load
% col 4 fraction const active current load
% col 5 fraction const reactive current load
load_con = [...
3 0 0 0 0;
4 0 0 0 0];
%upfc_con
% 1 - upfc number
% 2 - sending bus
% 3 - receiving bus
% 4 - shunt transformer resistance
% 5 - shunt transformer reactance
% 6 - series transformer resistance
% 7 - series transformer reactance
% 8 - shunt transformer turn ratio (n_sh)
% 9 - series transformer turn ratio (n_se)
% 10 - DC voltage (reference)
% 11 - capacitance (C)
% 12 - base voltage (Vb)
% 13 - 0
% 14 - 0
% 15 - line reactance
% 16 - number of UPFC states
% 1 - Vdc only
% 2 - Vdc, Vp1, Vq1, Upfc_PI_Vs, Upfc_PI_dc
% 17 - mode
% 1 - nonlinear simulation
% 2 - linearising
% 3 - input response
% 18 - way of forming A,B,C (upfc_con==1)
% 1 - state Vdc only: A=a_mat, B=[upfc], C=[upfc]
% 2 - state Vdc and expand system by PI-controllers (B,C based on UPFC)
% 3 - state Vdc and expand system by PI-controllers (B,C based on TG, EXC, UPFC)
% 4 - upfc_con == 1, closed loop approach

upfc_con = [ 1 3 4 0 .00025/.05^2 0 .05 .05 .25 31000 .055 230e3 0 0 .11 1 1 1];
% upfc_ctrl
% 1 - controller type
% 0 - no controller
% 1 - P type
% 2 - PT1 type
% 3 - I type
% 4 - Basic control:
% series:
% 1. line P/Q (pq-mode using PI), or
% 2. series compensation (PT1)
% 3. Vr/Vs (PI)
% 4. angle between Vr and Vs
% shunt: Vs and Vdc using PI-controllers
% 5 - shunt current controller
% 6 - decoupled line P/Q and Vs/Vdc using PIs
% 7 - LQ regulator for line P/Q and LQR for Vs/Vdc (using PIs to get reference values)
% 2 - Vs_ref
% 3 - Vs_flag
% 0 - Vs not controlled
% 1 - Vs controlled
% 4 - P_ref
% 5 - Q_ref
% 6 - constant K_PI_dc
% 7 - time constant T_PI_dc
% 8 - constant K_PI_Vs
% 9 - time constant T_PI_Vs
% 10 - constant k_PT1_Vp1
% 11 - time constant T_PT1_Vp1
% 12 - constant k_PT1_Vq1
% 13 - time constant T_PT1_Vq1
% 14 - time constant T_Vp2
% 15 - time constant T_Vq2
% 16 - prop. constant K ref
% 17 - prop. constant k_PI_V3
% 18 - time constant T_PI_V3
% 19 - n_ref (Vr/Vs)
% 20 - constant K_PI_V4
% 21 - time constant T_PI_V4
% 22 - alpha_ref (thetaR - thetaS) [deg]
upfc_ctrl = [4 1.03 1 .80 .15 .8 .1 .4 .05 .005 1 .005 1 .001 0.02 0.4 1 1 1 1 100 .005];

```

```
% upfc_weight (if controller type 4 is used) to determine active mode
% 1 - weight on Vp1, Vq1 (line P/Q)
% 2 - weight on Vp2, Vq2 (series compensation)
% 3 - weight on Vp3=0, Vq3 (Vr/Vs)
% 4 - weight on Vp4, Vq3=0 (angle(Vr)-angle(Vs))
upfc_weight = [1 0 0 0];
```